The role of deletions on chromosomes 7p and 20q in myeloproliferative disorders

Doctoral thesis at the Medical University of Vienna
for obtaining the academic degree

Doctor of Philosophy

Submitted by

Roland Jäger

Supervisor:
Robert Kralovics, PhD
CeMM – Center for Molecular Medicine
of the Austrian Academy of Sciences
Lazarettgasse 19/3, 1090 Vienna

Vienna, 06/2010

TABLE OF CONTENTS

ABSTRACT

Somatic mutations play a central role in the pathogenesis of myeloproliferative neoplasms (MPNs), triggering clonal hematopoiesis and establishing the disease phenotype. After the discovery of JAK and MPL mutations, continual technological advances now allow the identification of increasing numbers of genetic defects in MPN patients, most of them chromosomal aberrations such as deletions and acquired uniparental disomies. Efforts to map the genetic lesions to single genes resulted in the discovery of defects in the TET2 and CBL genes, however, the target gene(s) comprised in the most frequent chromosomal lesion in MPN, deletions on chromosome 20q (del20q), still remain to be identified. Therefore, we determined the role of del20q in the evolution of the malignant clone, characterized three independent MPN patient cohorts (a total of 822 patients) for del20q and assembled a del20q common deleted region (CDR) using microarray karyotyping of nine patients. We further identified *MYBL2* and *TOP1* as two putative tumor suppressors on 20q by mimicking deletion-caused haploinsufficiency using different shRNA knock-down strategies in vitro. Comparing our mapping data in patient material with the functional in vitro studies, we could see *MYBL2* within the del20q CDR, whereas *TOP1* mapped outside of the CDR, questioning the exclusive relevance of CDRs in the search for tumor suppressors.

Besides our work on del20q, a defect observed in the chronic phase of MPN, we were searching for cytogenetic aberrations associated with post-MPN transformation to acute leukemia. Leukemic transformation is a major complication of MPN, however, the genetic changes leading to transformation remain largely unknown. We screened nine patients with post-MPN leukemia for chromosomal aberrations using microarray karyotyping. Deletions on the short arm of chromosome 7 (del7p) emerged as a recurrent defect. We mapped the common deleted region to the *IKZF1* gene, which encodes the transcription factor Ikaros. We further examined the frequency of *IKZF1* deletions in a total of 29 post-MPN leukemia and 526 MPN patients without transformation and observed a strong association of *IKZF1* deletions with post-MPN leukemia in two independent cohorts. Patients with *IKZF1* loss exhibited complex karyotypes, and del7p was a late event in the genetic evolution of the MPN clone. *IKZF1* deletions were seen in both undifferentiated and differentiated myeloid cell types, indicating that *IKZF1* loss does not cause differentiation arrest but rather renders progenitors susceptible to transformation, most likely through chromosomal instability. Induced *Ikzf1* haploinsufficiency in primary murine progenitors resulted in elevated Stat5 phosphorylation and increased cytokine-dependent growth, suggesting that reduced expression of *IKZF1* is sufficient to perturb growth regulation. Thus, *IKZF1* loss is an important step in the leukemic transformation of a subpopulation of MPN patients.

ABSTRACT (German)

Somatische Mutationen spielen in der Pathogenese von Myeloproliferativen Neoplasien (MPN) eine wichtige Rolle, indem sie sowohl für die klonale Hämatopoese als auch das Krankheitsbild verantwortlich sind. Seit der Entdeckung der Mutationen in *JAK2* und *MPL* werden durch kontinuierliche technologische Fortschritte immer mehr genetische Defekte in MPN entdeckt. Die meisten davon sind chromosomale Aberrationen wie Deletionen und erworbene uniparentale Disomien. Bemühungen, diese genetischen Fehler auf einzelne Gene zu reduzieren, führten zur Entdeckung von Defekten in den Genen *TET2* und *CBL*. Die für die MPN-Pathogenese entscheidenden Gene in der am häufigsten auftretenden chromosomalen Aberration in MPN – den Deletionen auf Chromosom 20 (del20q) – konnten jedoch noch nicht identifiziert werden. Aus diesem Grund haben wir versucht die Rolle von del20q in der Evolution des malignen Klons zu bestimmen. Dazu haben wir del20q in drei unabhängige MPN Patientenkohorten (insgesamt 822 Patienten) charakterisiert sowie mithilfe von Mikroarray-Karyotypisierung eine „allgemein/gemeinsam deletierte Region" (CDR) zusammengestellt. Weiters konnten wir *MYBL2* und *TOP1* als putative Tumorsuppressoren auf Chromosom 20q identifizieren. Dies erreichten wir durch Anwendung von verschiedenen shRNA knock-down-Strategien in-vitro, womit wir die von Deletionen verursachte Haploinsuffizienz nachahmen konnten. Letztendlich fassten wir die Kartierungsdaten von neun del20q Patienten und die Daten aus den funktionellen in-vitro Studien zusammen und konnten feststellen, dass zwar *MYBL2* innerhalb der CDR liegt, jedoch *TOP1* außerhalb der CDR lokalisiert ist. Mit dieser Beobachtung stellen wir die exklusive Relevanz von CDRs in der Suche nach Tumorsuppressoren in Frage.

Neben unserer Arbeit an del20q, ein Defekt der in der chronischen Phase von MPN auftritt, waren wir auf der Suche nach zytogenetischen Aberrationen, welche bei der Transformation von MPN zu akuter myeloider Leukämie (post-MPN AML) auftreten. Leukämische Transformation ist eine der schwerwiegendsten Komplikationen in MPN. Die dazu führenden genetischen Veränderungen sind jedoch noch unklar. Mithilfe von Mikroarray-Karyotypisierung untersuchten wir neun Patienten mit post-MPN AML auf chromosomale Aberrationen. Dabei konnten wir Deletionen am kurzen Arm von Chromosom 7 (del7p) als wiederkehrenden Defekt identifizieren. Im Zuge der Kartierung der del7p CDR konnten wir den Defekt auf das *IKZF1* Gen lokal beschränken, welches den Transkriptionsfaktor Ikaros kodiert. Weiters untersuchten wir die Häufigkeit von *IKZF1* Deletionen in 29 post-MPN AML Patienten und 526 MPN-Patienten ohne Transformation und konnten in zwei unabhängigen Patientenkohorten eine starke Assoziation von *IKZF1* Deletionen mit post-MPN AML feststellen. Patienten mit *IKZF1* Deletion zeigten weiters einen komplexen Karyotyp, wobei sich del7p in der genetischen Evolution des MPN Klons als spät auftretender Defekt herausstellte. Wir konnten *IKZF1* Deletionen sowohl in undifferenzierten als auch in differenzierten myeloiden Zelltypen sehen. Dies deutet an, dass der Verlust des *IKZF1* Gens keine Blockade in der Zelldifferenzierung induziert, sondern eher die Progenitorzellen für leukämische Transformation empfindlich macht, wahrscheinlich durch chromosomale Instabilität. Induzierte Haploinsuffizienz für *Ikzf1* in Maus Primär-Progenitorzellen führte zu erhöhter Stat5-Phosphorylierung und gesteigertem Zytokin-abhängigem Wachstum. Dies legt nahe, dass reduzierte *IKZF1* Genexpression ausreicht um die Wachstumsregulierung zu stören. Demzufolge sind *IKZF1* Deletionen ein wichtiger Schritt in der leukämischen Transformation eines Teils der MPN Patienten.

1. INTRODUCTION

1.1. Clinical features of MPN

Myeloproliferative neoplasms (MPN) are clonal stem cell malignancies of the hematopoietic system. MPN is characterized by excessive production of blood cells of the myeloid lineage. Three classical disease entities are summarized as classic Philadelphia chromosome negative MPNs; polycythemia vera (PV), essential thrombocythemia (ET) and primary myelofibrosis (PMF) [1]. Whereas PV and ET involve an excessive production of red blood cells and platelets, respectively, PMF is characterized by replacement of the bone marrow with fibrotic tissue [2]. Besides the three common MPN entities, there is a large group of less frequent diseases summarized as non-classical MPNs; chronic neutrophilic leukemia (CNL), chronic eosinophilic leukemia (CEL), chronic myelomonocytic leukemia (CMML), juvenile myelomonocytic leukemia (JMML), hypereosinophilic syndrome (HES), systemic mastocytosis (SM) and others [1, 3].

Despite the different phenotypes, the three common MPN entities share clinical complications such as inherent tendency for thrombosis, bleeding and secondary leukemic transformation, albeit occurring at different frequencies. Thrombosis is a frequent event in PV and ET dramatically affecting morbidity and mortality in MPN. Whereas thrombosis does not significantly shorten life expectancy in ET, reduced survival due to thrombotic events can be observed in PV patients [4, 5]. Patients with advanced phase PV and ET may evolve to secondary myelofibrosis [6] which is, similar to PMF, associated with unfavorable prognosis and substantial decrease in survival [7-9]. Bone marrow fibrosis is associated with mobilization of hematopoietic progenitors from the bone marrow, leading to an increased number of circulating CD34+ progenitors in the peripheral blood [7]. The circulating progenitors populate the spleen and the liver resulting in hepatosplenomegaly. Subsequent complications arising from this are hepatic failure, bleeding, portal hypertension and heart failure.

Besides thrombosis, bleeding and infections, transformation to leukemia is a significant cause of death in MPN [4, 8-12].. The risk for leukemic transformation is highest in PMF (10–30% of cases), followed by PV (8-10%) and ET (4-5%). [4, 13]. The cause of this increased transformation rate in MPN is currently unknown, but could be a natural consequence of the genetic changes due to the accumulation of mutations and chromosomal lesions in the MPN clone. Alternatively, there is an ongoing discussion on the possible role of therapy in transformation. Commonly used cytotoxic agents such as hydroxyurea were shown to be leukemogenic in some studies [14, 15], and can impose a selective pressure on the MPN clone, mediating a competitive advantage for subclones with acquired leukemogenic mutations [16, 17]. Other studies suggest that increased risk of transformation is instead dependent on disease duration, resulting in an increase in transformation events over time [4, 18, 19].

1.2. Genetic defects in MPN pathogenesis

Besides clinical features, both classical and non-classical MPNs share stem cell derived clonality in myeloproliferation [2]. Not only clonality itself is shared, but also the mutations driving the clones, mediating a proliferative advantage and cytokine hypersensitivity to the outgrowing malignant cell. Cytokine hypersensitivity in MPN is a consequence of deregulated signal transduction caused by somatic mutations directly or indirectly involved in growth control [20].

Blood production is a tightly regulated process, since the function of the hematopoietic system is dependent on the rapid but controlled expansion of all lineages to supply the body's demand for blood cells and to generate an effective immune response to pathogens. Signals from cytokines binding to receptors on the cell surface are transduced by protein kinase signaling cascades, resulting in rapid activation of gene expression. Signal-independent constitutive activation of intracellular signal transduction pathways has been observed in hematological malignancies [20, 21] and found to be frequently caused by mutations of tyrosine kinases or their effector molecules (Figure 1.2.) [16].
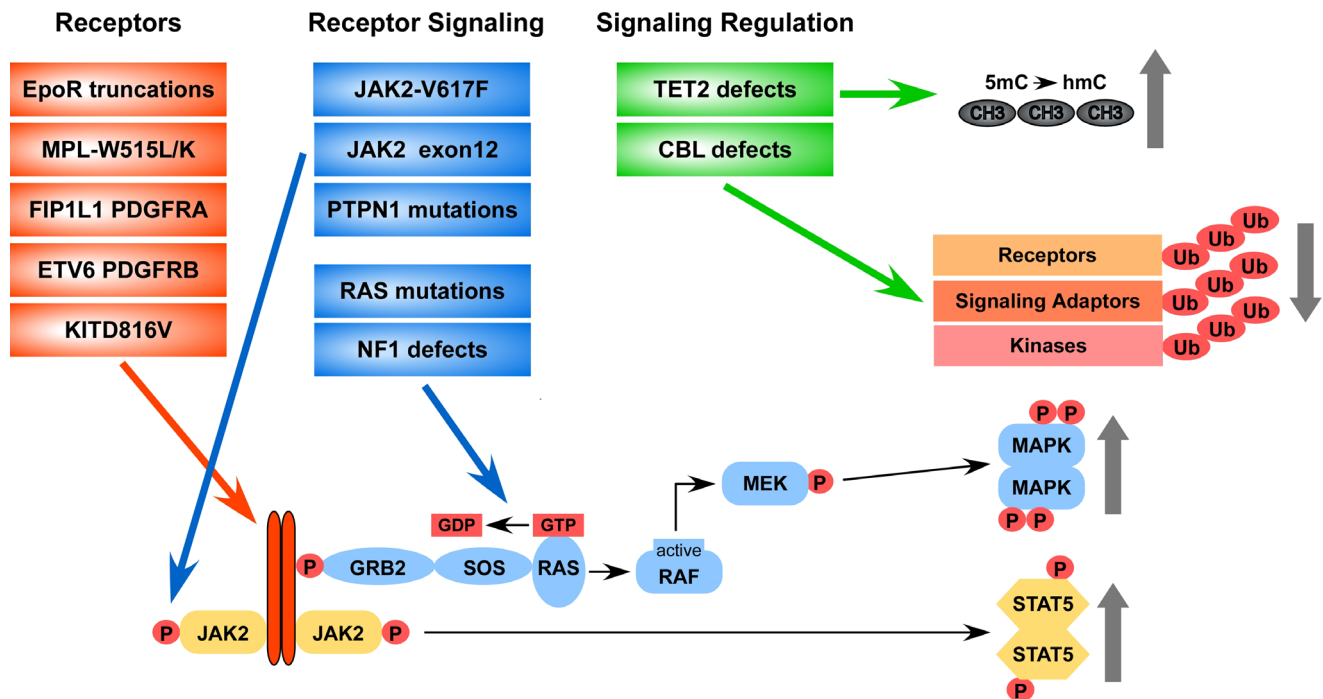
Figure 1.2.: Genetic defects and their downstream consequences in MPN
Red, blue and green boxes summarize germ line and somatic mutations in MPN and MPN-like phenotypes. Clonal advantage based on cytokine hypersensitivity can be triggered by genetic defects directly targeting receptors (red boxes) as well as mutations affecting elements of downstream signaling cascades (blue boxes) and genes coding for regulatory proteins such as TET2 and CBL (green boxes). Defects identified so far in MPN predominantly activate the JAK-STAT and the mitogen-activated protein kinase (MAPK) pathways. Whereas receptor and kinase mutations result in elevated phosphorylation response, phosphatase mutations such as in PTPN1 inactivate its negative regulation. MAPK signaling is direcly affected by RAS mutations, and indirectly enhanced by defects in NF1, a GTPase activating protein known to decrease signal potential of Ras by accelerating Ras-associated hydrolysis of guanosine triphosphate (GTP) into guanosine diphosphate (GDP) and phosphate. The ubiquitin ligase CBL regulates the degradation of cytokine receptors (EpoR, c-Kit), molecules important for signaling (such as the adapter protein Grb2), and tyrosine kinases (Jak2, Tyk2). Decreased ubiquitination of those factors consequently enhances signaling capacity. TET2 might be involved in epigenetic transcriptional regulation by enzymatically catalyzing the conversion of 5-methylcytosine to 5-hydroxymethylcytosine, as shown for another TET family member TET1. The identification of TET2 defects in MPN pathogenesis propose epigenetic deregulation as alternative mechanism to the altered transcriptional responses due to increased Stat5 and Mapk phosphorylation.

Besides the well studied fusion gene BCR-ABL in chronic myeloid leukemia (CML), other mutations of tyrosine kinases, their effectors or negative regultors outside of the three main MPN entities are FIP1L1-PDGFRA and ETV6-PDGFRB in subtypes of CEL [22-24], KITD816V in SM [25] as well as *RAS*, *NF1* and *PTPN1* mutations in JMML [26-28]. Within the three classical MPN entities, PV, ET and PMF, mutations associated with kinase signaling were found in the

thrombopoietin receptor gene *MPL* and, most prominently, the tyrosine kinase gene *JAK2* (Figure 1.2.) [2]

In 2005, a gain-of-function mutation in the *JAK2* kinase gene (JAK2-V617F) has been identified [29-32], present in more than half of MPN patients. Despite the striking role of JAK2-V617F in the disease, other mutations with lower frequency have also been described, most prominently activating mutations in exon 12 of *JAK2* [33-35] and in MPL [36, 37], as well as mutations recently found in the *CBL* [38] and *TET2* genes (Figure 1.2. and Table 1.2.) [39]. In addition to those mutations, a variety of chromosomal aberrations such as deletions and acquired uniparental disomies (UPDs) have been observed in the MPN clone. The "stochastic" mutation acquisition model of MPN pathogenesis has recently been proposed that argues for an absence of predetermined order in the acquisition of mutations and aberrations in MPN [16].

Table 1.2.: Frequencies of the most prominent mutations in classical MPNs

	PV	ET	PMF	*References*
JAK2-V617F	95%	50-60%	50-60%	(16-19)
JAK2 exon12	20% (JAK2-V617F negative PV)	-	-	35
MPL-W515L/K	-	1-9%	5%	(22, 61, 64)
TET2	16%	5%	17%	40
CBL	-	-	6%	(24)

1.2.1. The V617F mutation of JAK2

The discovery of a gain of function mutation in *JAK2* (JAK2-V617F) in more than half of MPN patients in 2005 [29-32] was a milestone in the MPN field 20 years after BCR-ABL was linked to CML. In CML, the discovery of the Philadelphia chromosome was followed by a series of scientific breakthroughs, including the characterization of the BCR-ABL fusion protein to an explosion of knowledge about kinase function and biology and finally the successful treatment of the disease by the development of still improving kinase inhibitors [41-44]. Based on those achievements in CML, the identification of JAK2-V617F gave hope for substantial

progress in the search for therapeutic strategies for MPN and the understanding of MPN pathogenesis. Indeed, the identification of JAK2-V617F was followed by many important findings and led to the initiation of clinical trials of Jak2 inhibitors. Among the most important findings in MPN pathogenesis was the involvement of cytokine signaling in the disease, which prompted efforts to identify additional genetic defects in MPN linked to cytokine signaling pathways. The function of the cytoplasmic tyrosine kinase Jak2 was found to be crucial for hematopoietic signaling, since it mediates cytokine receptor signaling for erythropoietin, thrombopoietin, interleukin-3, granulocyte colony-stimulating factor, and granulocyte-macrophage colony-stimulating factor [45]. The discovery of JAK2-V617F also strengthened the concept of relatedness of the MPN entities. It became clear that although the MPN entities have different phenotypes, they are still closely connected. William Dameshek's hypothesis of a common origin for the chronic myeloid disorders [46], originally based on observations of certain overlaps between the hyperproliferating cell types and on shared clinical features and complications, were subsequently supported by the shared genetic basis.

Occurrence of JAK2-V617F at high frequencies is restricted to PV (in 95% or patients), ET (50-60%) and PMF (50-60%), although it can be found at lower frequencies also in AML (5%), MDS (3%), CMML (6%), atypical myeloproliferative disorders (20%), HES (1%) and SM (6%) [30, 47-58]. It is still unclear how one mutation can lead to several distinct phenotypes. It has been suggested that it is the dose of mutant *Jak2* protein that determines the disease phenotype. Specifically, a JAK2-V617F transgene in a mouse model resulted in thrombocythemia when expressed at low levels, and polycythemia when highly overexpressed [59]. Another hypothesis proposing that it is instead genetic factors collaborating with JAK2-V617F that leads to distinct phenotypes is supported by a bone marrow transplant model in which expression of JAK2-V617F induced erythrocytosis with mild leukocytosis in C57Bl/6, whereas Balb/c mice developed erythrocytosis with increased leukocyte count and bone marrow fibrosis [60]. Genetic factors contributing to the phenotype might be present in the germ line, as in the mouse transplant model, but alternatively not yet identified somatic mutations may collaborate with JAK2-V617F to modify the disease phenotype. Known somatic mutations are unlikely to be involved in the disease phenotype

after the acquisition of JAK2-V617F, as none of those occurring together with JAK2-V617F cluster with any one particular MPN entity. However, a low JAK2-V617F mutational burden may be involved in the phenotypic modulation of MPN, perhaps in combination with other factors.

1.2.2. Other oncogenic mutations

Following the discovery of JAK2-V617F, the JAK2-V617F negative patients were subjected to a search for new mutations in the entire *JAK2* gene, the other JAK family members (*JAK1*, *JAK3* and *TYK2*) and the *STAT* genes, which are *JAK2* effectors. Although genes such as *JAK3* are known to be mutated in leukemia [61-65], no other *JAK* family members were found to be mutated in MPN. Instead, various mutations within exon 12 of the *JAK2* gene were identified in JAK2-V617F-negative patients [33, 34]. Similarly to JAK2-V617F in exon 14, exon 12 mutations are thought to inactivate the JH2 pseudokinase domain of Jak2, a domain with negative autoregulatory properties, resulting in a gain-of-function of the mutant Jak2 protein [64, 66].

Upstream of the JAK-STAT pathway, different somatic mutations were found in exon 10 of the *MPL* gene [36, 37, 67]. Binding of thrombopoietin to its receptor Mpl regulates maturation of megakaryocytes and platelet production by stimulating proliferation through activation of the JAK-STAT pathway [68]. MPL-W515L and –W515K mutations are early, stem cell derived events [69]. So far, they have only been observed in PMF and ET, but not in PV patients. Their frequencies are about 5% in PMF and, depending on the patient cohort, between 1 and 9% in ET [37, 67, 70]. Structurally, the *MPL* codon 515 mutations are responsible for an exchange of crucial amino acids in the juxtamembrane region of the protein by substituting either leucine or lysine for tryptophan. The functional characterization of the mutant protein suggested an impaired function of an autoinhibitory region, causing receptor activation in the absence of the ligand thrombopoietin [71]. Ectopic expression of the MPL-W515L allele resulted in cytokine-independent growth of both human UT7 and murine 32D and Ba/F3 cell lines, mediated by constitutive phosphorylation of Jak2, Stat3, Stat5, Erk and Akt [36]. In a mouse

bone marrow transplant model, expression of the mutant allele in the bone marrow resulted in an MPN-like phenotype with thrombocytosis, splenomegaly, splenic infarction and reduced life expectancy [36]. Investigations following the identification of the codon 515 mutations in MPL exon 10 resulted in the identification of rarer mutations in the same exon (MPL-S505N, MPL-A506T and MPL-A519T) and other *MPL* exons (S204F, Y591T, S204P), some of which remain to be confirmed and further characterized [72-74].

1.2.3. Loss of function of the tumor suppressor TET2

Another recently identified defect present in a substantial proportion of MPN patients are genetic alterations in the *TET2* gene, a member of the Ten-Eleven-Tanslocation (TET) family [39]. In addition to MPN, *TET2* mutations are found in various myeloid malignancies such as myelodysplastic syndromes (MDS) (19%), acute myeloid leukemia (AML) (24%), and CMML (22%) [39, 40, 75, 76]. Follow up studies confirmed the *TET2* mutation frequencies [40, 77, 78]. In MPN, *TET2* is mutated in 13% of all cases with the highest frequency in PMF (17%), followed by PV (16%) and ET (5%) [78] (Table 1). *TET2* loss-of-function can be caused by larger deletions containing the *TET2* gene as well as by mutations within *TET2*, such as amino acid substitutions, frame shifts generating stop codons and in-frame deletions, which are spread out along the entire coding region of *TET2* [79]. The *TET2* alterations are mostly biallelic, although there are still cases where an intact *TET2* allele combined with a deleted allele were observed, suggesting haploinsufficiency can still cause disease [39].

Interestingly, *TET2* expression has been found to be downregulated in granulocytes from MDS patients, independently from their *TET2* mutational status, providing some evidence for a higher frequency of impaired *Tet2* function through deregulation of transcription or epigenetic mechanisms [75]. Not much is known regarding how Tet2 contributes to normal and malignant hematopoiesis. Evidence for a role for Tet2 in epigenetic gene regulation comes from studies on another Ten-Eleven-Tanslocation family member, Tet1, which has been shown to catalyze the conversion of 5-methylcytosine in DNA to 5-hydroxymethylcytosine

(Figure 1.2.3.) [80]. However, the role of Tet2 in regulating hematopoiesis needs further investigation.
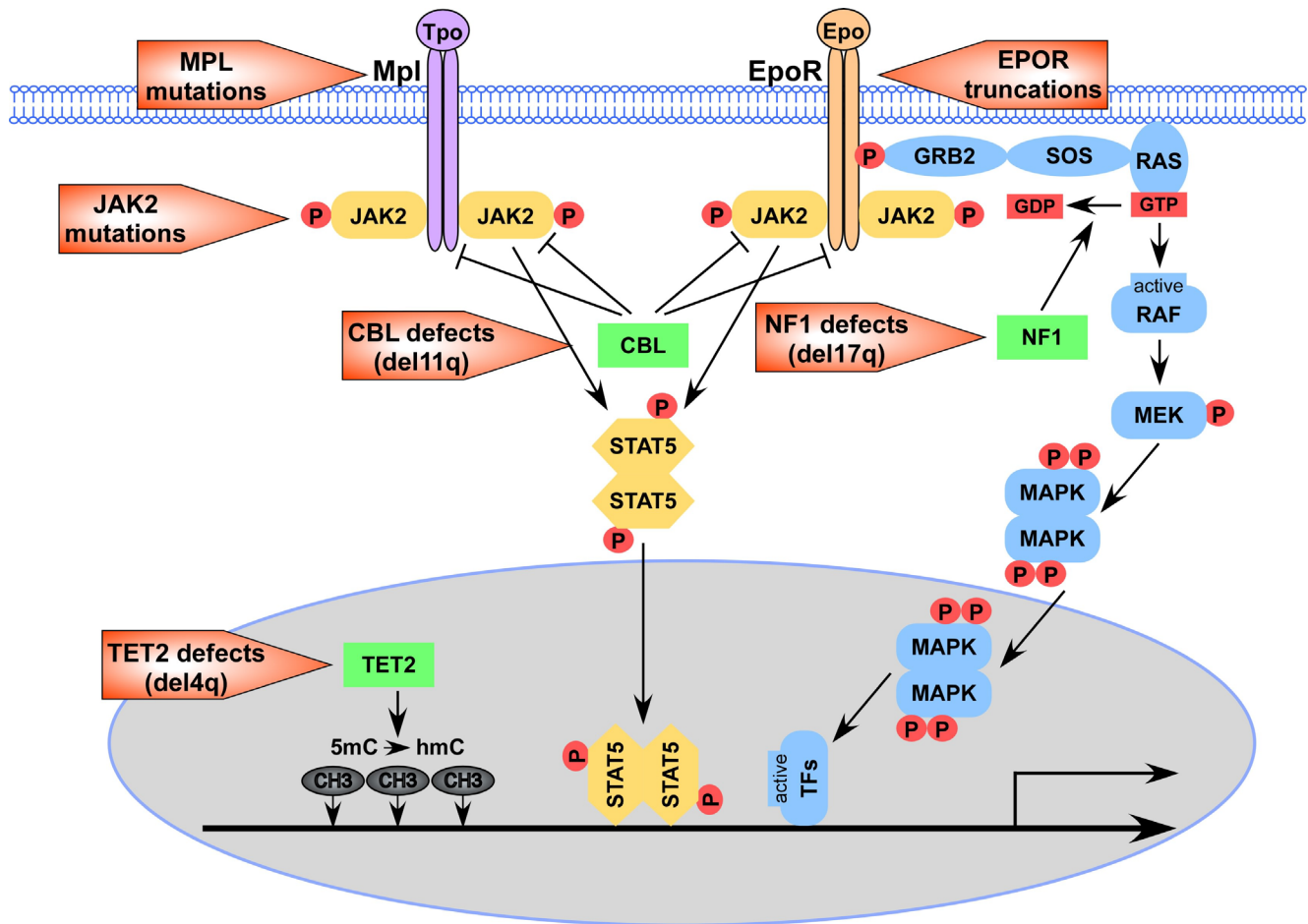
Figure 1.2.3.: Mechanisms and pathways targeted by mutations in MPN.
Schematic diagram of pathways involved in MPN pathogenesis. Red boxes summarize germ line and somatic mutations in MPN and MPN-like phenotypes. Clonal advantage based on cytokine hypersensitivity can be triggered by genetic defects directly targeting cytokine receptors, such as MPL mutations and EPO-R C-terminal truncations, as well as mutations affecting elements of downstream signaling cascades. Defects identified so far in MPN predominantly activate the JAK-STAT and the mitogen-activated protein kinase (MAPK) pathways. Gain of function mutations in JAK2 (JAK2-V617F and JAK2 exon 12 mutations) directly affect signal transduction, whereas loss of function mutations in CBL and NF1 intervene indirectly. The ubiquitin ligase CBL regulates the degradation of surface receptors and JAK2. NF1, a GTPase activating protein decreases signal potential of Ras, an important proto-oncogene in the MAPK pathway. Besides defects in cytokine signal transduction, mutations potentially directly affecting gene transcription have been found in TET2. TET2 might be involved in epigenetic transcriptional regulation by enzymatically catalyzing the conversion of 5-methylcytosine to 5-hydroxymethylcytosine, as shown for another TET family member TET1.

1.2.4. CBL mutations – defects in a complex regulator of hematopoiesis

Similar to TET2 , the recently identified mutations in CBL are not restricted to classical MPN, but can also be found in JMML (10-15%), CMML (13%), atypical aCML (8%) and HES/CEL (1%) [38, 81-83]. The frequencies of CBL mutations in classical MPN remain to be determined, however current studies hint that it is relatively rare (up to 2% in all MPN) [38]. CBL defects tend to associate with advanced disease state and poor prognosis [38]. The first reports of CBL mutations in human disease were in acute myeloid leukemia (AML) [84, 85]. The CBL mutations found in myeloid diseases are heterogeneous, including missense mutations, deletions, nonsense mutations and splice site alterations, most of them clustering around exons 8 and 9, which encode the linker and RING finger domains of the protein, both crucial for the function of this E3 ubiquitin ligase. Functional CBL attaches a ubiquitin molecule to growth-factor receptors and other cellular proteins and thereby targets them for degradation. Initial results from studies looking at the consequences of mutant CBL expression on JAK-STAT revealed aberrant STAT5 phosphorylation, pointing to a regulatory role of CBL in degradation of proteins required for JAK-STAT pathway activation.

In addition to the impact of CBL on cytokine receptor stability and regulation of the JAK-STAT pathway, there is evidence suggesting Cbl is a regulator of Ras trafficking [86]. The Ras proto-oncogenes are small GTPases that are involved in cellular signal transduction by activating signaling pathways such as the mitogen-activated protein kinase (MAPK) cascade, resulting an a cellular response on transcriptional level. In addition to JAK-STAT signaling, the MAPK pathway provides a parallel pathway of signal transmission from receptor tyrosine kinases [87]. Ras signaling links the Cbl mutations to another prominent defect in myeloid disorders, namely NF1 mutations. NF1 codes for the neurofibromin protein, a GTPase activating protein involved in Ras deactivation by accelerating Ras-associated hydrolysis of guanosine triphosphate into guanosine diphosphate and phosphate. Until recently, NF1 mutations had been reported only in CMML at a frequency of 15% [88]. In a recent report, rare NF1 gene deletions and a mutation were detected in a few MPN cases [89], placing the MAPK pathway in

an important position along with the JAK-STAT pathway, in MPN pathogenesis (Figure 1.2.3).

Cbl has clear properties of a classical tumor suppressor, with respect to both functional and genetic features. Specifically, the CBL mutated clone shows increased proliferative response with loss of function, even in the heterozygous state, although it still tends to become homozygous by undergoing UPD [81]. Cbl mutants do not have E3 ubiquitin ligase activity, but act as dominant negatives by inhibiting proteins within the Cbl family. However, Cbl mutants also show gain-of-function properties in the absence of wild-type Cbl, augmenting the cytokine hypersensitivity of the loss-of-function phenotype to a broader spectrum of cytokines, indicating oncogene-like characteristics of Cbl [81]. As a regulator of protein abundance more distant to JAK-STAT than the previously described prominent mutations, Cbl might control pleiotropic elements interacting with JAK-STAT, regulating the pathway in both directions [90]. One could summarize CBL defects as gain-of-function mutations of a tumor suppressor. It seems that wild-type Cbl has tumor suppressor functions, whereas mutant Cbl acts as an oncogene, redefining the strictly separated definition of these elements in cancer biology.

1.2.5. Cytogenetic aberrations in MPN

The oncogenic and tumor suppressor mutations present at substantial frequencies suggests that the MPN clone is both highly complex and heterogeneous. In addition, recent reports of newly identified cytogenetic aberrations reveal a large number of candidate genes for MPN pathogenesis. During the last few years, conventional metaphase cytogenetics has been complemented and partly replaced by microarray-based detection of loss of heterozygosity (LOH) using single nucleotide polymorphism (SNP) genotyping. With this method, screening for genetic aberrations can be performed with a much higher resolution, depending on the amount and distribution of probes on the microarray. Another crucial advantage over metaphase cytogenetics is the detection of copy number neutral LOH, which indicates an acquired uniparental disomy (UPD). UPD occurs through mitotic recombination and can

transform pro-proliferative defects (loss of functions of tumor suppressors and gain of function of oncogenes) from a heterozygous to a homozygous state [91]. As many genetic defects are shared between myeloid malignancies, recent studies using the SNP genotyping approach for the identification of new cytogenetic lesions report on combined patient cohorts, consisting of MPN, MDS, AML and rare non-classic MPNs such as CMML and JMML [75, 81, 82, 92-96]. Whole genome scans in these large combined cohorts generated a view of the variety of chromosomal aberrations throughout the genome, revealing clonal genomic abnormalities in up to 75% of patients with myeloid malignancies [96]. A large number of chromosomal aberrations are recurrent, most prominently UPDs on 1p, 1q, 4q, 7q, 11p, 11q, 14q, 17p and 21q, providing additional evidence for a direct involvement in pathogenesis [81]. Remarkably, 7q UPD was detected primarily in high risk patients confirming chromosome 7 defects and monosomy 7 as prominent markers for poor disease outcome in MDS and AML [92, 97].

The aim of high resolution mapping of cytogenetic lesions is the identification of single gene defects. The first successful result of this approach was the mapping of defects in *TET2* [38, 39, 75] and *CBL* [38, 81-83]. Interestingly, the well known genetic lesions, such as deletions on the long arm of chromosome 13 (del13q) and 20 (del20q) [20] are still relatively large and also the overlap of the recurrent events, the common deleted region, contains large number of genes. This might indicate either that there are several disease relevant genes within one deleted region or the mechanism generating the chromosomal lesion does not allow smaller deletions to occur.

1.3. Hereditary factors in MPN

The increasing number of known genetic defects in MPN as well as the observations of multiple acquisitions of oncogenic mutations in the same patient [98, 99] raises the question on the origin of genetic instability in MPN. Recent findings support a model of a random acquisition of the genetic lesions in the MPN clone [16]. Fixed sequential relationships between mutations could not be defined as all known defects seem to be acquired in a random order. However, none of the somatic lesions found in MPN to date can explain genetic instability.

Although JAK2-V617F positive cells have been shown to have increased genetic instability [100] many genetic lesions in patients are detected outside of the JAK2-V617F positive clone [17, 98, 99, 101] . One way to get closer to identifying the origin of genetic instability in MPN is by studying familial MPN. Familial MPN is characterized by an autosomal dominant inheritance with incomplete penetrance [20, 102]. The three MPN entities appear variably in a single affected family and all oncogenic mutations of *JAK2*, MPL and *TET2* detected in these families were somatically acquired [103-105]. Thus, in familial MPN there is a germ line predisposition to acquire somatic mutations that drive a clonal disease in the affected pedigree members. This predisposition is also the likely cause of low penetrance observed in the pedigrees. The main conclusion from familial MPN studies is, that germ line factors exist that predispose carriers to somatic mutagenesis. The only exception reported so far is the MPL-S505N mutation present in sporadic MPN [67] and in a family with autosomal dominant thrombocytosis [106]. The absence of germ line *JAK2* mutations could be explained by an incompatibility of the defect with embryogenesis, as supported by studies in a JAK2-V617F mouse model [59].

The concept of germ line disease initiating events in MPN changed dramatically in 2009, when three groups independently reported on a *JAK2* haplotype that preferentially associated with the presence of the JAK2-V617F mutation [99, 107, 108]. The GGCC haplotype (also known as 46/1) is a 330 kilobase chromosomal segment that includes the entire *JAK2* gene and two additional genes centromeric to *JAK2*. Individuals homozygous for the GGCC haplotype have an approximately five times higher risk of acquiring MPN than individuals not carrying the GGCC haplotype [99]. Two different hypothesis try to explain this strong interaction between somatic and germ line features at the *JAK2* locus. The "fertile ground" hypothesis assumes a physiological advantage for the mutation in mediating properties to grow out if acquired on the GGCC haplotype [107], whereas the hypothesis of "differential mutability" suggests a difference in mutagenesis rates between the two common *JAK2* haplotypes (Table 1.3.) [99].

Table 1.3. Comparison of the two models explaining the common *JAK2* haplotype

	Fertile ground model	Differential mutability model
Definition	Clones acquiring the mutation on the GGCC haplotype have a selective advantage over clones acquiring the mutation on the TCTT haplotype.	The GGCC haplotype mutates more frequently than the TCTT haplotype.
Pro	MPL mutations occur more frequently in GGCC haplotype carriers	There are examples of APC and TP53 mutations associated with specific haplotypes
Contra	No evidence for JAK2 non-synonymous SNPs on the GGCC haplotype No evidence for a different mRNA expression pattern	Strong evidence of differential mutability is still absent
To be clarified…	Can neighboring genes (INSL4 and INSL6) genes play a role? Can the GGCC haplotype exert a trans-regulatory effect on other genes? Is the JAK2-V617F burden higher in GGCC carriers?	Can haplotypes differ in replication fidelity or DNA repair efficiency?

JAK2 exon 12 mutations were shown to also be preferentially acquired on the GGCC haplotype [109]. However, the relationship of other mutations such as MPL, *TET2* and *CBL* with the haplotype still remains to be investigated. Interestingly, recent correlation studies report on statistically significant effects of the GGCC haplotype on survival in PMF and even susceptibility for devolving ET independent of *JAK2* mutational status [110, 111], indicating an even higher complexity of the phenomenon.

2. HYPOTHESIS

Besides oncogenic mutations such as JAK2-V617F, cytogenetic aberrations are prominent genetic defects in the MPN clone. Whereas chromosomal gains and copy number alteration neutral acquired uniparental disomies (UPDs) are thought to amplify gain-of-function mutations in oncogenes or loss-of function mutations in tumor suppressor genes, chromosomal deletions may directly lead to haploinsufficiency or even total loss of tumor suppressors. During the last decades, classical cytogenetics revealed abnormal karyotypes in MPN at frequences ranging from 10–15% in PV and 35% in PMF [11, 20, 112-114]. Beyond the most frequent ones are deletions on chromosome 20q (del20q), present in the bone marrow of up to 10% of all MPN patients [115-117]. Del20q is not restricted to MPN, it can be found in other myeloid malignancies such as myelodysplastic syndrome (4%) [118] or acute myeloid leukemia (3%) [119], and therefore represents a prominent candidate region for a common tumor suppressor driving clonal expansion in the myeloid compartment if inactivated. In the last years, microarray technologies made it possible to detect cytogenetic aberrations by SNP genotyping and copy number analysis at high resolution. As a basis for all our projects we run the complete MPN patient cohort of the Medical University Vienna (380 individuals) on Affymetrix 6.0 microarrays, which opened us a view onto various cytogenetic aberrations and confirming del20q as one of the most frequent recurrent deletions in MPN (Figure 2.).

Common deleted regions (CDRs), representing the stretch of DNA absent in all patients positive for a specific deletion, are thought to harbor the relevant tumor suppressor(s). Intensive del20q CDR mapping in large patient cohorts resulted in several CDRs of different sizes for MPN, MDS and AML [120-124], the smallest being a combined MPN/MDS CDR of 2 mega-basepairs (Mb), encompassing 9 genes [115]. However, to date, it was not possible to identify a gene mutation within the CDR that is functionally linked to the expansion of the del20q clone. Further, the role of del20q in the hierarchy of genetic defects in the MPN clone especially in context with JAK2-V617F is still unclear. Studies in patients with JAK2-V617F and del20q suggested that del20q preceded the acquisition of JAK2-V617F [125], however, this remains to be evaluated.

Having access to three different patient cohorts, we aimed to investigate the role of del20q in the clonal evolution on progenitor cell level and characterize the cohorts for the frequencies of del20q. We further aimed to assemble an MPN-specific CDR and identify the tumor suppressor(s) within this CDR by mimicking deletion-caused haploinsufficiency using different RNAi strategies.
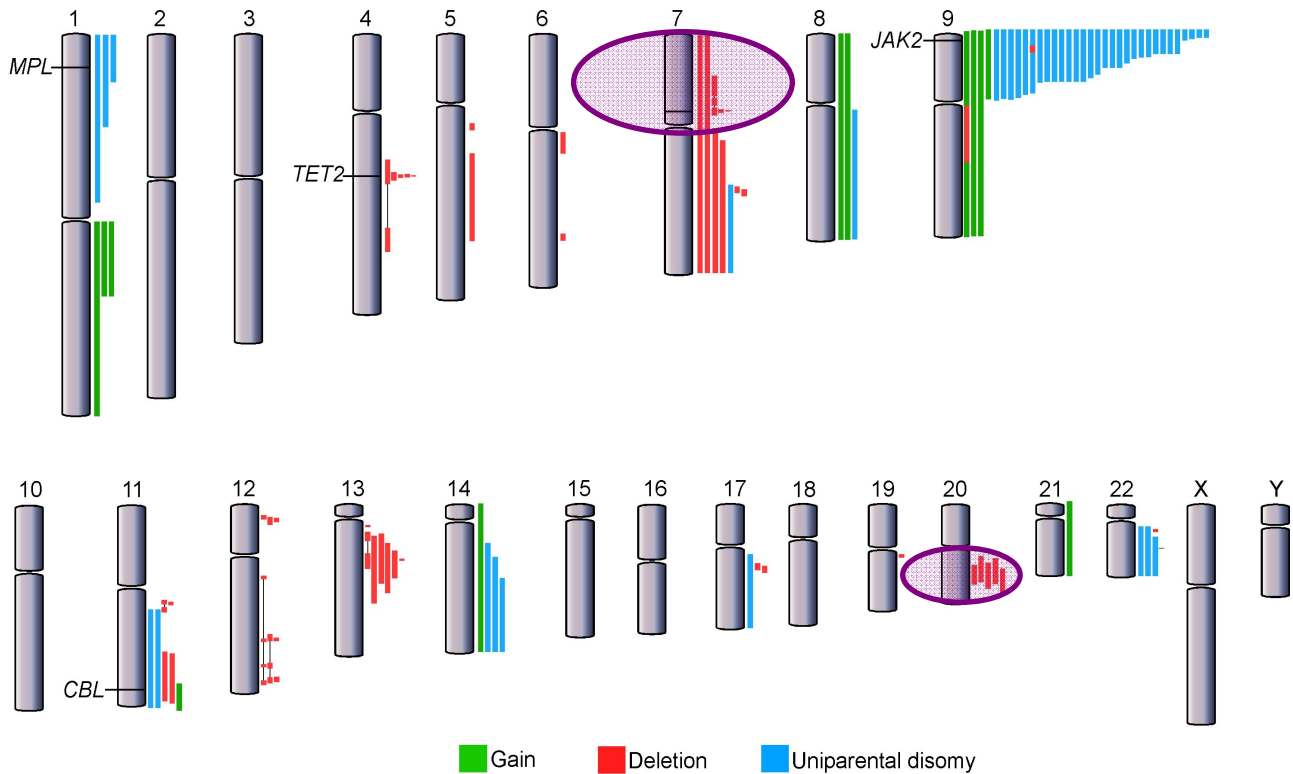
Figure 2. Roadmap to MPN genetics. Analysis of the Viennese MPN patient cohort (380 individuals) revealed a variety of chromosomal aberrations, gains (green), deletions (red) and UPDs (blue), several of them occurring recurrently. The most frequent cytogenetic aberration is UPD on chromosome 9p, known to be responsible for the transition of heterozygous JAK2-V617F to the homozygous state. Further recurrent genetic lesions are targeting previous reported and well described genetic lesions such as MPL mutations as well as TET2 and CBL defects. Del20q (highlighted in purple) was confirmed to be a frequent event also in the Viennese chronic phase MPN patient cohort. Del7p events (highlighted in purple) were identified and mapped specifically in patients transformed to post-MPN leukemia.

Del20q is a frequent defect in MPN generally observed in the chronic phase of the disease. However, a major risk factor in MPN is transformation from the chronic phase MPN to acute myeloid leukemia (AML) is [126]. The genetic changes associated with post-MPN leukemic

transformation are poorly understood. Although *JAK2* mutations were suspected to be linked with post-MPN leukemic transformation, clinical studies have failed to demonstrate a significant association [51, 127]. Moreover, in JAK2-V617F positive patients, the leukemic transformation frequently occurs on a JAK2-V617F negative background suggesting the existence of JAK2-V617F-dependent and -independent pathways of transformation [128, 129]. In a recent study a significant clustering of *TET2* mutations with post-MPN leukemia was reported, however, *TET2* defects were not specific for the transformation [130]. A specific link to post-MPN transformation was provided by the identification of somatic mutations in the *IDH1* and *IDH2* genes[131], the former proven to be strongly associated with normal karyotype[132].

To gain further insights into the genetic basis of the transition from chronic phase MPN to post-MPN leukemia, we aimed to analyze transformed MPN patients for chromosomal aberrations using high-resolution microarray karyotyping and examine cytogenetic defects for specific association with post-MPN leukemia. A recurrent deletion on chromosome 7 with a CDR comprising a single gene happened to show this association (Figure 2). We further aimed to evaluate the temporal role of this single gene defect in the evolution of the malignant clone and to functionally characterize the defect and its consequences.

3. METHODS

3.1. Patient cohort, cell sorting, DNA isolation, JAK2 and MPL mutation analysis

A total of 480 patients from Vienna (Austria), 252 from Pavia (Italy) and 90 from Brno (Czech Republic) were included in this study. The study was approved by local ethics committees. Peripheral blood samples were collected after written informed consent of the patients. Granulocytes and peripheral blood mononuclear cells (PB-MNCs) were isolated using density gradient centrifugation. Blasts were separated from the PB-MNC fraction by magnetic cell sorting (Miltenyi Biotech) for markers present on the leukemic blasts. Genomic DNA was isolated applying a standard protocol. Allele-specific PCR for the JAK2-V617F mutational analysis was carried out using a previously described protocol [125]. Allele-specific PCR for the MPL-W515L was performed based on the same methodology, but with the sense primer MPL515-F GTTTCTTCCGAAGTCTGACCCTTTTTG, and the 5'-6-carboxyfluorescein labeled antisense primers MPL515-RG GTAGTGTGCAGGAAACTGCC, and MPL515-RA AAAGTAGTGTGCAGGAAACTGCA using 62.2^{o}C annealing temperature.

3.2. Microarray genotyping, loss of heterozygosity and copy number analysis

Genomic DNA from peripheral blood granulocytes was used for microarray genotyping. Genotyping was done using the Genome-Wide Human SNP 6.0 arrays (Affymetrix) according to the manufacturer's protocols. Evaluation of copy number and loss of heterozygosity (LOH) was performed using the Genotyping Console version 3.0.2 software (Affymetrix). Screening of patients for LOH in the *IKZF1* gene locus was done by comparing SNP genotypes of granulocytes (clonal myeloid cells) with genotypes of buccal mucosa or T-cells (control polyclonal tissue) in each patient. Only patients heterozygous in the control tissue were informative for the LOH analysis. Two single nucleotide polymorphisms (rs6421315 and rs7806674) located in the *IKZF1* locus with an average heterozygosity frequency of over 0.4 were used for LOH analysis. Since the two SNPs are in linkage disequilibrium (D'=0.05 in the HapMap CEU population) the overall informativity of the LOH analysis with these two markers was 71%. Genotyping for rs6421315 and rs7806674 was performed using commercial Taqman assays C__3121415_10 and C____358427_10

(Applied Biosystems). PCR and genotyping was done using the 7900HT Real Time PCR System (Applied Biosystems) as recommended by the manufacturer. We also performed a real-time PCR based copy number measurement using the commercially available assay Hs00805103_cn (Applied Biosystems) to validate the presence of copy number changes of *IKZF1* detected by microarray and LOH analyses and to analyze samples for which no control paired tissue was available. The copy number assay was performed as recommended by the manufacturer.

3.3. Microsatellite PCR

Microsatellite PCR based LOH screening within the del20q CDR was performed as previously described [29] using primer sequences and labeling as listed in table 3.3..

Table 3.3.: Primers used for microsatellite based LOH screening

Microsatellite	Forward Primer	Reverse Primer	length
D20S858	FAM-TGGGTGATACAGACACAGTGAC	gtttctTCTCCAAGTAGTTGACAGATTTCC	168-208
D20S899	gtttcttAGAAATGCTTTCAGAGCC	HEX-GTCAACATGAATAATACCATCTTAG	175-187
D20S96	HEX-CACTGCAACTCTAACCTGGG	gtttcttCCTGTATGCTGCATTTCCTG	99-133
D20S861	FAM-TCATGTCATTCAGTCTGACTCTA	GTTTCTTCACATTTTTTACAGGAATTATTG	90-102

3.4. Sequencing

Sequence analysis of the 7 coding *IKZF1* exons (including exon junctions 70-150 bases pairs 5' and 3' from each junction) as well as JAK2-exon14 was performed using the BigDye Terminator v3.1 Cycle Sequencing chemistry and 3130xl Genetic Analyzer (Applied Biosystems). Primer sequences for PCR and sequencing are shown in Table 3.4.

Table 3.4. Primer sequences used for IKZF1 exon sequencing

	Forward	Reverse
Exon1	AGCATAGGGGTTCTTTATCTCTC	AATAGCCCCTATTCCTCCCC
Exon2	CTCATGCCACCCTCTCAAG	TATGCCAGTTGAGGGAACAC
Exon3	TGCTCTCCCCTTGGTATTTG	TACCACTTGGAACCAATCGC
Exon4	TCTATCAAACCTGCAGCCG	ACTCAGGGTTAGCCAGCAAG
Exon5	CCAAGTCCGTAACAGTTTTAGC	AACTTCCCTCCCTCCTAGCC
Exon6	AGGGCCTGGCTCTTGTAGG	TTTCCCTTTCTTCCACCCTC
Exon7_1	CCTCCCCGGTTGTAGATTTC	GCTCCTCCTTGAGCGACAG
Exon7_2	CTCCAAGGCCAAGTTGGTG	TCCAGTCCAGTCTATGCTGC

Exon numbering was based on Mullighan et al., Nature 453:110-114, 2008.

3.5. Genotyping of hematopoietic progenitors

Peripheral blood mononuclear cells were isolated using standard density gradient centrifugation. Cells were plated in the H4431 methylcellulose media at a density of 10^5 cells/ml (StemCell Technologies). After culturing for 14 days, colony forming units (CFUs) representing burst forming units-erythroid (BFU-E) and granulocytic-monocytic colony forming units (CFU-GM) were harvested and DNA was extracted as previously described [99]. Each CFU was assayed for a maximum the 4 clonal markers JAK2-V617F, del13q and del7p and del20q. JAK2-V617F mutational status was determined by sequence analysis of JAK2-exon14 as previously described [29]. Deletions on chromosome 13q were detected by loss of heterozygosity analysis using microsatellite PCR for *D13S153*. Deletions on 7p were detected by TaqMan LOH analysis using the commercial TaqMan assay C__3121415_10 (Applied Biosystems). Del20q was detected by microsatellite PCR as described in Methods 3.3.

3.6. Vectors, lentiviral packaging – IKZF1 knock down

Three shRNA constructs targeting the *Ikzf1* transcript and one random oligonucleotide control, not homologous to any mouse transcripts, were designed for ligation into pLKO.2 lentiviral vector (kindly provided by Sebastian Nijman), which carries the puromycin-resistance gene and drives shRNA expression from a human U6 promoter [133]. All shRNA constructs were sequence verified after cloning. Three different constructs targeting the *Ikzf1* mRNA were tested in duplicates for knock-down efficiency against the random oligonucleotide in the cytokine dependent murine pro-B cell line Ba/F3-EpoR (Ba/F3 cells expressing the erythropoietin receptor) as shown in Figure 4.1.7.1. The target sequences of the constructs are listed in Table 3.6.

Table 3.6. Target sequences for shRNAs within the Ikzf1 mRNA.

Construct	Target sequence 5'-3'	mRNA target in mouse
IKZF1-shRNA_1	AGAGCGATGCCACAACTAC	Ikzf1
IKZF1-shRNA_2	GATAGCTGGTTATGCCTCC	Ikzf1
IKZF1-shRNA_3	TAGTGGCTTCAGGAGCTCT	Ikzf1
random control	AGGCTGCTTGCACGATCTA	none

The shRNA performing best in mimicking haploinsufficiency (mRNA knock-down to 50%) was further tested in four independent knock-down experiments in murine lin⁻ mouse bone marrow cells (Figure 4.1.7.2.A) and consequently used for the functional experiments. TaqMan Gene expression assays Mm01187878_m1 for *Ikzf1* and Mm01545399_m1 for *Hprt1* as reference were used for determination of knock-down efficiency (Applied Biosystems). Viral packaging and preparation of viral supernatant was performed in HEK293T cells as described elsewhere [133, 134].

3.7. *Primary cell isolation and viral transduction*

Bone marrow was isolated from tibia and femurs of C57BL/6 mice. After red blood cell lysis, bone marrow cells were cultured in StemPro-34 serum free medium with nutrient supplement (Invitrogen) supplied with each 10ng/ml recombinant SCF, Flt3-L, GM-CSF, IL-3 and IL-6 (R&D Systems). The cells were depleted for adherent cells by incubation for 24 hours at a density of 10^6 cells/ml, followed by magnetic sorting of progenitor cells using the lineage cell depletion kit (CD2, CD3, CD11b, CD14, CD15, CD16, CD19, CD56, CD123, and CD235a) (Miltenyi Biotech). Viral supernatant was applied on lin⁻ mouse bone marrow cells for 20 hours in a volume ratio of 1:1 with supplemented media. Viral transduction was followed by selection on puromycin (2.5 ug/ml) for 4 days.

3.8. *Proliferation assay – primary cells*

Lentivirally transduced cells with shRNA constructs targeting the *Ikzf1* transcript and a random oligonucleotide control were assayed for proliferation capacity using a colorimetric assay. Cell densities of 2500 and 5000 cells per well were plated in triplicates in a 96-well plates on a dilution series of the cytokine mix (50 to 0 ng/ml each) of mouse SCF, Flt3-L, GM-CSF, IL-3 and IL-6 (R&D Systems). Proliferation was determined using the Cell Proliferation Kit II XTT (Roche) on days 5 and 4 after plating for the plating densities 2500 and 5000, respectively.

3.9. Intracellular pStat5 and Stat5 mRNA assays

Lentivirally transduced, puromycin selected lin⁻ mouse bone marrow cells were starved in StemPro-34 serum free medium (Invitrogen) with or without nutrient supplement for 20 hours. Starved cells were counted and aliquots of 1.5×10^5 cells were used for subsequent experimental processing. Both Ikzf1 knock-down and control cells were incubated with three different concentrations of IL-3 (0 ng/ml baseline, 0.025 ng/ml, 0.05 ng/ml) for 10 minutes at 37°C. Phosophorylated Stat5 level was determined using the BD Phosflow reagents (BD Biosciences). Following the IL-3 incubation cells incubation cells were processed in Fix Buffer I, Perm Buffer III and Stain Buffer according to the manufacturer's protocols (BD Biosciences). Intracellular pStat5 was stained using 10 µl the PE Mouse Anti-Stat5 (pY694) antibody in 100 µl total cell suspension for 2 hours, followed by two washing steps and subsequent FACS analysis on a FACSCalibur instrument using the BD CellQuest software (BD Biosciences). An aliquot of IL-3 stimulated cells were processed for RNA isolation and Stat5 mRNA level was determined using the TaqMan Gene expression assays Mm00839861_m1 for *Stat5a* and Mm01545399_m1 for *Hprt1* as reference (Applied Biosystems).

3.10. Gene expression profiling

For human expression profiling, chord blood collected from 5 donors was separated into granulocytes and mononuclear cells (MNCs) using gradient centrifugation. MNCs were sorted into CD34+ and CD34- fractions by magnetic cell sorting (Miltenyi Biotech) for CD34. For murine expression profiling, bone marrow isolated from femur and tibia of three C57/Bl6 mice was sorted into Lineage marker negative (lin-) and positive (lin+) fractions by magnetic cell sorting using the lineage cell depletion kit (CD2, CD3, CD11b, CD14, CD15, CD16, CD19, CD56, CD123, and CD235a) (Miltenyi Biotech). Gene expression was determined using TaqMan Assays listed in table 3.10. for mouse and human del20q target genes, using HPRT1 assays Hs99999909_m1 and Mm01545399_m, respectively, for normalization. Real time PCR was done using the 7900HT Real Time PCR System (Applied Biosystems) as recommended by the manufacturer.

Table 3.10. TaqMan Assays used for del20q gene expression profiling

human TaqMan assays		mouse TaqMan assas	
MAFB	Hs00534343_s1	Mafb	Mm00627481_s1
TOP1	Hs00243257_m1	Top1	Mm00493749_m1
PLCG1	Hs00234046_m1	Plcg1	Mm01247293_m1
ZHX3	Hs00390053_m1	Zhx3	Mm00770117_m1
LPIN3	Hs01037256_g1	Lpin3	Mm00499085_m1
EMILIN3	Hs01377845_m1	Emilin3	Mm00812794_m1
CHD6	Hs00260089_m1	Chd6	Mm00557576_m1
PTPRT	Hs00179247_m1	Ptprt	Mm00451782_m1
SFRS6	Hs00740177_g1	Sfrs6	Mm00471475_m1
L3MBTL	Hs01096637_g1	L3mbtl	Mm01239972_g1
SGK2	Hs00367639_m1	Sgk2	Mm00449845_m1
IFT52	Hs00211198_m1	Ift52	Mm00549112_m1
MYBL2	Hs00231158_m1	Mybl2	Mm00485340_m1
GTSF1L	Hs00746221_s1	Gtsf1	Mm01298416_m1
TOX2	Hs00262775_m1	Tox2	Mm01247701_m1
JPH2	Hs00375310_m1	Jph2	Mm00517621_m1

3.11. Stable transfections – Amaxa delivery of shRNA constructs to cell lines

UT7/TPO and Baf3/EPO cells were cultured in RPMI-1640 medium (Invitrogen) supplemented with 10% FCS (Invitrogen) and high concentrations of the essential cytokines (UT7/TPO: 20% of CM cell line supernatant, tested to be sufficient for maximal UT7/TPO growth; Baf3/EPO: 1 U/ml recombinant erythropoietin ERYPO, Janssen-Cilag). Stable knock-downs in UT7/TPO and Baf3/EPO cell lines were achieved using Amaxa (now Lonza) nucleofection of shRNA constructs cloned into the psiSTRIKE vector using the siSTRIKE™ U6 Hairpin Cloning System - Puromycine (Promega) according to the manufacturers instructions. The shRNA sequences were based on the Promega siRNA Target Designer. ShRNAs against human targets used in the primary del20q CDR screen in UT7/TPO as well mouse shRNAs targeting murine Mybl2 are listed in table 3.11. Two different shRNA constructs targeting one gene transcript were transfected if not indicated otherwise. For controls, an empty psiSTRIKE vector lacking the shRNA insert was transfected in the primary screen. In the validation steps, scrambled shRNA controls were used (Table 3.11). Cells

were selected on puromycin (1 ug/ml) for 4 days followed by measurement of knock-down efficiency and proliferation assay.

Table 3.11. shRNAs used for del20q CDR transcript knock-down. Sequences listed are 5' to 3' including the loop and extensions forming sticky ends for siSTRIKE cloning

SFRS6	shRNA_1	ACCGCAGTTGGCAAGATTTAAATTCAAGAGATTTAAATCTTGCCAACTGCTTTTTC
	shRNA_2	ACCGGATGGCACAGAAATAAATTTCAAGAGAATTTATTTCTGTGCCATCCTTTTTC
L3MBTL	shRNA_1	ACCGAGAAATATCTGGAAGAAATTCAAGAGATTTCTTCCAGATATTTCTCTTTTTC
	shRNA_2	ACCGATAAAGATCCACTTTGATTTCAAGAGAATCAAAGTGGATCTTTATCTTTTTC
IFT52	shRNA_1	ACCGTCTTGAACAGGGAAATTATTCAAGAGATAATTTCCCTGTTCAAGACTTTTTC
	shRNA_2	ACCGGAAGATTCAGAGCTTAAATTCAAGAGATTTAAGCTCTGAATCTTCCTTTTTC
MYBL2	shRNA_1	ACCGTGACCTGAGTAAATTTGATTCAAGAGATCAAATTTACTCAGGTCACTTTTTC
	shRNA_2	ACCGTCATCGAGCTGGTTAAGATTCAAGAGATCTTAACCAGCTCGATGACTTTTTC
GTSF1L	shRNA_1	ACCGTGCAATGCATCAGAATAATTCAAGAGATTATTCTGATGCATTGCACTTTTTC
	shRNA_2	ACCGGAGCCAGAAGCCTTTGAATTCAAGAGATTCAAAGGCTTCTGGCTCCTTTTTC
TOX2	shRNA_1	ACCGAACCCGAAGAAGAAGAAATTCAAGAGATTTCTTCTTCTTCGGGTTCTTTTTC
	shRNA_2	ACCGAGTCGGAAGTGCATTTCATTCAAGAGATGAAATGCACTTCCGACTCTTTTTC
MYBL2 - scrambled	scramb_1	ACCGTAACAGGCTAGAATGTTTTTCAAGAGAAAACATTCTAGCCTGTTACTTTTTC
	scramb_2	ACCGATGCCGCGATAGTTAGATTTCAAGAGAATCTAACTATCGCGGCATCTTTTTC
Mybl2 - mouse	shRNA_1	ACCGCTCAAGCGACAGAAGAAATTCAAGAGATTTCTTCTGTCGCTTGAGCTTTTTC
	shRNA_2	ACCGGACAATGCTGTGAAGAATTTCAAGAGAATTCTTCACAGCATTGTCCTTTTTC
Mybl2 - mouse scrambled	scramb_1	ACCGAGAGGCCAGCAAAAATCATTCAAGAGATGATTTTTGCTGGCCTCTCTTTTTC
	scramb_2	ACCGGATGTAAGACGGACAATTTTCAAGAGAAATTGTCCGTCTTACATCCTTTTTC

3.12. Transient transfections – Delivery of synthetic siRNAs to UT7/TPO

Transient knock-down of MYBL2 in UT7/TPO cells was performed by delivering a 5'FAM-labeled synthetic siRNA oligonucleotide (Sigma-Aldrich) and its corresponding scrambled oligonucleotide (sequences of both described elsewhere [135]) using HiPerFect Transfection Reagent (Quiagen). Parallel transfections of target and scrambled control siRNAs in a highly precise setup following the manufacturer's instructions allowed detection of almost equal transfection efficiency for both fractions using FACS analysis for fluorescent FAM.

3.13. Measurement knock-down efficiencies – Real Time PCR and Western Blotting

Knock-down experiments were validated by comparing the mRNA level of knock-down cells to the one from the control cells by Real Time PCR performed on a 7900HT Real Time PCR System (Applied Biosystems) as recommended by the manufacturer. TaqMan assays used for quantification are listed in Table 3.10. Each mRNA level was normalized by the mRNA

level of HPRT1 (TaqMan assays Hs99999909_m1 (human) and Mm01545399_m (mouse)). For one representative Mybl2 knock-down experiment in Baf3/EPO cells, we checked the comparability of the knock down on mRNA level and protein level by Western Blotting (Figure 4.2.4.3). Cell homogenate (100 µg) was separated by electrophoresis on a 10% SDS polyacrylamide -gel and transferred to polyvinylidene difluoride membranes. Antibodies specific for Mybl2 (H-115: sc-13028, Santa Cruz Biotechnology) and β-actin (Sigma-Aldrich) were used at dilutions of 1/8000 and 1/500, respectively. Immunoreactive proteins were detected by enhanced chemiluminescent protocol (GE Healthcare).

3.14. Proliferation assay – cell lines

Stably and transiently transfected cells knock-down and control cells were assayed for proliferation capacity using a colorimetric assay. Cell densities of 5000 (UT7/TPO) and 2000 cells per well were plated in triplicates in a 96-well plates on a dilution series of the appropriate cytokine (thrombopoietin for UT7/TPO and erythropoietin for Baf3/EPO). For thrombopoietin gradient, supernatant of the CM cell line was spiked into the regular media, whereas human recombinant erythropoietin (ERYPO, Janssen-Cilag) could be added in Units per ml (U/ml) as concentration was provided by the manufacturer. Proliferation was determined using the Cell Proliferation Kit II XTT (Roche) on days 6 and 5 after plating for UT7/TPO and Baf3/EPO, respectively.

3.15. Screen for del20q tumor supressors (pooled bar-coded shRNA setup)

Three to five shRNAs per gene were designed targeting the 16 genes within the extended del20q common deleted region (see 4.2.5.). The shRNA sequences were designed based on the iRNAi freeware and are listed in table 3.15. Annealed oligonucleotides were cloned into a pool of pLKO.2 lentiviral vectors comprising 100 different LUA tags (kindly provided by Sebastian Nijman), which could be later on read and quantified with the Luminex XMap Technology. Bacterial colonies were plated and colonies were picked, sequenced and prepped until each shRNA (Table 3.15) was present associated with a unique bar-code (Figure 3.15.A). All shRNA constructs were sequence verified after bacterial prep. The

pLKO.2 vector carries a puromycin-resistance gene and drives shRNA expression from a human U6 promoter [133]. After viral packaging and preparation of viral supernatant in HEK293T cells (described elsewhere [133, 134]), Baf3/EPO cells were transduced indepdently with the different constructs (Table 3.15) and additional 4 empty control constructs (bar code, but no shRNA insert) in a 96-well format. After 4 days of puromycine selection, cells were pooled, a baseline DNA sample was taken and the cell pool was passeged for 100 days in the presence of 0.08 U/ml and 1 U/ml recombinant erythropoietin ERYPO (Janssen-Cilag) (Figure 3.15.C). The experiment was performed in three biological replicates, independently handled form the viral transduction on. Cell aliquots were taken weekly for subsequent DNA isolation and Luminex relative quantification of the bar codes in the pool.

Table 3.15. shRNAs used for the pooled bar-coded knock down of del20q target genes.
Sequences listed are 5' to 3' and represent the 19-mer targeting the transcript

| Gene	shRNA	Sequence	Gene	shRNA	Sequence
Mafb	shRNA_1	CGACTTCGACCTTCTCAAG	L3mbtl	shRNA_1	GTAGTGGCCTAGACGTTGG
	shRNA_2	CGGTAGTGTGGAGGACCGC		shRNA_2	AGTGCGACCCCCTCACAGC
	shRNA_3	GGTAGCAGCAAGCTGAGTC		shRNA_3	GTGGACCATTGAAGAGGTC
	shRNA_4	GAAGTCAACCCAGGGCTGG		shRNA_4	AGGTTACAAGGAAGAGGAG
Top1	shRNA_1	GAGGAAGAGGATGGTAAAC	Sgk2	shRNA_1	GCGCAAGTCGGACGGAGCC
	shRNA_2	GTCCGACATGATAACAAGG		shRNA_2	CGTGGAAGGACCTGCTGAC
	shRNA_3	GAGAGCAAGTGGATGGGAA		shRNA_3	CATCTATTTGGACTCACGA
Plcg1	shRNA_1	GACGATGGACCTTCCCTTC	Ift52	shRNA_1	CAATGCCCAGGCTCTCACC
	shRNA_2	CAAGGCCAAAGGCAAGAAG		shRNA_2	CAGGATGCCAAACATATCC
	shRNA_3	GCCAGATACCAGCAGCCAT		shRNA_3	ACATATCCTTGAACACATC
Zhx3	shRNA_1	CAGCTTTCTGAAGAACTCC	Mybl2	shRNA_1	GGAAAGTCGACACGGGAGG
	shRNA_2	CCAAAGCTGAGCTCTGCTA		shRNA_2	CAGCCTGCTCAACCAGGGT
	shRNA_3	GACCGCACAGCAGCGTCAT		shRNA_3	GATGGGTTCTGAGAACTTG
Lpin3	shRNA_1	ACTGCAGTGGATTCTCCTC		shRNA_4	GCTCAAGCGACAGAAGAAA
	shRNA_2	GACTGGACACACCAGGGCA		shRNA_5	GGACAATGCTGTGAAGAAT
	shRNA_3	GCCACTGCCGTATGTGGAC	Gtsf1	shRNA_1	TCTTTCACAGGAAGAGGCT
Emilin3	shRNA_1	GACCAGAGGCCACCTGAGG		shRNA_2	TACAACGCCTGCCACGTGG
	shRNA_2	GACCCCACCCCAATTTATC		shRNA_3	GCGCATCTCATCTGAATAA
	shRNA_3	CCCCAGCCTCGCAAGGAAC	Tox2	shRNA_1	GAAGGAGTACCTGAAAGCC
Chd6	shRNA_1	CTCGAGGGGATGAACTGGC		shRNA_2	GATGAGTGACGGAAATCCA
	shRNA_2	CTCCTATGAGCGGGAAATG		shRNA_3	GCCTACGCTCTCTTCTTCA
	shRNA_3	TACTGGCCAGCTAGGCAGT	Jph2	shRNA_1	GACAGGACCCCTCAACTCC
Ptprt	shRNA_1	TGTGGGGCAGAACGCCACG		shRNA_2	GAACGACAAGCGCTCGGGC
	shRNA_2	CCTCGATTCGCTACACTAC		shRNA_3	CATCGGCCTGGCTATCCTA
	shRNA_3	TGAAGGGGTTGTGGACATC			
Sfrs6	shRNA_1	GGTCCCGTTCTAGATCTCG			
	shRNA_2	TGGGTACGGTTTCGTGGAG			
	shRNA_3	GCTTTCTGAGCCACAGCCT			
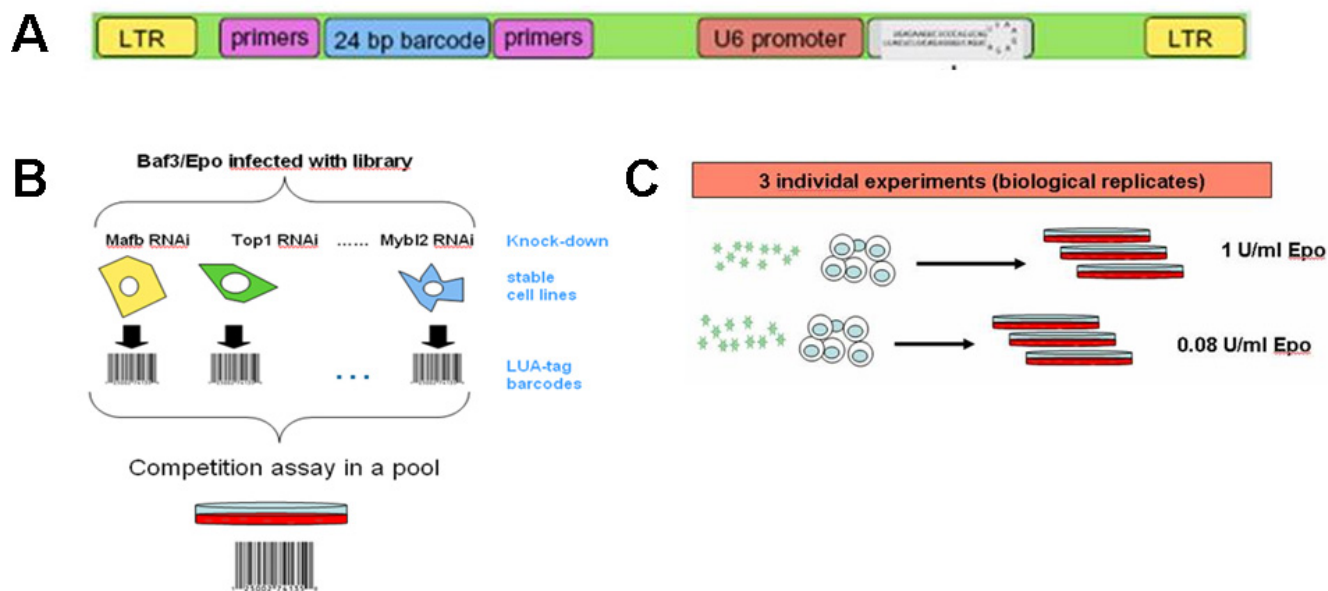
Figure 3.15. Outline of the screen for del20q tumor supressors in a pooled bar-coded shRNA setup. (A) Between two LTR signals for lentiviral packaging, shRNA templates, driven by a human U6 promotor, are associated with a unique LUA-tag (24-bp bar code). **(B)** Baf3/EPO cells were independently tranduced with the bar-coded shRNA constructs and then pooled for a proliferative competition assay. **(C)** Cells were cultered under two different cytokine concentrations, 0.08 U/ml and 1 U/ml recombinant erythropoietin (Epo). The experiment was performed in three independent biological replicates per concentration.

3.16. Competitive proliferation assay (candidate vs. control bar-coded shRNA setup)

Validation of the top-scoring candidate in the screen (see Results 4.2.5) was technically performed as described in Methods 3.15. The competition of a pool of constructs was reduced to a "shRNA construct vs. empty bar-coded Control" setup. Cells transduced with Top1 shRNAs effective in the screen, either Top1 shRNA_1 or Top1 shRNA_2 were plated in a one to one ratio with control cells. A baseline DNA sample was taken and cells were cultured for 26 days in presence of 0.08 U/ml recombinant erythropoietin ERYPO (Janssen-Cilag). The experiment was performed in three biological replicates, independently handled form the viral transduction on. Cell aliquots were taken in regular intervals for subsequent DNA isolation and Luminex quantification of the bar codes.

3.17. Luminex quantification of bar-coded shRNAs

The relative quantity of bar-codes corresponding to the abundance of a specific knock-down in the pool was determined using the Luminex xMap technology [136]. DNA from cell aliquots taken for Luminex quantification (described in Methods 3.15 and 3.16) was isolated using the Wizard Genomic DNA Purification Kit (Promega). Bar-codes integrated into the cells' genomes was amplified in 34 PCR cycles using forward primer 5'-cgattagtgaacggatctc-3' and reverse primer 5'-gaaggtgagaacaggagc-3' from 1ug genomic DNA in total. Bar codes were further linear amplified using the biotinylated primer 5'-[Btn]tgaggatagcagagaagg-3' in 30 cycles. 1ul of the biotinylated product was hybridized to 15ul of xMAP beads set 2.1 (Luminex) in TMAC buffer in a total volume of 50ul. The reaction was heated to 94°C for 2min and then incubated at 40°C for 90min. Then, 40ul 1:200 TMAC diltution of streptavidin-phycoerythrin conjugate (SAPE) (Invitrogen) was added and incubation was continued for 10min. After a washing step (TMAC buffer) samples were resuspended in TMAC and analyzed on a Bio-Plex 200 instrument (Luminex). For the del20q pool, scores were calculated by summing up ascending and descending slopes of the trend of relative abundance of bar-codes in the pool over the first 50 days. For the validation (Competitive proliferation assay, candidate vs. control bar-coded shRNA setup), fluorescence signals were recalculated into percent signal of day 0 baseline signal.

4. RESULTS

4.1. Deletions on chromosome 7p – a genetic defect at post-MPN leukemic transformation

4.1.1. High-resolution genomic analysis of patients with post-MPN leukemia

Of the 339 MPN Viennese patients included in this study, 9 patients were diagnosed with post-MPN leukemic transformation. To gain insight into the genetic changes that precede this event we studied these 9 transformed MPN patients using high-resolution SNP microarrays. Since leukemic blasts display a high degree of genomic instability resulting in extremely complex karyotypes, we focused the analysis on terminally differentiated clonal myeloid cells from these patients. Granulocyte DNA samples taken either at the time or before leukemic transformation were used for genotyping. Loss of heterozygosity (LOH) due to deletions and UPD was scored in all patients followed by analysis of copy number. Acquired genetic lesions were detected in 7 of the 9 patients (Table 4.1.1.). Defects of chromosome 9p were the most frequent, including the previously characterized 9pUPD and 9p gains [29, 91, 117]. We detected two cases of chromosome 7p deletions (patients 444, 455), two different chromosome 13q deletions (patients 203, 444), and several other non-recurrent lesions (Table 4.1.1). Most of the detected deletions spanned large genomic regions except for the common deleted region on chromosome 7p (del7p). The combined deleted region on chromosome 7p assembled from two deletion events was 0.36 Mb in size and included the *IKZF1* and the *FIGNL1* genes encoding the transcription factor *Ikaros* and the *fidgetin-like 1* protein, respectively.

Table 4.1.1. Summary of cytogenetic lesions in 9 post-MPN leukemic patients.

UPN	Dg.	JAK2-V617F	loss (position, Mb)	UPD (position, Mb)	gain (position, Mb)
140	PV	+	-	-	-
203	PMF	+	chr13: 19.3-20.3	-	trisomy chr8
245	PV	+	-	chr9: ter-34.4 chr14: 23.6-ter	-
419	PV	+	-	chr9: ter-37.1	-
420	PV	+	chr5: 89.19-139.0	chr9 :ter-32.9	-
429	PV	+	-	-	chr9: ter-18.2
444	PMF	+	chr4: 101.1-107.7 chr4: 136.9-145.5 chr7: 22.45-35.5 chr7: 38.45-45.05 chr7: 46.95-53.2 chr13: 29.4-36.6 chr13: 44.35-54.45	chr9:ter-33.4	-
455	PV	+	chr6: 64.5-80.05 chr7: 50.18-50.55 chr8: 115.96-118.6 chr12: 90.55-93.55 chr12: 108.8-110.8 chr12: 120.0-123.1	chr9:ter-40	-
487	PV	+	-	-	-

UPN, unique patient number; Dg., diagnosis; ter, chromosomal end; Mb, mega base pairs; chr, chromosome

4.1.2. Frequency of del7p in MPN and mapping of the common deleted region

To determine the frequency of *IKFZ1* deletions in chronic phase MPN patients, we developed screening assays based on LOH and copy number measurements by quantitative PCR (qPCR). Two SNPs (SNP1 and SNP2) located in introns 0 and 2 (Figure 4.1.2.1) were genotyped in DNA samples isolated from non-myeloid control cells and myeloid cells from the same patient. LOH was scored in each patient displaying a heterozygous genotypic call in the control DNA and a homozygous call in the myeloid cell derived DNA (Figure 4.1.2.2.).
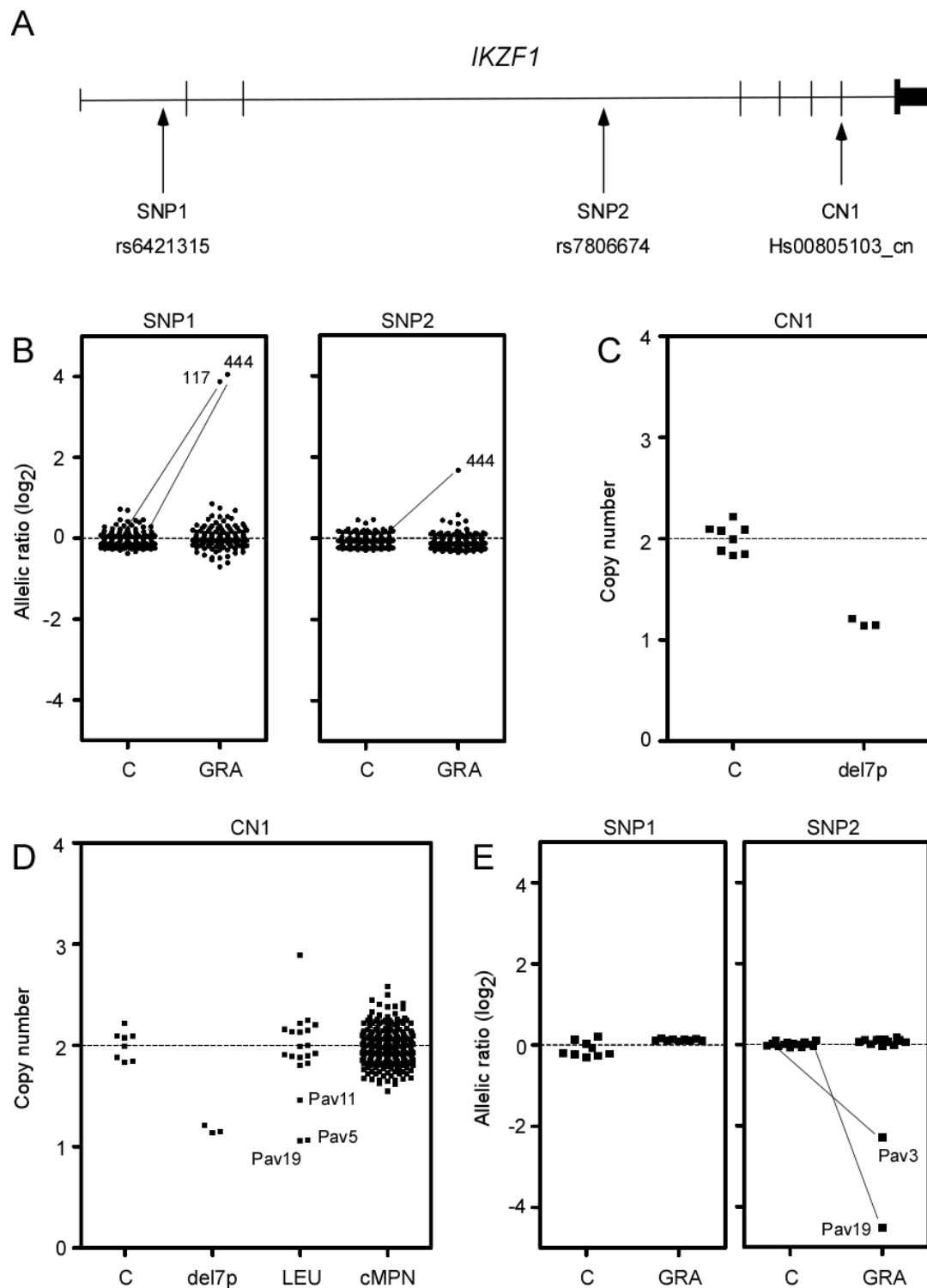
Figure 4.1.2.1.. Frequency of *IKZF1* deletions in two independent MPN patient cohorts. (A) Relative position of the assays used for the *IKZF1* deletion analysis. Location of the single nucleotide polymorphisms rs6421315 (SNP1) and rs7806674 (SNP2) and the copy number assay Hs00805103_cn (CN1) is indicated with arrows within the *IKZF1* gene. Vertical bars represent *IKZF1* exons 0 to 7. **(B)** Analysis of loss of heterozygosity (LOH) in the Vienna MPN cohort. Patients

heterozygous for at least one of the two SNPs (SNP1, SNP2) in the control tissue (C) were tested for LOH in granulocyte DNA (GRA). Granulocyte allelic ratios deviating from 0 (log2) were scored as LOH. Patient 444 with a microarray validated *IKZF1* deletion was used as a positive control. **(C)** *IKZF1* deletion analysis by copy number measurement. DNA from healthy individuals (*n=8*) was used as a control for diploid copy number (C). Three patients (117, 444, 455) with either microarray- or LOH-based evidence of chromosome 7p deletion (del7p) exhibited significant reduction of *IKZF1* copy number (*P<0.01*). The copy number values shown represent means of triplicate measurements for each DNA sample. **(D)** *IKZF1* deletion analysis in the Pavia patient cohort (*n=240*) using the CN1 copy number assay. Significant copy number reduction was detectable in three patients (Pav11, Pav5, Pav19) in the post-MPN leukemic group (LEU). None of the patients in the chronic MPN group (cMPN) exhibited a copy number value below 1.5 used as a threshold. For comparison, the copy number values of healthy controls (C) and positive controls (del7p) are shown as well. **(E)** *IKZF1* deletion analysis in the Pavia leukemic MPN patient cohort using LOH analysis. Only heterozygous patients for SNP1 and SNP2 in the control tissue (C) were included in the analysis. Two patients (Pav19, Pav3) showed significant deviation from allelelic ratio of 0 (log2) in the granulocyte DNA (GRA) consistent with LOH for the SNP2 assay.

Of 315 patients analyzed, 135 were informative (i.e. heterozygous in the control DNA) for SNP1 and 146 for SNP2. Patient 444 was used as a positive control as this patient was informative for both SNPs. A total of 217 patients were informative for at least one of the SNPs. One patient (117) with a diagnosis of PMF exhibited LOH for SNP1 but was uninformative for SNP2 (Figure 4.1.2.1.B). We confirmed the presence of the deletions by a copy number assay mapping to exon 6 (Figure 4.1.2.1.A) in all three patients (444, 455, 117) with either microarray- or LOH-based evidence of 7p deletion (Figure 4.1.2.1.C). In the entire MPN patient cohort from Vienna informative for del7p analysis (*n=225*), del7p was present in 3 patients (1.3%). To test the del7p frequency in an independent patient cohort, we analyzed an additional 240 MPN patients from Pavia. Twenty of these patients had post-MPN leukemia and 220 were in the chronic phase of MPN. The exon 6 copy number assay was preferred for del7p analysis in the Pavia cohort since paired DNA samples (control tissue and myeloid cells) were available only for the 20 post-MPN leukemia patients. The analysis of *IKZF1* copy number revealed 3 patients (Pav5, Pav11, and Pav19) with del7p in post-MPN leukemia and none in the chronic phase MPN cohort (Figure 4.1.2.1.D). Although the copy number value for patient Pav11 was close to the cutoff value (copy number 1.5), it was confirmed in repeated analysis and was consistent with a minor population of del7p positive cells in this patient. LOH analysis using paired control and myeloid DNA samples was performed only in the post-MPN leukemic patients. In addition to Pav19, patient Pav3 tested positive for LOH with the SNP1 assay (Figure 4.1.2.1.E).

Interestingly, patient Pav3 showed a copy number of 2 using the exon 6 assay indicating that an intragenic deletion of *IKZF1* is likely in this patient with a centromeric deletion breakpoint between intron 0 and exon 6. To map the common deleted region, all patients with a detectable del7p were genotyped by microarray analysis (117, 444, 455, Pav3, Pav5, Pav11, Pav19). One patient (117) had a 1.55 Mb deletion spanning across the *IKZF1* locus and two patients (Pav11, Pav19) displayed monosomy 7 (Figure 4.1.2.3.A).
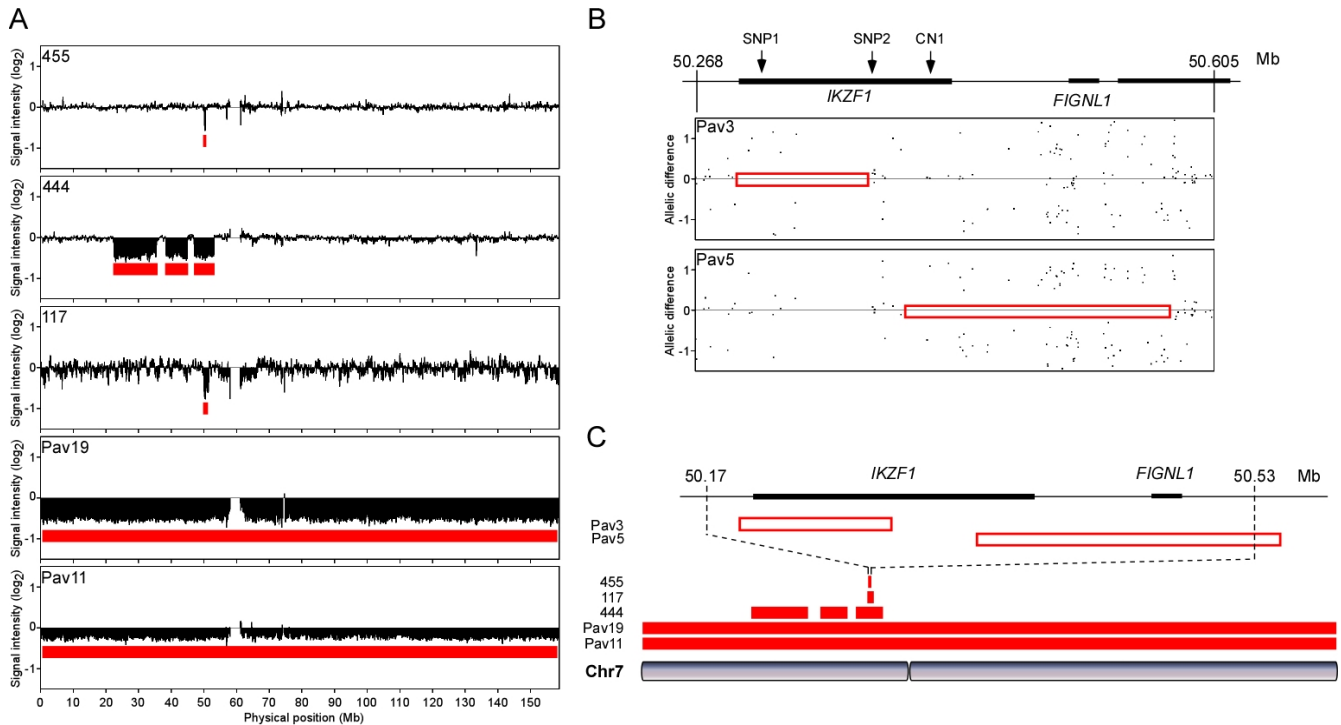

Figure 4.2.2.3. Mapping of the common deleted region in MPN patients with chromosome 7 deletions (A) Probe signal intensity (log2) across chromosome 7 is shown in five patients (455, 444, 117, Pav19, Pav11) with large deletions. Red horizontal bars indicate the reduction of probe signal intensity. X axis represents the physical position on chromosome 7 in mega base pairs (Mb). Loss of signal intensity across the entire chromosome (consistent with monosomy) was present in two patients (Pav19 and Pav11). **(B)** Genotypes of single nucleotide polymorphisms (SNPs) within the *IKZF1* and *FIGNL1* gene loci in two patients with small chromosome 7 deletions. Each dot represents a SNP genotypic call between positions 50.268 and 50.605 Mb (X axis). Both patients (Pav3, Pav5) exhibit a stretch of homozygous calls in granulocyte DNA (red horizontal boxes) within the *IKZF1* gene consistent with loss of heterozygosity. Within the regions indicated by red boxes, there is a complete absence of heterozygous genotypic calls (allelic difference of 0). **(C)** Summary of the deletion analysis on chromosome 7 (Chr7). The common deleted region (physical position 50.17-50.53 Mb) is delineated with dotted line. The relative positions of *IKZF1* and *FIGNL1* genes are shown as black horizontal lines.

In patients Pav3 and Pav5, the microarrays did not provide sufficient resolution to detect a microdeletion by decreased probe signal intensity but a stretch of homozygosity within the *IKZF1* gene was detected consistent with the presence of LOH in these patients (Figure 4.1.2.3.B). Combining the data from all patients, the common deleted region contained only the *IKZF1* gene (Figure 4.1.2.3.C).

4.1.3. Clinical phenotype of del7p patients

The distribution of del7p events in the Viennese chronic MPN and post-MPN leukemia patients showed a significant association (P=0.0042) of del7p with leukemic transformation (Table 4.3.1.). Similarly, the association was present in the Pavia cohort as 4 patients from the post-MPN leukemia group were positive whereas none in the chronic phase were (Table 4.1.3.). In summary, the association of del7p (and monosomy 7) with leukemic transformation was highly significant in all the cohorts analyzed (Table 4.3.1.). Six of the seven patients with del7p transformed to acute myeloid leukemia (AML). Patient 117 did not transform, however, the patient exhibited features of advanced phase PMF such as pancytopenia and increased blasts in the peripheral blood. The mean age of del7p patients at MPN diagnosis was 56.4 years (range 39-75). In del7p patients with AML, the mean time between MPN diagnosis and leukemia was 7.7 years (range 0.3-17.6). The common clinical features of the del7p patients included anemia, thrombocytopenia, and increased percentage of blasts in peripheral blood. All of the patients with post-MPN leukemia tested positive for the JAK2-V617F mutation whereas patient 117 was positive for MPL-W515L.

Table 4.1.3.. Association of del7p with post-MPN leukemic transformation.

Cohort	del7p	Chronic MPN	post-MPN leukemia	P (Fisher's exact test)
Vienna	absent	216	7	
	present	1	2	0.0042
Pavia	absent	220	16	
	present	0	4	< 0.0001
Combined	absent	436	23	
	present	1	6	< 0.0001

4.1.4. Leukemic blasts carry del7p and JAK2-V617F

To determine whether *IKZF1* loss predisposes patients to leukemic transformation we tested if the leukemic blasts originated from progenitors carrying the *IKZF1* defect. We used DNA available from sorted leukemic blasts from 3 patients (444, Pav19, Pav11) and determined the copy number of *IKZF1* by qPCR (Figure 4.1.4.). In all these patients the blasts carried the del7p or monosomy 7. In all three patients the leukemic blasts also tested positive for the JAK2-V617F mutation by allele-specific PCR (data not shown).
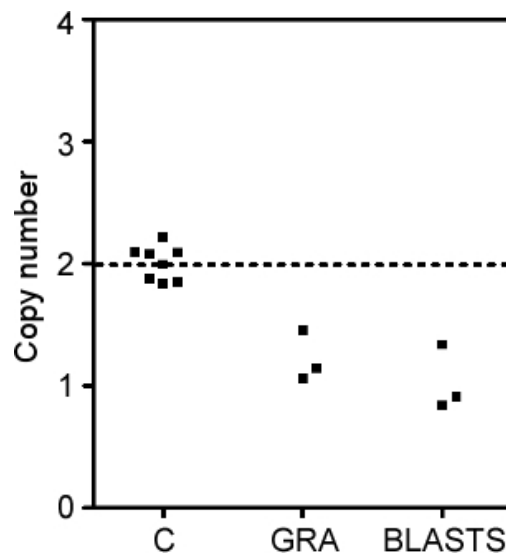

Figure 4.1.4. *IKZF1* deletion analysis in leukemic blasts. Sorted leukemic blasts were analyzed in three patients (444, Pav19, Pav11) carrying chromosome 7p deletion or monosomy 7 in granulocytes (GRA). In all three patients, the *IKZF1* copy number analysis revealed presence of *IKZF1* deletions also in the leukemic blasts (BLASTS). The CN1 copy number assay was used for the analysis. The copy number of healthy controls (*n=8*) is shown for comparison (C).

4.1.5. Absence of IKZF1 point mutations in del7p and MPN patients

To distinguish between two mechanisms of tumor suppressor inactivation (complete loss of function or haploinsufficiency) we performed sequence analysis of the seven coding *IKZF1* exons and exon-intron junctions in all patients with del7p. No mutations were found on the undeleted allele of *IKZF1* in these patients. In patient 117 for whom total granulocyte RNA was available for expression analysis, we detected *IKZF1* mRNA expression from the remaining *IKZF1* allele (data not shown). Thus, haploinsufficiency is the most likely genetic

mechanism affecting *IKZF1* in del7p patients. To examine the possibility that *IKZF1* haploinsufficiency can occur by point mutations rather than deletions, we sequenced the *IKZF1* exons in all the remaining post-MPN leukemia patients (*n=23*) and 73 chronic phase MPN patients but none of these carried *IKZF1* point mutations (data not shown).

4.1.6. Deletion of chromosome 7p is a late genetic event in MPN

To determine the if del7p occurred early or late in the genetic evolution of the MPN clone, we monitored mutation and deletion burdens in granulocytes of two del7p patients in serial samples over time. In both patients, one being positive for JAK2-V617F (444) and the other for MPL-W515L (117), increased *IKZF1* deletion burden was detected as a late event after the acquisition of oncogenic mutations (Figure 4.1.6.1.).
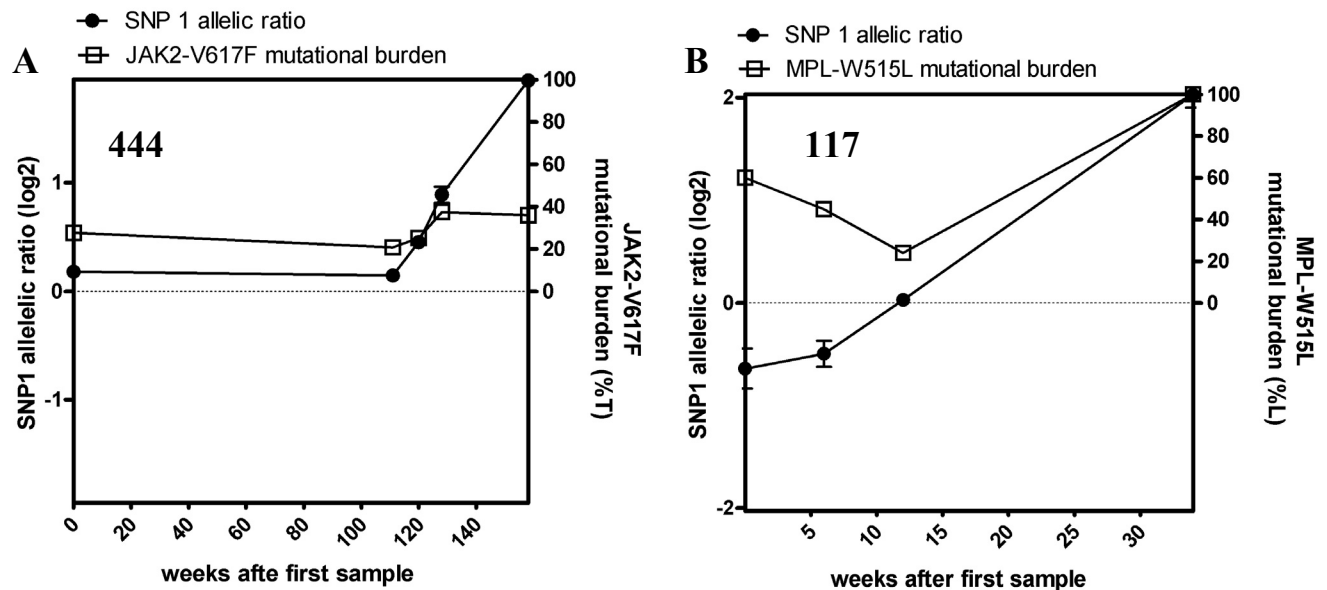

Figure 4.1.6.1. Oncogene mutation and deletion burdens in granulocytes of two patients with IKZF1 deletion over time. Each datapoint represents different sampling over time (X axis). The IKZF1 deletion burden is monitored as described for the SNP1 loss of heterozygosity assay (see Figure 4.1.2.2) and plotted on the left Y axis as log2 of allelic ratio. Increasing deviation from log2 allelic ratio 0 indicates accumulation of cells with IKZF1 deletion over time. The right Y axis shows oncogene mutational burdens as percentage of mutant allele. **(A)** Analysis of JAK2-V617F mutation burden and IKZF1 deletion burden in patient 444 over time. In five serial samples the JAK2-V617F mutation burden increases from around 20% at first sampling to 40% at week 160, whereas IKZF1 deletion first shows up at week 120 and reaches full clonality in granulocytes at week 160. **(B)** Analysis of MPL-W515L mutation burden and IKZF1 deletion burden in patient 117 over time. During the first 15 weeks after first sampling, SNP1 allelic ratio indicates the absence of IKZF1 deletion in the granulocytes, MPL-W515L mutation burden decreases from 60% to 25%. After week 15, a del7p positive subclone arises, followed by rapid establishment of full clonality for both defects at week 35.
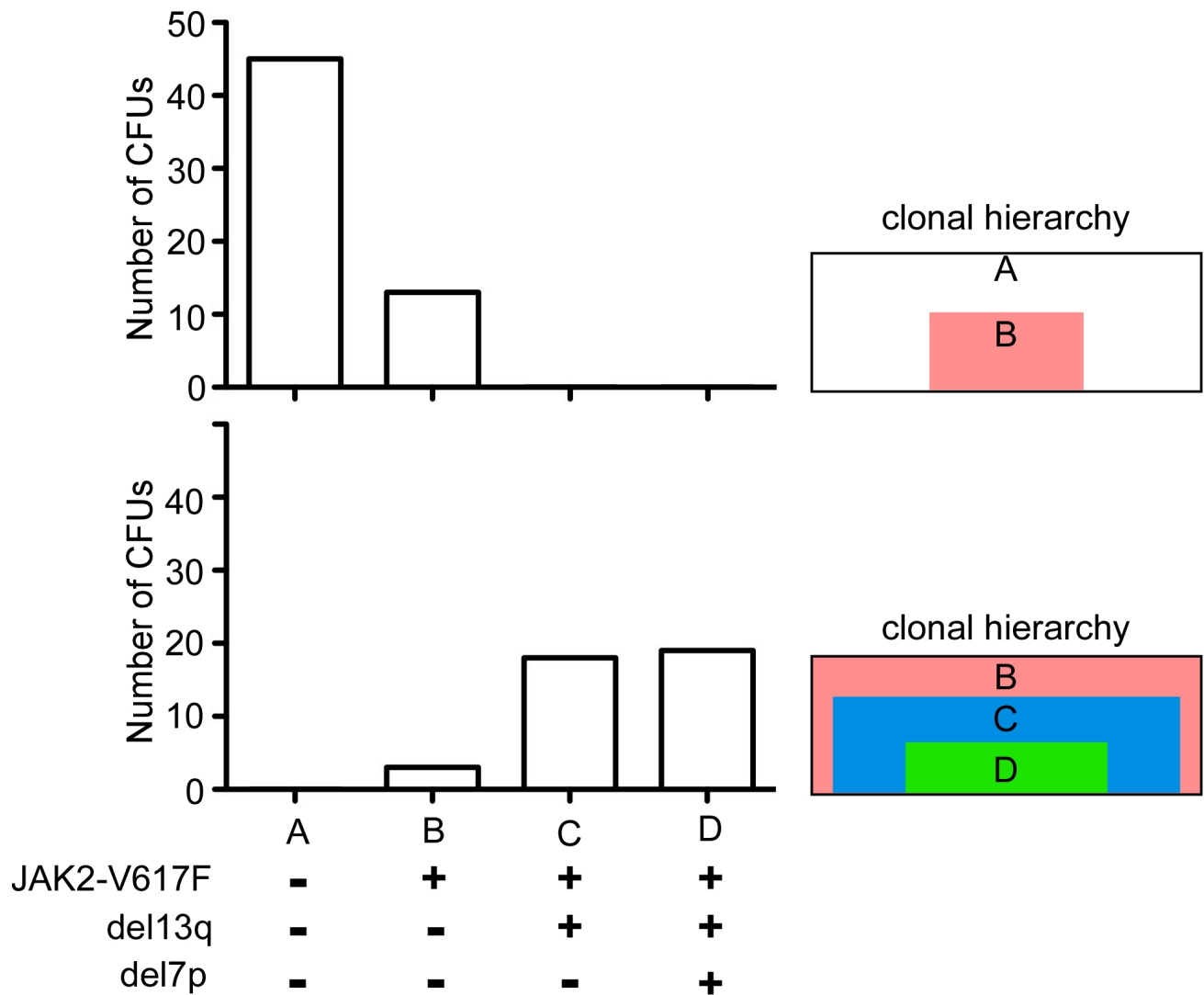
Figure 4.1.6.2. Clonal evolution of the hematopoietic progenitor pool in a patient with deleted *IKZF1*. Peripheral blood mononuclear cells from two serial blood samples taken from patient 444 were plated in methylcellulose (top panel, sample before leukemia; bottom panel, sample at leukemia). Colony forming units (CFU; primarily consisting of erythroid burst-forming units and granulocytic-monocytic CFUs) were individually isolated and genotyped for the presence of JAK2-V617F, deletions on chromosomes 13q (del13q) and 7p (del7p). Four genotypic classes were observed (A-D). The clonal hierarchy of progenitors was deduced from the genotypic classes. The boxes on the right depict the clonal hierarchy of the progenitor pool at the time of sampling. Each colored box represents a progenitor subpopulation: genotypic class A is negative for all three lesions analyzed (white); genotypic class B represents progenitors single positive for JAK2-V617F (pink); genotypic class C represents progenitors carrying del13q and JAK2-V617F (blue); genotypic class D is positive for all three clonal markers (green).

In addition, an early DNA sample from patient Pav5 did not test positive for del7p (data not shown), all together indicating that loss of IKZF1 is a genetic event acquired late in the disease progression.

To further analyze the hierarchy of genetic defects in progenitor cells, we examined colony forming units (CFUs) in patient 444 from whom we had peripheral blood cells. In two serial samples (before and at transformation) we genotyped CFUs for del7p, JAK2-V617F and del13q. In the sample before transformation, the majority of colonies did not carry any of those defects, but a JAK2-V617F positive clone was already present (Figure 4.1.6.2.). In the later sample drawn at leukemic transformation, all BFU-E and CFU-GM colonies were positive for JAK2-V617F, most of them also carrying del13q. Del7p was acquired on JAK2-V617F – del13q double-positive background, resulting in a triple-positive subclone (Figure 4.1.6.2.). Therefore, the order of acquisition of aberrations in patient 444 was JAK2-V617F followed by del13q and finally del7p.

4.1.7. Loss of IKZF1 increases cytokine sensitivity of primary progenitor cells

The functional consequences following complete loss of Ikaros as well as expression of the Ik6 dominant negative isoform have been studied extensively in both cell lines and mouse models [137-140]. The use of RNAi offers a unique opportunity to model somatic monoallelic gene losses. To investigate the functional impact of *IKZF1* haploinsufficiency on clonal expansion, we mimicked the defect in mouse primary progenitor cells using a shRNA-based knock-down approach. We used Ba/F3-EpoR cells and tested three independent shRNA constructs targeting *Ikzf1* for knock-down efficiency against a random oligonucleotide control. One of the three constructs (shRNA_1) reduced *Ikzf1* mRNA to approximately 50% (Figure 4.1.7.1.) and was subsequently tested in four independent experiments in murine lineage marker negative (lin⁻) bone marrow primary cells. In the primary cells, the shRNA_1 construct exhibited similar knock-down efficiency as in Ba/F3-EpoR (Figure 4.1.7.2.A). To assay the functional consequences of Ikaros haploinsufficiency, lin⁻ hematopoietic progenitors stably transfected with the *Ikzf1* shRNA_1 or control constructs were assayed for proliferation capacity in the presence of increasing cytokine concentrations. We reproducibly observed

that cells deficient for Ikaros showed increased cytokine sensitivity, but did not acquire cytokine independent growth (Figure 4.1.7.2.B).
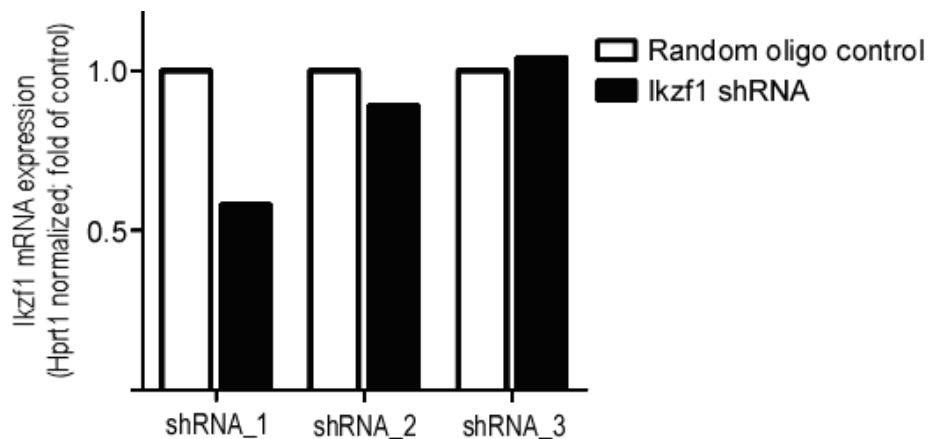
Figure 4.1.7.1. **Assaying shRNAs targeting Ikzf1 for knock-down efficiency**. Three different short hairpin RNA constructs (shRNA_1 to shRNA_3) were tested for their ability to reduce Ikzf1 mRNA level in Ba/F3-EpoR cells. Ikzf1 mRNA expression was normalized with the expression level of Hprt1 mRNA. The shRNA constructs directed against Ikzf1 were compared with a random sequence shRNA control oligonucleotide (random oligo). Ikzf1 shRNA_1 showing a knock-down efficiency of approximately 50% was chosen to be tested in murine lineage marker negative bone marrow primary cells.

Figure 4.1.7.2. Effects of *Ikzf1* knock-down on proliferation capacity of mouse primary progenitor cells. (A) A short hairpin RNA (shRNA) construct effectively reduces *Ikzf1* mRNA level in murine lineage marker negative bone marrow primary cells. *Ikzf1* mRNA expression was determined by real-time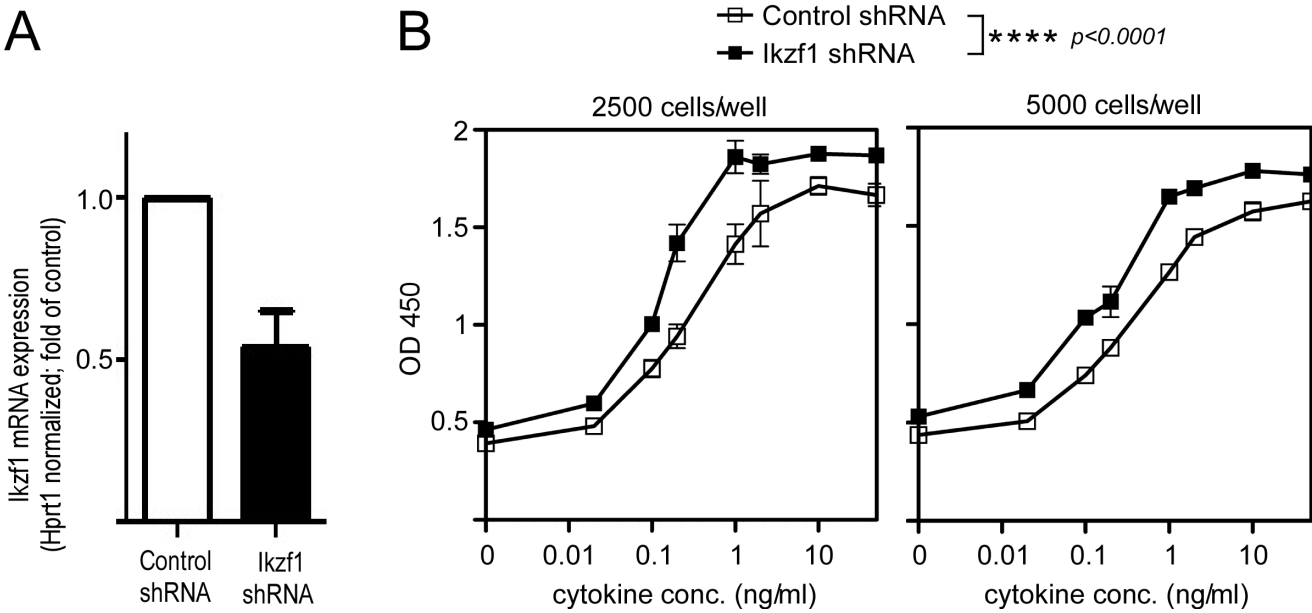 PCR and was normalized with the expression level of *Hprt1* mRNA. The shRNA construct directed against *Ikzf1* (*Ikzf1* shRNA) was compared with a random sequence oligonucleotide shRNA control (Control shRNA) in four independent experiments. The lentiviral shRNA construct shows a knock-down efficiency of approximately 50% compared to the control shRNA **(B)** Proliferation of mouse lineage marker negative bone marrow cells transduced with either the *Ikzf1* shRNA (*Ikzf1* shRNA) or the control random sequence shRNA construct (Control shRNA). Cell growth was assayed in the presence of increasing cytokine concentration. As cell density is crucial for proliferation and survival of primary progenitors, the assay was plated at two different densities, 2500 and 5000 cells/well, followed by the readout on experimental day five and four, respectively. The mean (±SD) of optical density at 450 nm (OD450) of triplicate results is shown (error bars are hidden behind the symbols in some cases). Statistical analysis applying two-way ANOVA revealed a significant difference between control and Ikzf1 knock-down for both plating densities (****$P<0.0001$). Bonferroni posttest revealed differences to be restricted to medium cytokine concentrations (0.02-10 ng/ml), not being significant at baseline and plateau.

4.1.8. Ikaros haploinsufficiency increases Stat5 phosphorylation in primary progenitor cells

As overexpression of the Ik6 dominant negative isoform in cell lines was shown to activate the JAK-STAT pathway [16], we examined the intracellular phoshorylated Stat5 (pStat5) level in the lin⁻ bone marrow cells. Due to cell number limitations we used FACS analysis of intracellular pStat5 staining with a monoclonal antibody specific for pStat5 (Figure 4.1.8.1.A). After starvation of cells transduced with either the Ikzf1 or control shRNA constructs stimulation with IL-3 resulted in a statistically significant increase of pStat5 level (Figure 4.1.8.1.B). Elevated levels of pStat5 were already present at baseline in Ikzf1 deficient cells (Figure 4.1.8.1.B). Opposed to the pStat5 level, the total Stat5 mRNA level measured by quantitative PCR did not differ between Ikaros knock-down and control primary cells (Figure 4.1.8.2).
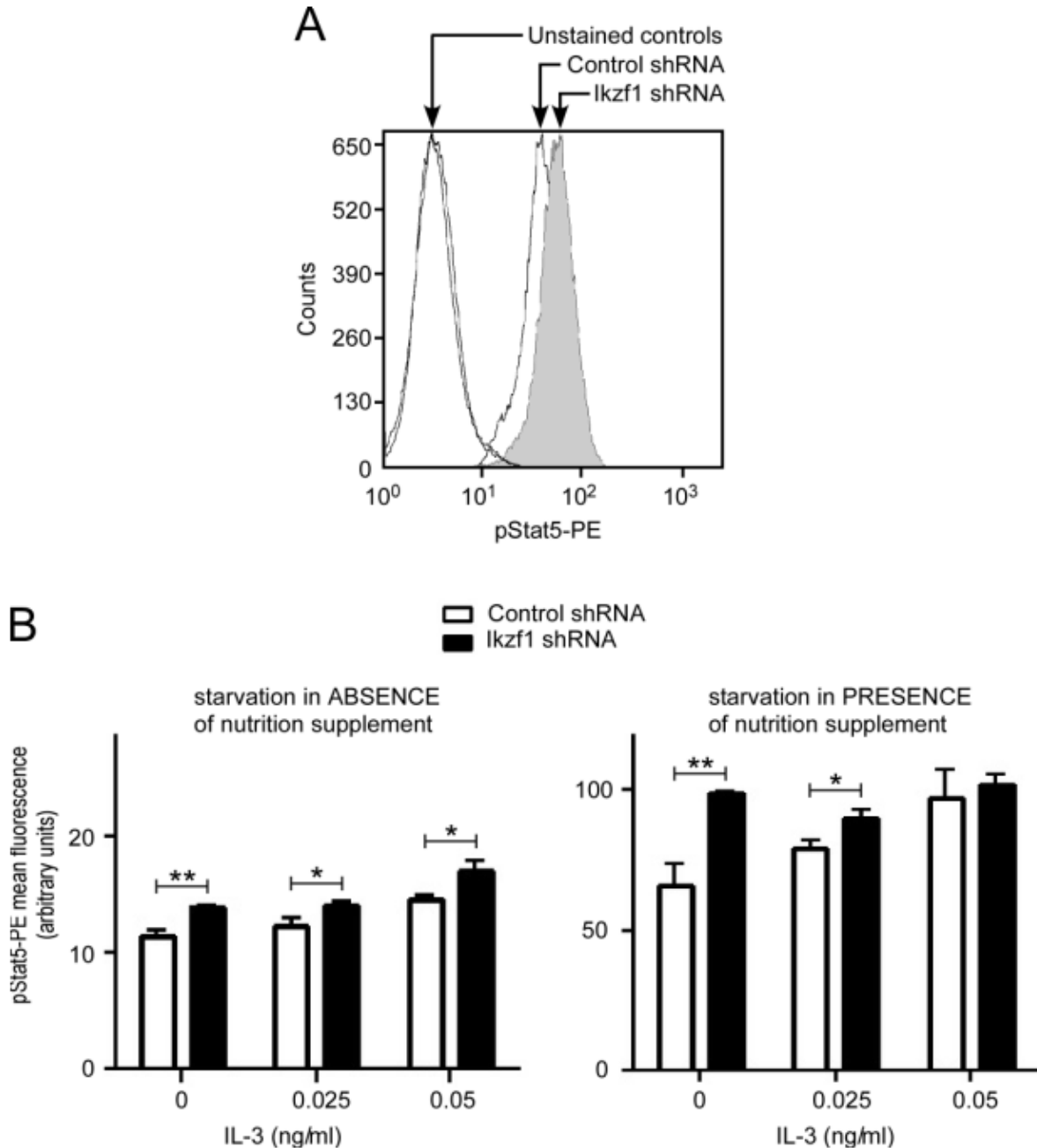
Figure 4.1.8.1. Effects of *Ikzf1* knock-down on Stat5 phosphorylation in mouse primary progenitor cells. (A) Cell sorting analysis of intracellular Stat5 phosphorylation (pStat5) following IL-3 stimulation in control (Control shRNA) and *Ikzf1* knock-down (Ikzf1 shRNA) mouse lineage marker negative primary bone marrow cells. Baseline fluorescence is depicted by unstained controls. The graph is representative for experiments performed for 3 concentrations of IL-3 in each 5 replicates as shown in (D). **(B)** Stat5 phosphorylation in murine lineage marker negative bone marrow primary cells following starvation either in the absence or the in presence of StemPro-34 nutrition supplement. Mean (±SD) of 5 replicates are shown for baseline phosphorylation (0 ng/ul IL-3) and induction with 0.025 ng/ml and 0.5 ng/ml IL-3 for both starvation conditions. Significance of observed differences in Stat5 phosphorylation between Control (Control shRNA) and *Ikzf1* knock-down (Ikzf1 shRNA) cells was determined using unpaired t-test (*P < 0.05, **P < 0.01).
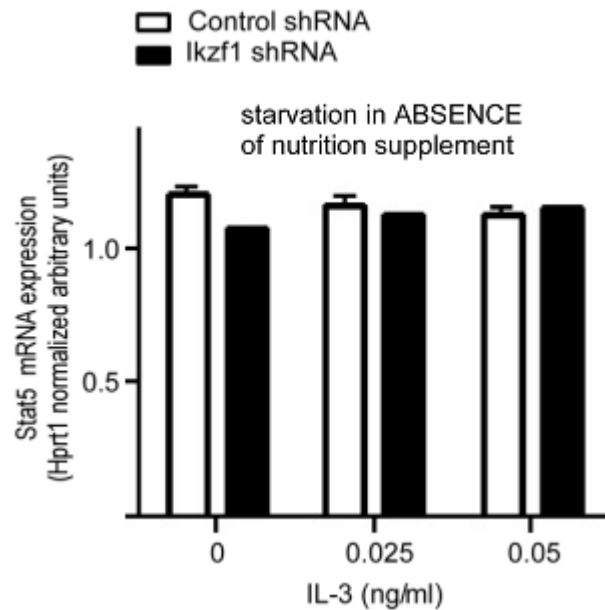
Figure 4.1.8.2. Effects of *Ikzf1* knock-down on total *STAT5* expression in mouse primary progenitor cells. *Stat5* mRNA levels determined by quantitative PCR in control (Control shRNA) and *Ikzf1* knock-down (Ikzf1 shRNA) murine lineage marker negative bone marrow primary cells after starvation in the absence of nutrition supplement and treatment with 0 ng/ml (baseline), 0.025 ng/ml and 0.5 ng/ml IL-3. *Stat5* mRNA expression was normalized with the expression level of *Hprt1* mRNA. Statistical analysis using unpaired t-test did not reveal any significant differences between the control and Ikzf1 knock-down at any IL-3 concentration.

4.2. Deletions on chromosome 20q – a frequent defect in chronic phase MPN

4.2.1. Screen for del20q events in three independent patient cohorts

Del20q represents one of the most common chromosomal abnormalities in MPN, reported at frequencies of 5-10% in bone marrow. [11, 20, 112-115]. However, presence of a defect in bone marrow stem cells and progenitors does not provide information on the effect of the genetic lesion on hematopoiesis. Therefore, we aimed to search for del20q in present in peripheral granulocytes detectable due a substantial clone size. We had access to granulocyte DNA from a total of 822 patients from three independent cohorts (Vienna, Austria; Pavia, Italy; Brno; Czech Republic) (Table 4.2.1.). In order to determine the frequency of del20q in the three cohorts, we screened for LOH and low copy number using microsatellite PCR, TaqMan SNP genotyping assays and TaqMan Copy Number Assays. Combined results from LOH screening using PCR for microsatellites d20s858, d20s899, d20s96, d20s861 and TaqMan Genotyping Assays C____660473_10, C___1408969 and C__25619579_10 combined with copy number analysis (Hs01792874_cn) showed in a total of 9 del20q events, resulting in an average frequency of 1.1% (Table 4.2.1.).

Table 4.2.1. Del20q events identified in three independent patient cohorts

Cohort	Patients	Del20q	% del20q	UPN
Vienna	480	4	0.8%	117, 146, 384, 446
Pavia	252	5	2.0%	Pav_ITA_Ang, Pav_Coh_147, Pav_Coh_153, Pav_Leu_15c, Pav_Coh_155
Brno	90	0	0%	n/a
total	822	9	1.1%	n/a

4.2.2. Del20q acts independently and can occur before and after JAK2-V617F

Determination of the role of del20q in the evolution of the malignant MPN clone is crucial for understanding its role in pathogenesis. Pre-JAK2-V617F defects are thought to establish

clonal hematopoiesis and predispose the clone for acquisition of the oncogenic mutations, whereas post-JAK2-V617F mutations might rather have a role in determining the disease phenotype. So far, studies in patients with del20q and JAK2-V617F showed that the size of the del20q clone by far exceeded the size of the clone carrying JAK2-V617F, suggesting that del20q preceded the acquisition of the JAK2-V617F mutation [125]. However, the order of acquisition of genetic lesions in the clone can only be determined on progenitor cell level. To determine the temporal relationship between the occurrence of del20q and the oncogenic mutations JAK2-V617F and MPL-W515L, we performed colony assays in methylcellulose, picked single BFU-E and CFU-G colonies grown in the presence of erythropoietin and genotyped each colony individually for del20q and JAK2-V617F or MPL-W515L, respectively. We plated the colony assay from two patients showing evidence for LOH at the del20q CDR locus in a minor clone (102, 233, 234, 346, 369), indicated by tendencies to hemizygous presence of microsatellites or reduced copy number, but absence of clear LOH. Genotyping was done for the oncogenic mutations, del20q and del13q as second chromosomal aberration reported to occur at high frequency besides del20q [20]. The assays used for colony genotyping allowed distinguishing between heterozygous/hemizygous and homozygous defects due to 9pUPD and 1pUPD for JAK2-V617F and MPL-W515L, respectively. All 5 patients investigated showed a minor population of del20q positive progenitors, occurring in various combinations with the other defects investigated, forming different genotypic classes (Table 4.2.2.). In all cases, the oncogenic mutation was preceding del20q, as illustrated by the presence of JAK2-V617F–positive colonies with and without del20q. Patients 233 and 234 appear to have acquired del20q in a cell heterozygous for JAK2-V617F, whereas in patient 369 the transition to del20q occurred in a cell homozygous for JAK2-V617F (Figure 4.2.2.1.). In patients 102 and 369, we found a more complex pattern, indicating multiple acquisition of del20q (Figure 4.2.2.2.). The acquisition of del20y outside of JAK2-V617F in patient 102 indicates that the two lesions act independently. Out of total 12 genotypic classes possible when looking at the 4 markers, we could observe 7 genotypic classes in our patients (Table 4.2.2.). Each patient shows a different combination of genotypic classes and therefore a different clonal composition of the progenitor pool (Figure 4.2.2.1.).

Table 4.2.2.: Genotypic classes of progenitors based on mutation and deletion status in five patients from the Vienna MPN cohort

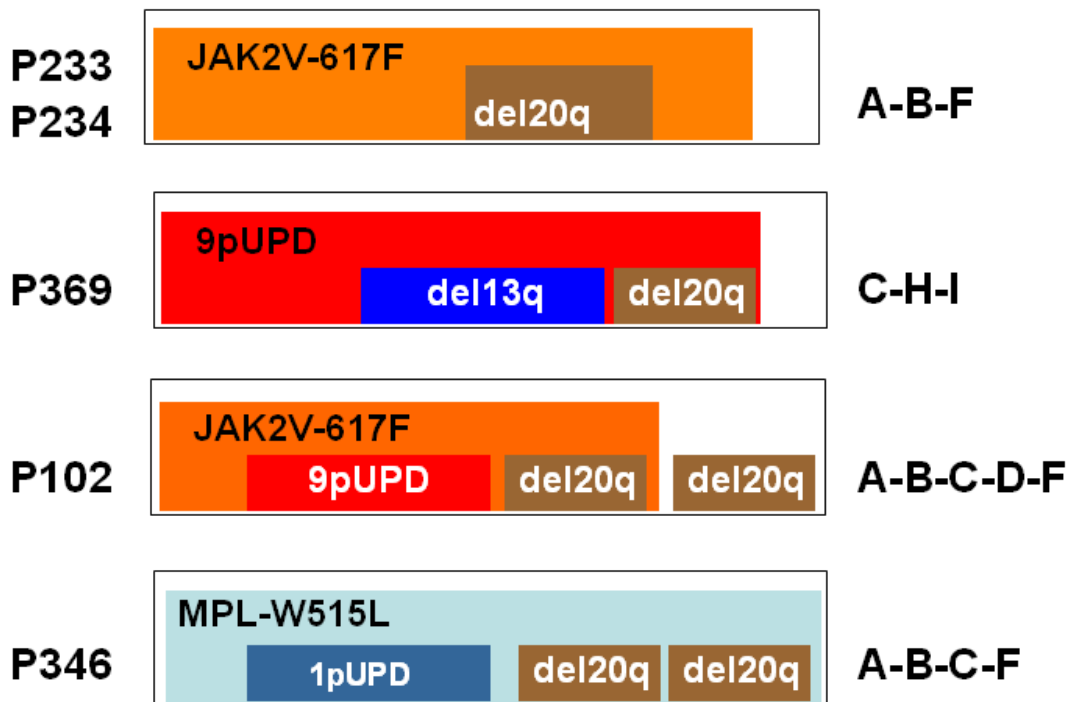|	GENOTYPIC CLASSES											
	A	B	C	D	E	F	G	H	I	J	K	L
Oncogene mut.: heterozygous	-	+	-	-	-	+	+	-	-	-	+	-
Oncogene mut.: homozygous	-	-	+	-	-	-	-	+	+	-	-	+
del20q	-	-	-	+	-	+	-	+	-	+	+	+
del13q	-	-	-	-	+		+	-	+	+	+	+
	Percentage of GENOTYPIC CLASSES within in CFUs											
PATIENTS	A	B	C	D	E	F	G	H	I	J	K	L
P233	36	62	0	0	0	1	0	0	0	0	0	0
P234	42	56	0	0	0	3	0	0	0	0	0	0
P369	0	0	81	0	0	0	0	4	15	0	0	0
P102	59	33	3	4	0	1	0	0	0	0	0	0
P346	10	82	5	0	0	3	0	0	0	0	0	0

Figure 4.2.2.1. Clonal evolution of the hematopoietic progenitor pool in a patient with del20q. Peripheral blood mononuclear cells from five patients with indication of a del20q minor clone (233, 234, 369, 102, 346) were plated in methylcellulose. Colony forming units (CFU; primarily consisting of erythroid burst-forming units and granulocytic-monocytic CFUs) were individually isolated and genotyped for the presence of the oncogenic muations (JAK2-V617F of MPL-W515L), deletions on chromosomes 13q (del13q) and 20q (del20q). Seven genotypic classes were observed (A, B, C, D, F, H, I). The clonal hierarchy of progenitors was deduced from the genotypic classes. Each colored box represents a progenitor subpopulation (see Table 4.4.2.). 9pUPD represents homozygous JAK2-V617F and 1pUPD homozygous MPL-W515L.
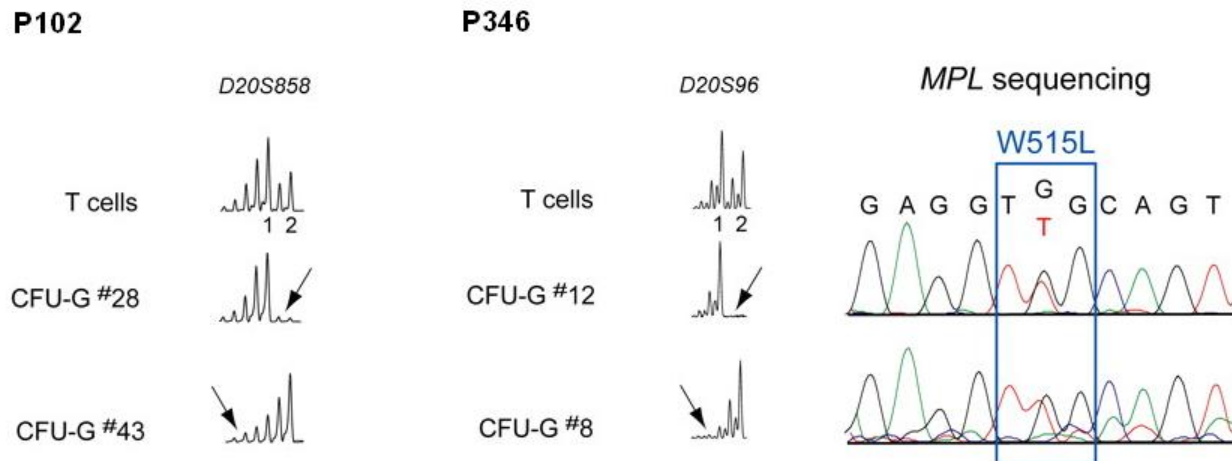
Figure 4.2.2.2. Multiple del20q and 9pLOH events in colonies from 3 MPD patients. The deleted region on chromosome 20q was mapped in individual colonies from patients 102 and 346 using microsatellites PCR for DS858 and D20S96, respectively. T-cell DNA was used to define the 2 alleles for each informative microsatellite. In patient 102, del20q in colony no. 28 created a different haplotype than the deletion in colony no. 43 (marked by arrows), indicating that 2 del20q events occurred independently and affected the chromosome 20q of different parental origin. Similarly, two separate del20q events affecting the chromosome 20q of different parental origin occurred in patient 346. The chromatograms for the MPL-W515Lmutation are shown for the 2 colonies analyzed.

4.2.3. The del20q common deleted region contains several non-expressed genes

Deletions such as del20q result in hemizygous loss of a distinct amount of genes. Some of them are not relevant due to cell type specific lack of expression, whereas others act as tumor suppressors and are therefore responsible for the outgrowth of the malignant clone. In order to identify the tumor suppressor(s) in del20q, we applied an shRNA based knock-down approach in the UT7/TPO cell line, mimicking haploinsufficiency for all genes comprised in a previously reported CDR [115] determined by combined G-banding, fluorescence in-situ hybridization (FISH) or microsatellite PCR analysis (Figure 4.2.3.1.).

To get information about the relevance of the individual knock-downs, we determined expression of the nine target genes in the hematopoietic system (Figure 4.2.3.2.). Out of the nine genes, three genes (*PTPRT, SGK2* and *JPH2*) were not expressed in hematopoietic cells, and one additional gene (*TOX2*) did not show expression in CD34+ hematopoietic stem cells (Figure 4.2.3.2.). Evaluation of our model system of choice, the megakaryoblast derived UT7/TPO cell line, revealed expression of all del20q genes expressed in the human CD34+ hematopoietic compartment (Figure 4.2.3.3.).
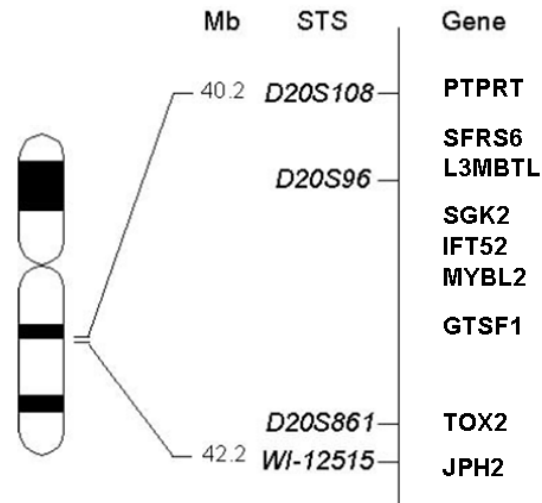
Figure 4.2.3.1. Del20q common deleted region according to Bench et al., Oncogene, 2000. The CDR spans two Mb (physical position 40.2 to 42.2) and contains nine genes (PTPRT to JPH2). Abbrevations: Mb (Mega base pairs), STS (Sequence-tagged sites).
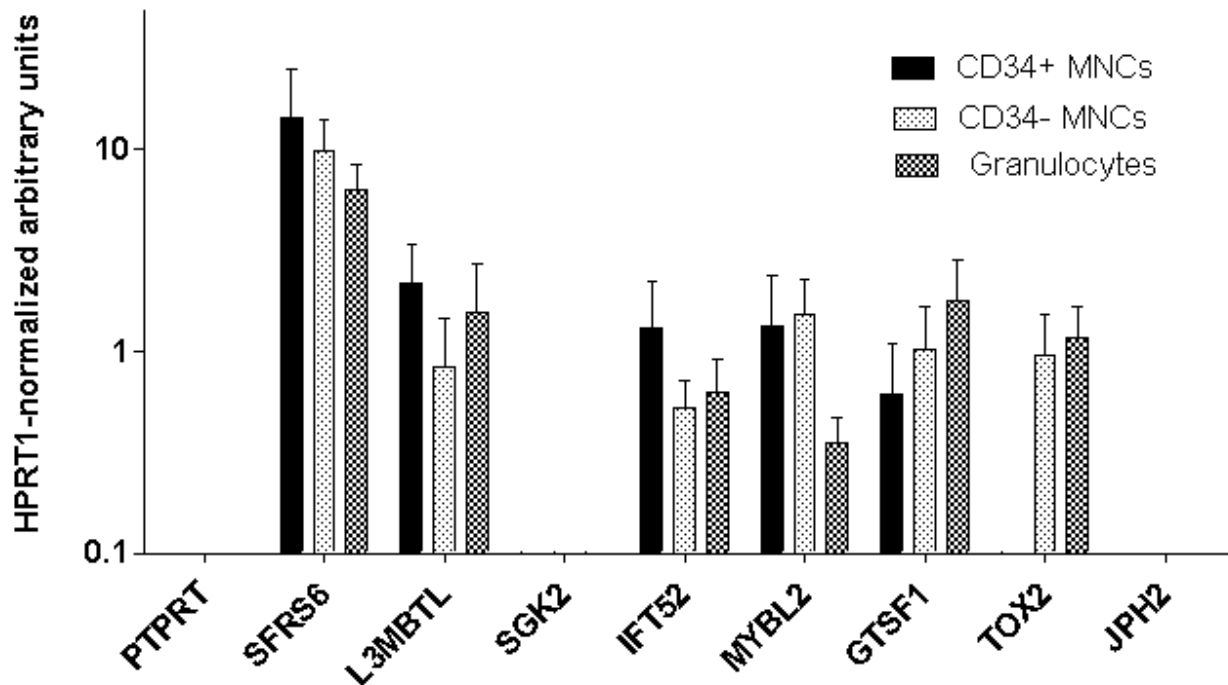
Figure 4.2.3.2. Gene expression profile of the del20q common deleted region in the human hematopoietic system. CD34 positive and CD34 negative mononuclear cells (MNCs), as well as granulocytes, all isolated from human cord blood, were assayed for mRNA level relative to the HPRT1 house-keeping gene. The nine genes within the del20q CDR (*PTPRT-JPH2*) are depicted as located on chromosome 20q (centromeric to telomeric). Results represent the mean (±SD) of measurements in specimen from 5 different individuals.

Figure 4.2.3.2. Gene expression profile of the del20q common deleted region in UT7/TPO. Gene expression level of the nine genes within the del20q CDR (*PTPRT-JPH2*) relative to HPRT1 was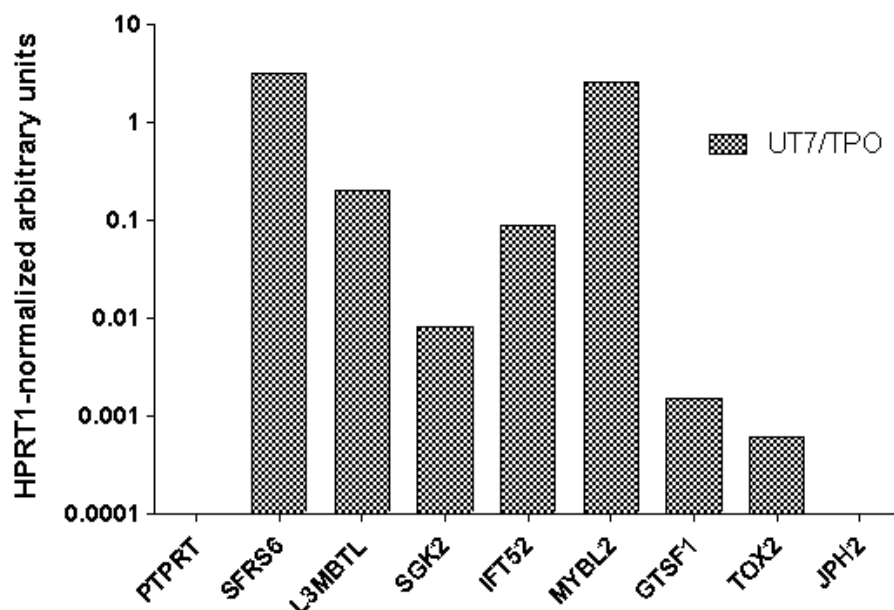 determined in mRNA extracted from UT7/TPO cells. Order of genes corresponds to their appearance on chromosome 20q (left-right, centromeric-telomeric.

4.2.4. Mybl2 is a putative tumor suppressor targeted by del20q

Based on the results from the expression analysis, we applied an shRNA based knock-down approach on the six genes within del20q that showed expression in hematopoietic cells (*SFRS6, L3MBTL, TOX2, IFT52, GTSF1L, MYBL2*). Using the siSTRIKE (Promega) strategy, we cloned two shRNA constructs per target and subsequently delivered both into thrombopoietin dependent UT7/TPO cells using Amaxa electroporation. After selection on puromycine, knock-down efficiency was measured and the proliferation capacity of the stably transfected cells compared to an empty vector control was assayed. We could not observe proliferative advantage of the *SFRS6, L3MBTL, TOX2, IFT52 or GTSF1L* knock-down cells over the control, however, *MYBL2* knock-down cells repeatedly showed thrombopoietin independent hyperproliferation (Figure 4.2.4.1). We could validate the MYBL2 knock-down induced proliferative advantage in UT7/TPO cells in an experimental setup using transient transfection with synthetic siRNAs (Figure 4.2.4.2). Further, knock-down of Mybl2 in the erythropoietin dependent mouse cell line Baf3/EPO using different shRNA constructs consistently resulted not in cytokine independent, but cytokine hypersensitive growth (Figure 4.2.4.3.).
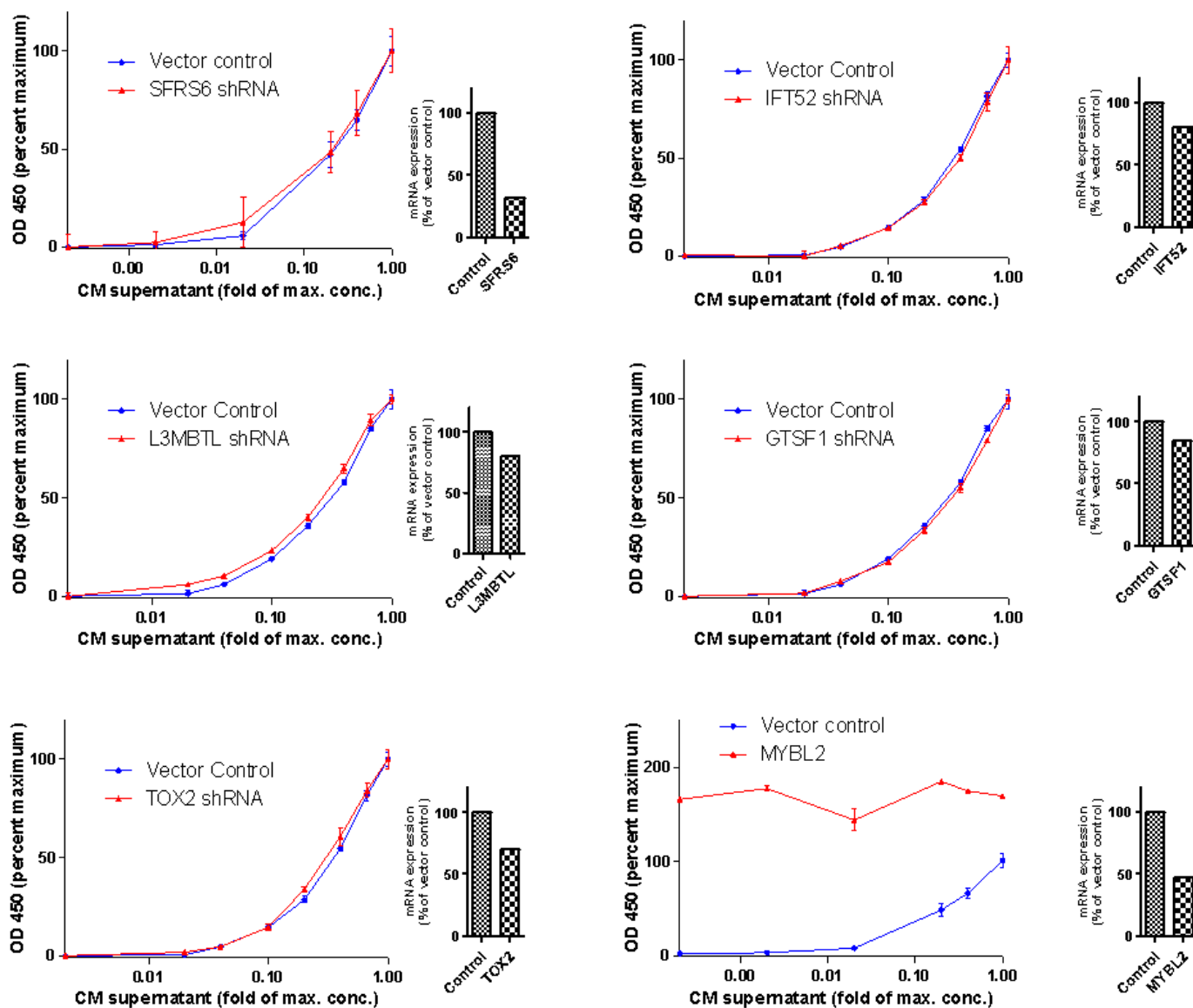
Figure 4.2.4.1. Effects of del20q target gene knock-down on proliferation capacity of UT7/TPO cells. Short hairpin RNA (shRNA) constructs effectively reduce mRNA levels of the del20q target genes (*SFRS6, L3MBTL, TOX2, IFT52, GTSF1L, MYBL2*) in the thrombopoietin dependent cell line UT7/TPO. Knock-down efficiencies compared to an empty control construct having no shRNA (Control) were determined by real-time PCR and were normalized with the expression level of *Hprt1* mRNA. Proliferation of UT7/TPO cells with either the target gene shRNA or the empty vector control (Vector Control) was assayed in the presence of increasing thrombopoietin concentration contained in the supernatant of the CM cell line (CM supernatant). The assay was plated at 5000 cells/well, followed by the readout on experimental day six. The mean (±SD) of optical density at 450 nm (OD450) of triplicate results is shown (error bars are hidden behind the symbols in some cases). Statistical analysis applying two-way ANOVA revealed no significant differences between control and target gene knock-downs except for the MYBL2 knock down (P<0.0001), the latter showing thrombopoietin independent increased proliferation in a range between 160% and 200% of the maximal proliferation of the control.
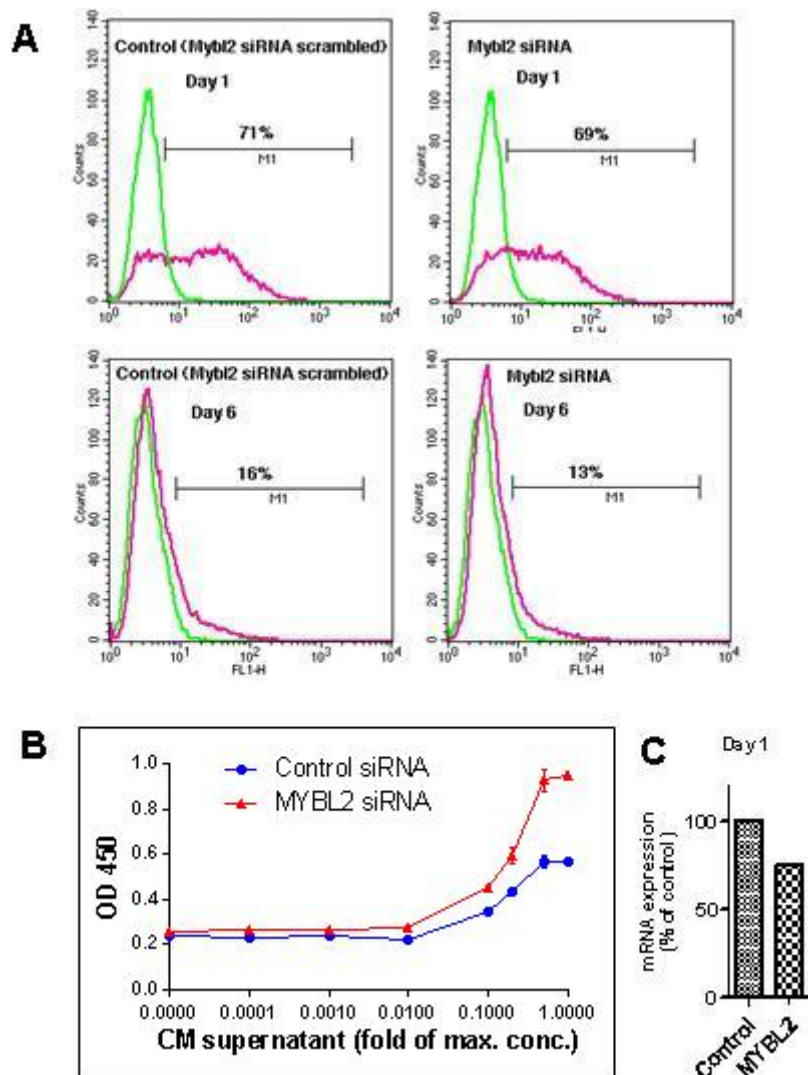
Figure 4.2.4.2. Effects of transient MYBL2 knock-down on proliferation capacity of UT7/TPO cells. (A) UT7/TPO cells were transiently transfected with synthetic control oligonucleotides (MYBL2 siRNA scrambled) and synthetic siRNA oligos targeting *MYBL2* (MYBL2 shRNA), both siRNAs were double stranded and 5'-FAM labeled. Control and MYBL2 siRNAs show similar transfection efficiencies on day 1 after transfection (71% vs. 69% of cells positive for FAM), in both cell fractions siRNA containing cells are diluted out through cell division (16% vs. 13% FAM positive cells on day 6). **(B)** Proliferation of UT7/TPO cells transiently transfected with either the *MYBL2* siRNA or the scrambled Control shRNA. Cell growth was assayed in the presence of increasing thromobopoietin concentration contained in the supernatant of the CM cell line (CM supernatant). The assay was plated at 5000 cells/well, followed by the readout on experimental day six. The mean (±SD) of optical density at 450 nm (OD450) of triplicate results is shown (error bars are hidden behind the symbols in some cases). Statistical analysis applying two-way ANOVA revealed a significant difference between control and *MYBL2* knock-down (p<0.0001). Bonferroni posttest revealed differences to be restricted to thrombopoietin concentrations 0.01 fold of the maximum CM supernatant concentration (p<0.01). **(C)** The efficient knock-down of MYBL2 mRNA to 70% (close to a haploinsufficient condition) was confirmed by real-time PCR, normalized with the expression level of *Hprt1* mRNA.
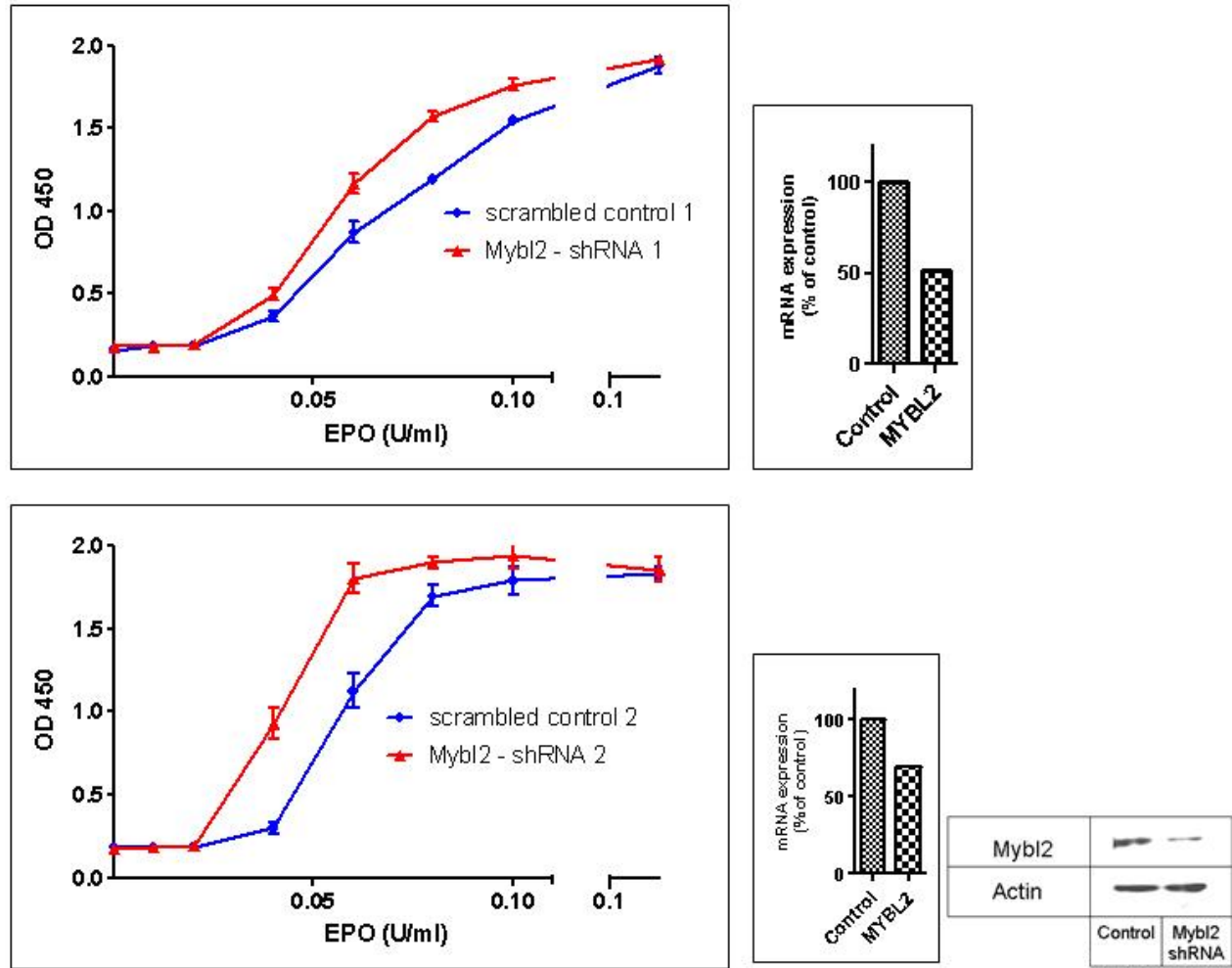
Figure 4.2.4.3. Effects of two different *Mybl2* shRNAs on proliferation capacity of Baf3/Epo cells. The erythropoietin dependent Baf3/EPO murine cell line was transiently transfected with shRNA constructs targeting *Mybl2* (Mybl2-shRNA 1 and Mybl2-shRNA 2) or their corresponding controls containing the scrambled sequences (scrambled control 1 and scrambled control 2, respectively. Knock-down efficiency of both constructs was confirmed using real-time PCR (for Mybl2-shRNA 1) and western blotting (for Mybl2-shRNA 1 and Mybl2-shRNA 2).Cell growth was assayed in the presence of increasing erythropoietin (EPO) concentrations The assay was plated at 2000 cells/well, followed by the readout on experimental day five. The mean (±SD) of optical density at 450 nm (OD450) of triplicate results is shown (error bars are hidden behind the symbols in some cases). Statistical analysis applying two-way ANOVA revealed a significant difference between control and Mybl2 knock-down for both shRNAs ($p < 0.0001$).

4.2.5. Top1 acts as a second putative tumor suppressor in a competitive RNAi setup

In addition to the classical shRNA based knock-down approach used for the identification of the tumor suppressor features of *MYBL2* (see 4.2.4), we applied a "pooled knock-down" approach using bar-coded shRNAs. As described in detail in under "Methods 3.15", every

shRNA is assigned to a 24 base-pair bar-code, which can be read using the Luminex XMap technology. Mimicking haplonsufficiency for one gene per cell, we pooled all knock-downs in equal amounts and screened for proliferative advantage in a competition setup under reduced cytokine concentrations. This strategy allowed us to include a larger number of genes, therefore we planned the experiment using a del20q CDR based on highly reliable microarray karyotyping CDR mapping data [17, 141], including 16 genes in total. Centromeric of the 9 genes (Figure 4.2.3.1.) used for the approach described in 4.2.4., seven more genes mapped this extended CDR, that are *MAFB, TOP1, PLCG1, ZHX3, LPIN3, EMILIN3*, and *CHD6* (Figure 4.2.5.1.). In a first step, we determined expression of the nine target genes in the hematopoietic system (Figure 4.2.5.1.).
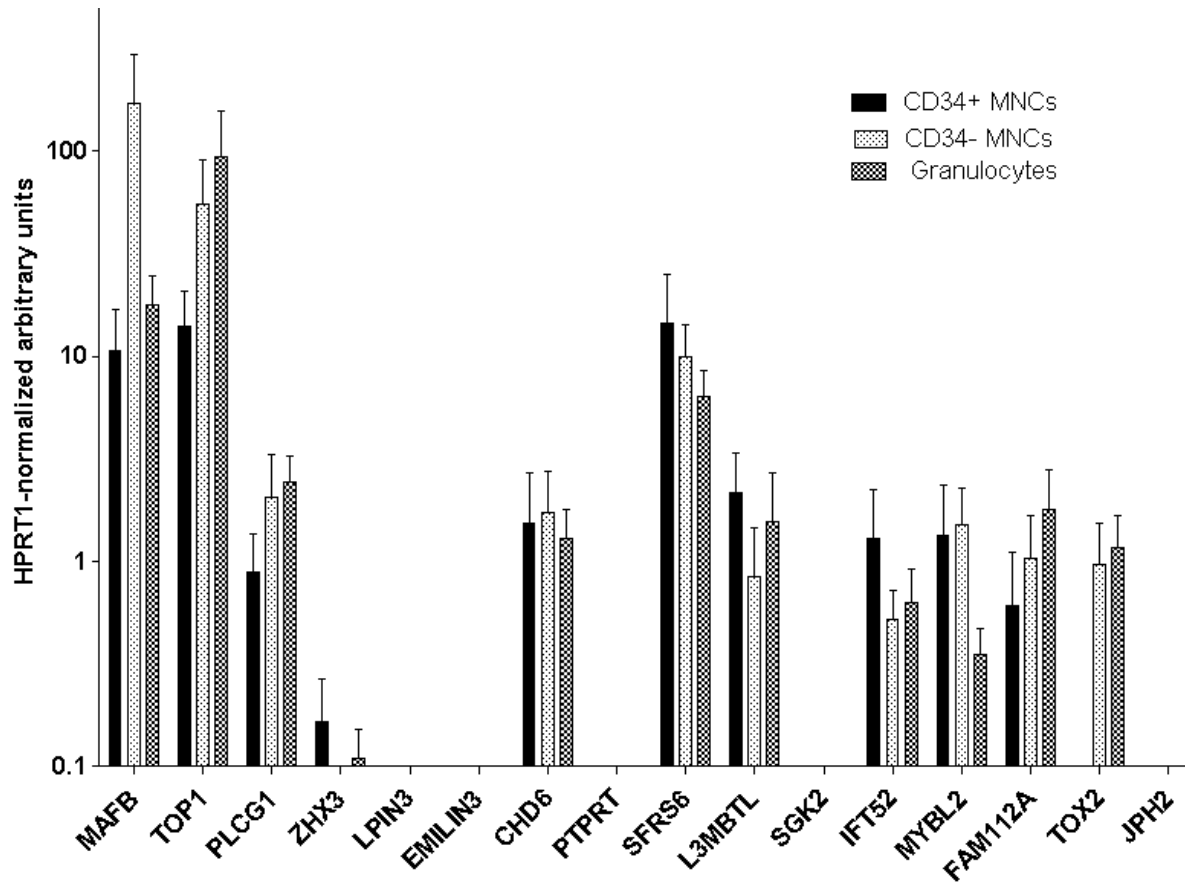
Figure 4.2.5.1. Gene expression profile of the extended del20q common deleted region in the human hematopoietic system. CD34 positive and CD34 negative mononuclear cells (MNCs), as well as granulocytes, all isolated from human cord blood, were assayed for mRNA level relative to the HPRT1 house-keeping gene. The sixteen genes within the extended del20q CDR (*MAFB - JPH2*) are depicted as located on chromosome 20q (centromeric to telomeric). Results represent the mean (±SD) of measurements in specimen from 5 different individuals.

Out of the sixteen genes, five genes (*LPIN3, EMILIN3, PTPRT, SGK2 and JPH2*) lacked expression in hematopoietic cells (Figure 4.2.3.1.). Since we designed the experiment for knock-down of mouse transcripts we evaluated the target gene expression in mouse early progenitors and bone marrow (Figure 4.2.5.2.) and the murine Baf3/EPO cell line (Figure 4.2.5.3.). We could observe high similarity in hematopoietic gene expression between human, mouse and Baf3/EPO cells (Figure 4.2.5.1 - 4.2.5.3).
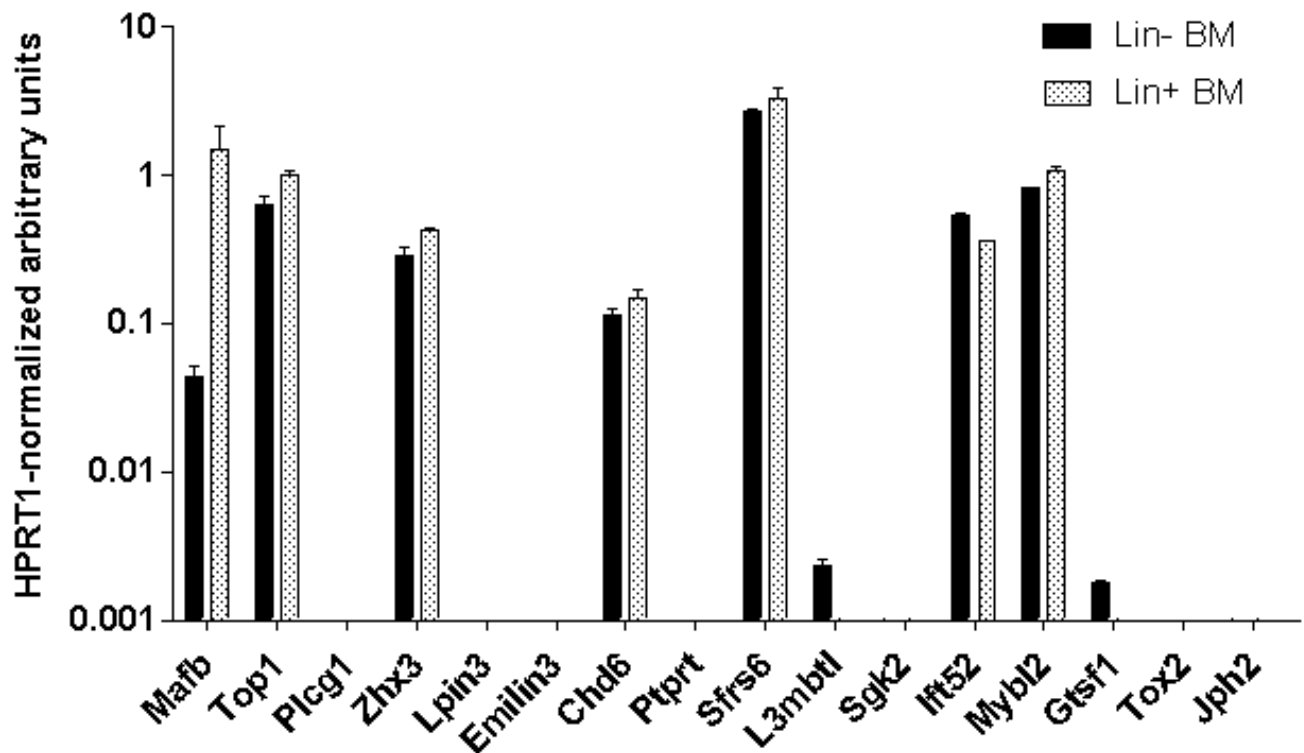
Figure 4.2.5.2. Gene expression profile of the extended del20q common deleted region in mouse early progenitors and bone marrow. Lineage marker negative (Lin-) and positive (LIN+) mouse bone marrow cells (MNCs), isolated from femur and tibia of C57/Bl6 mice, were assayed for mRNA level relative to the *Hprt1* gene. The sixteen genes within the extended del20q CDR (MAFB - JPH2) are depicted as located on chromosome 20q (centromeric to telomeric). Results represent the mean (±SD) of measurements in specimen from 3 different mice.
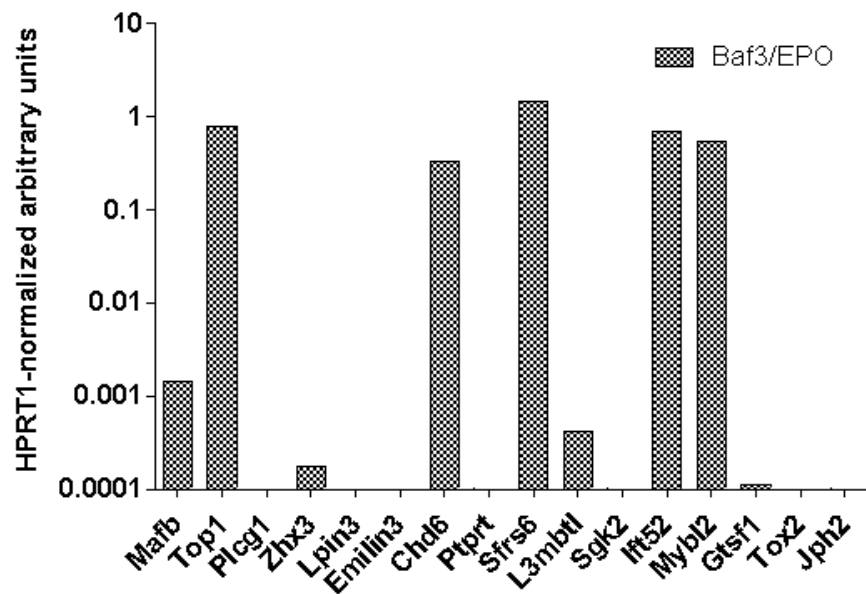
Figure 4.2.5.3. Gene expression profile of the del20q extended ommon deleted region in Baf3/EPO cells. Gene expression level of the sixteen genes within the extended del20q CDR (*Mafb-Jph2*) relative to *Hprt1* was determined in mRNA extracted from Baf3/Epo cells. Order of genes corresponds to their appearance on chromosome 20q (left-right, centromeric-telomeric).

In a next step, we cloned shRNA constructs targeting the sixteen genes into lentiviral bar-coded vectors, transduced Baf3/EPO cells with the individual constructs, pooled the transduced cells in equal amounts and cultured them under reduced erythropoietin concentrations (see Methods 3.15). Analyzing the abundance of the individual bar codes assigned to specific shRNAs in DNA samples taken in regular intervals over a time period of 100 days, we could observe *Top1* knock-down cells to exhibit competitive advantage over all other knock-downs (Figure 4.2.3.4). Cumulative scores were calculated from each three independent biological replicates for two different erythropoietin concentrations. The bar-code performing best was associated with *Top1* knock-down and showed an 8.6 fold higher score than the second best performing knock down, that was Gtsf1l at lowest erythropoietin concentration (Figure 4.2.3.4.A). This difference decreased for a less competitive condition (*Top1* followed by L3mbtl), indicating *Top1* hyperproliferation to be based on cytokine hypersensitivity. Importantly, two different shRNAs targeting *Top1* dominated the pool within and between the different biological replicates, arguing against an off-target effect (Figure 4.2.3.4.B). Constant knock-down efficiency could be proved for both constructs (Figure 4.2.3.4.C).

A

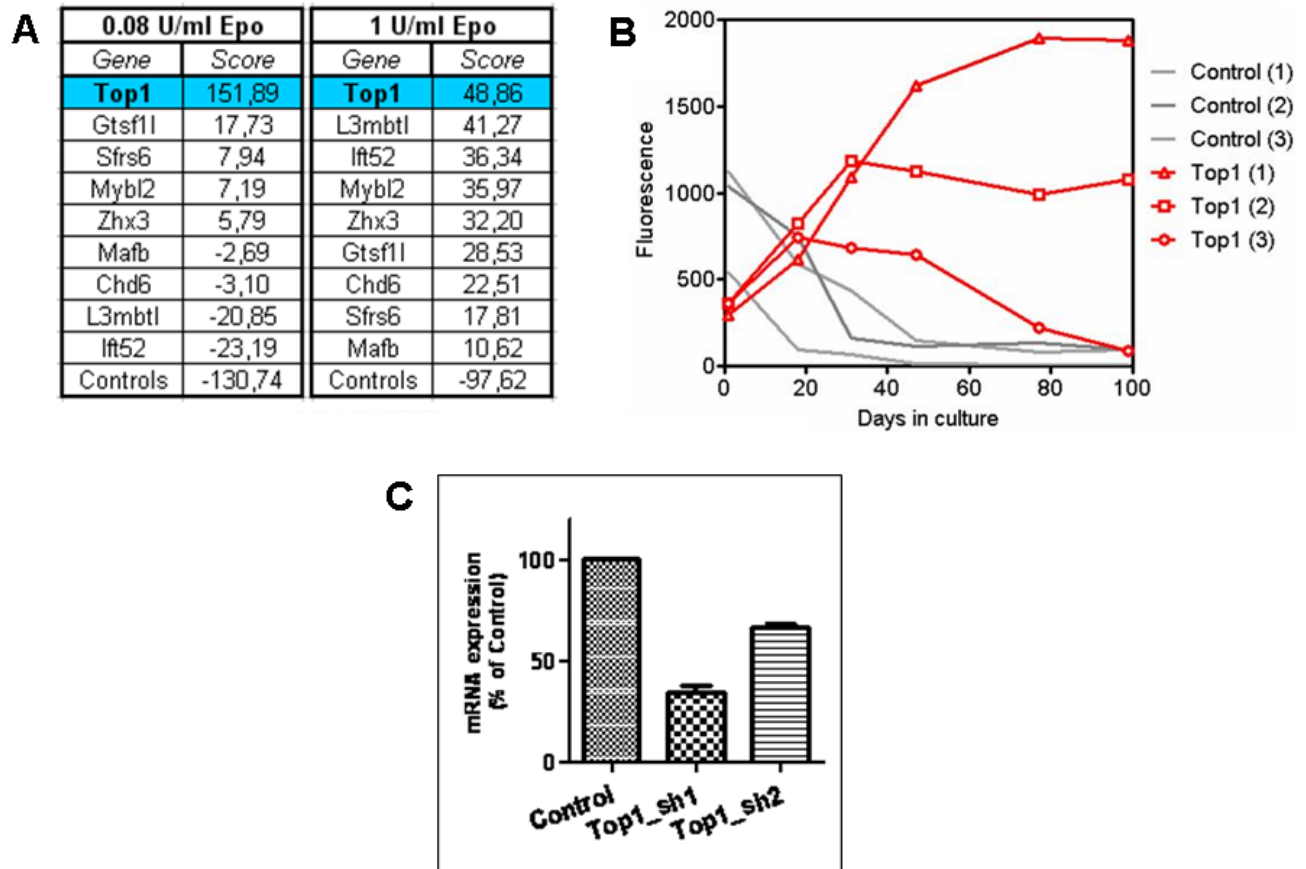| 0.08 U/ml Epo		1 U/ml Epo	
Gene	*Score*	*Gene*	*Score*
Top1	**151,89**	**Top1**	**48,86**
Gtsf1l	17,73	L3mbtl	41,27
Sfrs6	7,94	Ift52	36,34
Mybl2	7,19	Mybl2	35,97
Zhx3	5,79	Zhx3	32,20
Mafb	-2,69	Gtsf1l	28,53
Chd6	-3,10	Chd6	22,51
L3mbtl	-20,85	Sfrs6	17,81
Ift52	-23,19	Mafb	10,62
Controls	-130,74	Controls	-97,62

Figure 4.2.5.4. Identification of cytokine hypersensitivity based proliferative advantage of *Top1* knock-down cells in a competitive screen. (A) Cumulative score based on summing up ascending and descending slopes of the trend of relative abundance of bar-codes in the pool over 50 days. Score is depicted for all nine del20q target genes expressed in the hematopoietic system. Each gene was targeted by three different shRNA constructs. Three different control constructs, having a bar-code but no shRNA were spiked into each experimental replicate (Controls). The two tables represent two independent experiments at low (0.08 U/ml) and medium (1 U/ml) erythropoietin, each of the two experiements is based on three biological replicates. **(B)** Representative graphical display of *Top1* and Control constructs in one of the three biological replicates at 0.08 U/ml erythropoietin. Two different *Top1* shRNAs (*Top1* (1) and *Top1* (2) start to dominate after day 20 post pooling. A third *Top1* shRNA (*Top1* (3)) and three Control constructs (bar-coded, no shRNA) do not positively effect proliferation and are therefore out-competed. For reason of clearness, other constructs in the pool are not shown. Fluorescence values are arbitrary based on the readout on the Luminex XMap beads. **(C)** Validation of knock-down efficiency. The two *Top1* shRNA constructs successful in the screen effectively reduce *Top1* mRNA level in Baf3/EPO cells. *Top1* mRNA expression was determined by real-time PCR and was normalized with the expression level of *Hprt1* mRNA. The shRNA constructs directed against *Top1* were compared with a bar-coded empty control (Control) in each three independent experiments. The lentiviral shRNA construct shows a knock-down efficiency of approximately 60% and 40%, respectively

We could further validate the tumor suppressor features of *Top1* in a competitive proliferation assay, where we assayed cells transduced with the two different effective shRNA constructs

for their ability to outgrow cells transduced with control constructs. Mixing *Top1* knock-down cells with control cells in a one to one ratio, we reproducibly observed both *Top1* knock-downs to proliferate better under reduced cytokine concentrations, resulting in a significant shift of the ratio towards the knock-down cells (Figure 4.2.3.5).
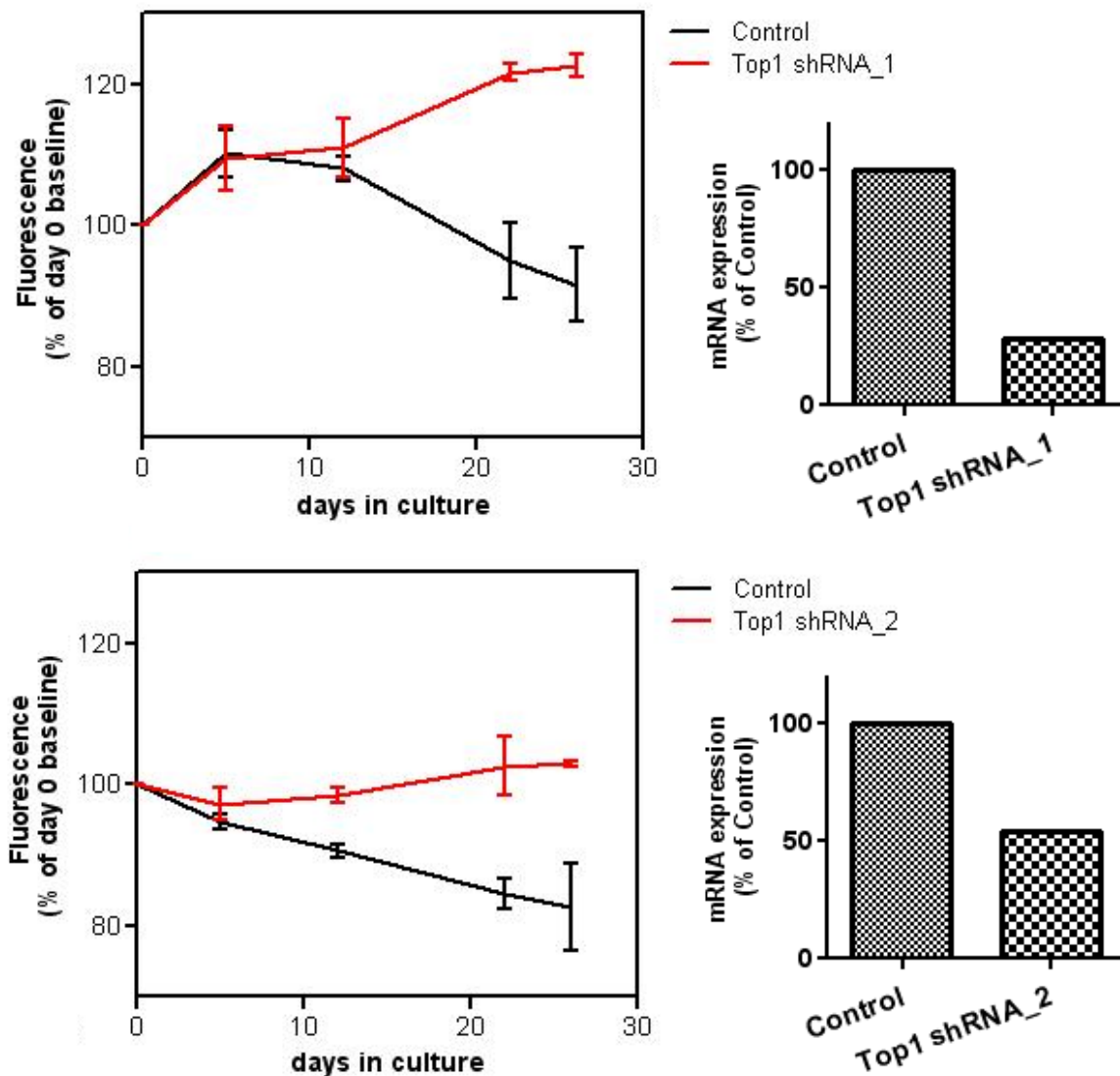
Figure 4.2.5.5. Validation of Top1 tumor suppressor features in Baf3/EPO cells. Cells transduced with Top1 shRNAs effective in the screen, either Top1 shRNA_1 or Top1 shRNA_2 were plated in a one to one ratio with control cells (Control). Arbitrary fluorescence units (Fluorescence) corresponding to the abundance of the bar codes over a time of 26 days are shown in percent of the baseline from DNA taken on day 0. Statistical analysis applying two-way ANOVA revealed a significant difference between control and *Top1* knock-down for both Top1 shRNA constructs. Bonferroni posttest revealed significant differences (P<0.001) after culture day 22 and 12 for Top1 shRNA_1 and Top1 shRNA_2, respectively. Both setups show the mean (±SD) of three independent biological replicates. Knock-down efficiency was validated *by* real-time PCR, comparing Top1 mRNA expression in knock-down cells (Top1 shRNA_1 and Top1 shRNA_2) to control cells (Control), both normalized with the expression level of *Hprt1* mRNA.

4.2.6. **TOP1 is outside of the del20q CDR assembled from two patient cohorts**

In parallel to the functional approaches described in 4.2.4. and 4.2.5., both based on common deleted regions assembled from the literature [115, 17, 141], we aimed to map our own combined Vienna-Pavia del20q CDR. Therefore, we assayed all del20q events identified through different screening methods (see 4.2.1.) on Affymetrix 6.0 SNP genotyping microarrays, providing us exact mapping data for the deletion breakpoints. In total we could analyze four del20q patients from the Vienna cohort (117, 146, 384, 446) and 5 patients from Pavia (Pav_ITA_Ang, Pav_Coh_147, Pav_Coh_153, Pav_Leu_15c, Pav_Coh_155), resulting in a 6.4 Mb CDR between the chromosome 20 physical positions 40.6 an 47 Mb (Figure 4.2.6.).
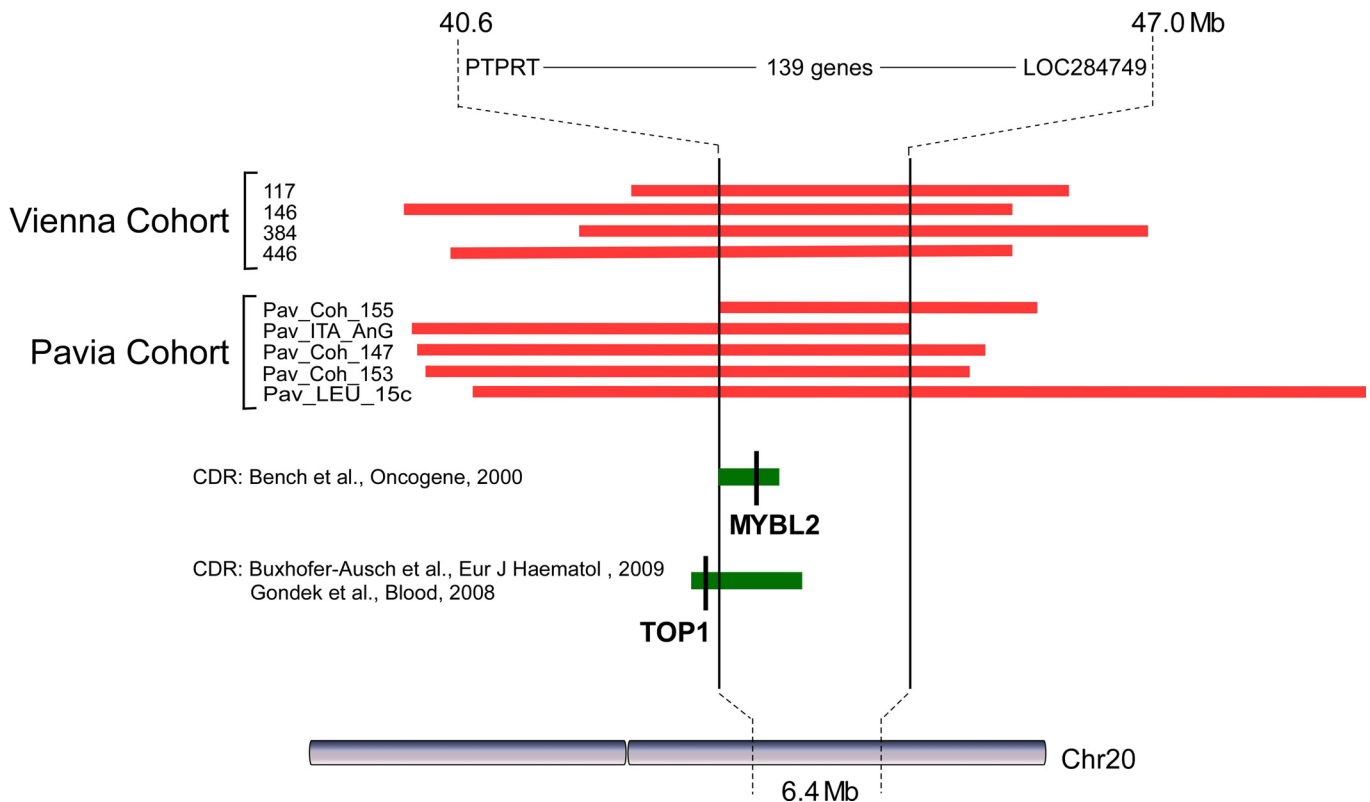
Figure 4.2.6. Mapping of the combined Vienna-Pavia MPN del20q CDR. Summary of the deletion analysis on chromosome 20 (Chr20) in the four Vienna and five Pavia del20q patients. Red horizontal bars indicate size and physical positon of each deletion. The common deleted region (physical position 40.6-47.9 Mb) is delineated with dotted line and contains 141 genes, from PTPRT to LOC284749. Green horizontal bars depict the CDRs derived from literature for the functional knock-down approached applied in chapters 4.2.4 and 4.2.5, the short black vertical lines depict the exact position of the MYBL2 and TOP1 genes within the CDRs.

The centromeric and telomeric breakpoints are upstream of the gene *PTPRT* and downstream of the hypothetical protein locus *LOC284749*, respectively, comprising 141 genes in total (Figure 4.2.6.). Comparing this CDR to the location of the newly identified putative tumor suppressors *MYBL2* and *TOP1*, *MYBL2* is located within the CDR, whereas the TOP1 locus is clearly upstream of the centromeric CDR-defining breakpoint and therefore outside of the del20q CDR (Figure 4.2.6.).

5. DISCUSSION

5.1. Ikaros defects in MPN at transformation to AML

We have studied the clonal genetic alterations in MPN at the time of leukemic transformation in a small cohort of patients using high-resolution SNP arrays. Chromosome 7p deletions emerged as a novel recurrent defect and by mapping the common deleted region we identified the *IKZF1* gene as the target of these deletions. Further examination of the frequency of *IKZF1* deletions in chronic phase MPN revealed a significant association of *IKZF1* deletions with leukemic transformation, which was replicated in an independent MPN patient cohort. In summary, hemizygous loss of *IKZF1* (including monosomy 7) was detected in 21% of post-MPN leukemia and 0.2% of non-leukemic MPN patients. We identified only one patient with *IKZF1* deletion that did not progress to leukemia but had advanced phase PMF as well as several other complications.

The transcription factor Ikaros encoded by the *IKZF1* gene has a pleiotropic function in the regulation of hematopoiesis [142, 143]. Complete or partial deficiency of Ikaros function in mice induced multiple hematopoietic defects including lymphoproliferative disorders and B- and T-cell leukemia [137-139, 144]. Multiple defects were also observed in the myeloid lineages, such as anemia and thrombocythemia [145]. Mice haploinsufficient for the transcription factor c-Myb exhibited similar myeloid abnormalities associated with a marked reduction of Ikaros mRNA expression [146]. These functional studies in mouse models strongly suggest that decreased Ikaros function is oncogenic. In accordance with the mouse phenotypes, defects in the *IKZF1* gene have been seen at high frequencies in human B- and T-cell malignancies. Specifically, a dominant negative isoform of Ikaros (Ik6) was detected in lymphoid malignancies attributed to aberrant splicing of *IKZF1* mRNA [137, 147, 148]. Most recently *IKZF1* deletions were found in approximately 84% of BCR-ABL positive acute lymphoid leukemia (ALL) [149]. Deletions of various sizes were detected on chromosome 7p including frequent intragenic deletions of *IKZF1* between exons 3 and 6 responsible for the expression of the Ik6 Ikaros isoform [149]. In our study we observed intragenic deletions in two cases but none of these was predicted to produce the Ik6 isoform. In the vast majority of ALL cases, only hemizygous deletions of

IKZF1 were found, similar to our findings in MPN. Although point mutations of *IKZF1* were detected in a few cases of chronic myeloid leukemia in lymphoblastoid crisis, their frequency was reported to be low [149, 150]. Accordingly, we did not detect any sequence alterations of *IKZF1* in post-MPN leukemia with or without *IKZF1* deletions.

It is still unclear exactly how Ikaros haploinsufficiency promotes the development of myeloid leukemia in MPN, although several hypotheses arise. As we detected *IKZF1* deletions in multiple cell types including progenitor cells and terminally differentiated granulocytes, it is unlikely that Ikaros haploinsufficiency induces differentiation arrest in the myeloid compartment (Figure 5.1.1.A). However, since anemia was present in 5 of 7 MPN patients with *IKZF1* deletion, it is possible that erythroid commitment might be impaired in these patients in accordance with the murine data [145].

We found that the *IKZF1* deletion was acquired as a late event in the clonal evolution of myeloid progenitors, occurring after the acquisition of JAK2-V617F and del13q. Due to the strong association of the *IKZF1* deletion with the transformation event, it is likely that after deletion of *IKZF1* myeloid progenitors acquire an increased susceptibility for transformation (Figure 5.1.1A). This may occur due to increased chromosomal instability as all MPN patients with *IKZF1* deletions displayed multiple cytogenetic defects (Table 4.1.1.). Another possible mechanism is the involvement of Ikaros in the JAK/STAT signaling pathway. Mutations of the Jak2 kinase that lead to dramatic increase in its kinase activity (such as *JAK2* fusions, JAK2-T875N and JAK2-R683) have been directly implicated in leukemogenesis [151-159]. The possible interaction of Ikaros with the JAK/STAT pathway in leukemic transformation is underlined by recent findings in childhood ALL, where *JAK* mutations (in particular *JAK2* mutations) were significantly associated with *IKZF1* defects [65]. In this study *IKZF1* lesions were present in 70% of *JAK* mutation positive, but in only 25.7% of *JAK* mutation negative pediatric ALL cases [65]. A functional insight into the possible involvement of Ikaros in the JAK/STAT pathway is provided by a study where cells expressing the dominant negative Ikaros isoform were shown to exhibit increased Jak2 and Stat5 phosphorylation as well as cytokine hypersensitivity [140].
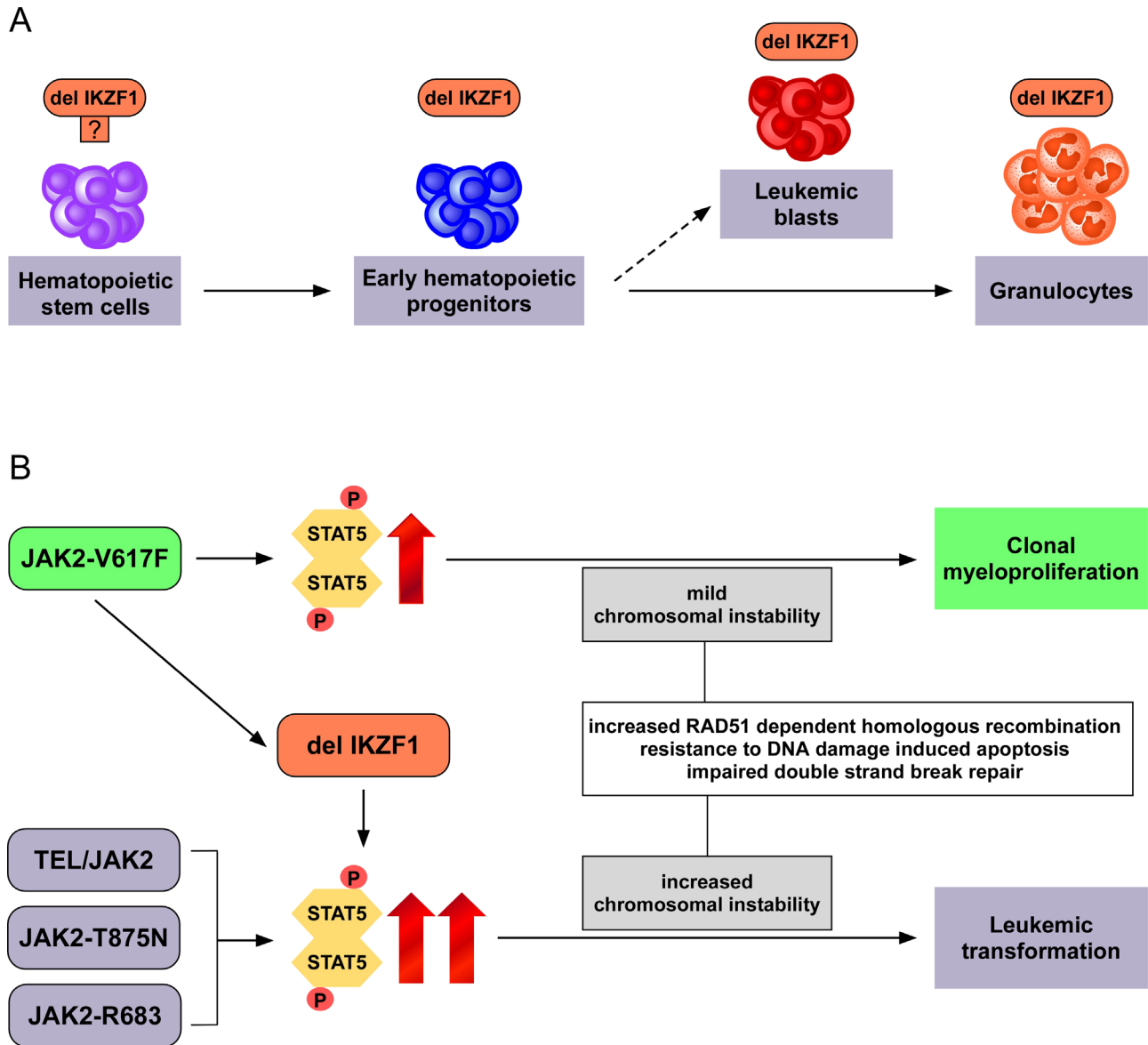
Figure 5.1.1. Model of Ikaros induced leukemic transformation in MPN (A) Deletion of *IKZF1* (del IKZF1) is present in early progenitors, terminally differentiated granulocytes and likely also in the hematopoietic stem cells. Deletion of *IKZF1* does not induce differentiation arrest, but rather increases the likelihood of acquiring defects associated with leukemic transformation. **(B)** Acquisition of the JAK2-V617F mutation leads to increased phosphorylation of Stat5, resulting in mild chromosomal instability, clonal expansion and a myeloproliferative phenotype. Ikaros deficiency additively elevates the level of pSTAT5 that further increases chromosomal instability. Leukemic transformation is triggered by strong JAK2 mutants (TEL/JAK2, JAK2-T875N and JAK2-R683) and mild mutants (JAK2-V617F) combined with additional somatic mutations (del IKFZ1). Stat5 hyperphosphorylation induced chromosomal instability is the key factor in the transformation process. Increased JAK/STAT activity is known to increase RAD51 dependent homologous recombination, induce resistance to DNA damage induced apoptosis (58) and increase the frequency of DNA double strand breaks (59).

Similarly, we could induce cytokine hypersensitivity of mouse primary progenitors with shRNA-mediated Ikzf1 deficiency. We also showed that the cytokine hypersensitivity induced by Ikzf1 deficiency is associated with elevated pStat5 levels in primary mouse progenitors (Figure 4.1.8.1 – 4.1.8.2.).

There exists both JAK2-V617F-dependent and -independent pathways of leukemogenesis in MPN since leukemic cells are often JAK2-V617F negative in otherwise JAK2-V617F positive patients [128, 129]. Ikaros deficiency might contribute to JAK2-V617F dependent leukemogenesis by further increasing the activity of the JAK/STAT pathway (Figure 5.1.1B). Increased activity of the JAK/STAT pathway due to presence of JAK2 mutations (TEL-JAK2 fusion, JAK2-V617F) was shown to induce genomic instability by increasing Rad51-dependent homologous recombination [100], elevating resistance to DNA damage induced apoptosis [160] and increasing the frequency of DNA double strand breaks (Figure 5.1.1.B) [161]. Stat5 phosphorylation plays a central role in these processes, as Stat5 was shown to directly transactivate the *RAD51* promoter in cells transformed with the TEL-JAK2 fusion protein [162]. Increased Rad51 level facilitates homologous recombination [163]. Further, Stat5 positively regulates the anti-apoptotic function of Bcl-xl [164-166] and is essential for transformation in JAK2-V617F and BCR-ABL mouse models [167, 168]. Increased Stat5 phosphorylation as a consequence of Ikaros deficiency (Figure 4.1.8.1 – 4.1.8.2.) might deregulate those pathways resulting in elevated transformation likelihood in MPN (Figure 5.1.1B).

Alternatively, a recent report on a nuclear function of JAK2 showed that constitutively active JAK2 causes unregulated displacement of heterochromatin protein 1α (HP-1α) [169]. HP-1α is known to have potential tumor suppressive functions such as reduction and control of mitotic recombination [170, 171], transcriptional repression within the heterochromatin [172] and functions in DNA repair [173]. As Ikaros is known to have a role in the recruitment and positioning of HP-1α [174], loss of Ikaros might have an additive effect on this deregulation further contributing to JAK2-V617F induced phenotypes (Figure 5.1.2.).
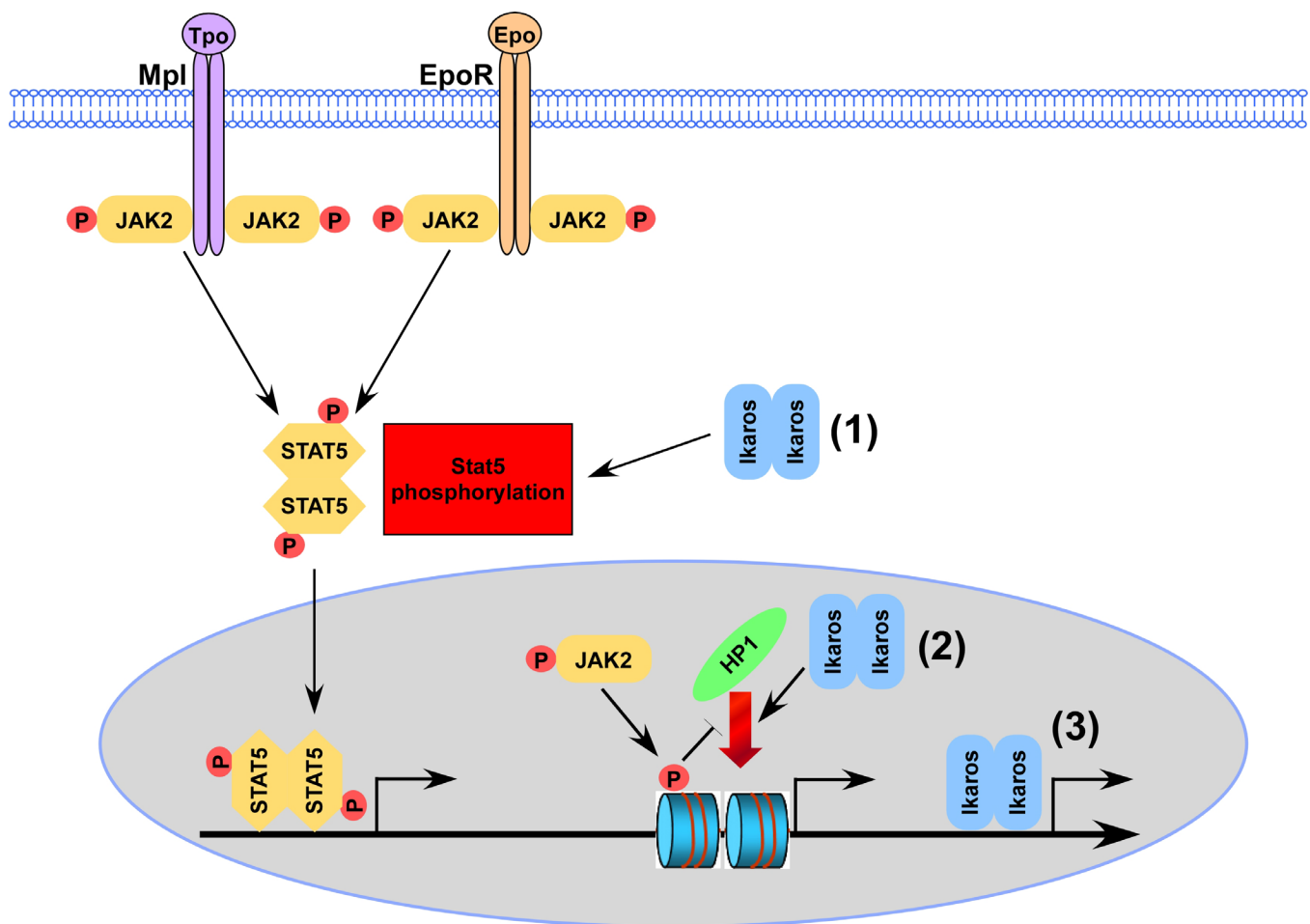
Figure 5.1.2. Possible mechanisms of Ikaros defects affecting gene transcription Ikaros deficiency induces increased Stat5 phosphorylation (1), resulting in deregulation of Stat5-dependent pro-proliferative gene transcription and induction of chromosomal instability. Alternatively, Ikaros is known to have a role in the recruitment and positioning of HP-1α (2). Loss of Ikaros might have an additive effect on hyperphosphorylated, constitutively active JAK2, that has been found to cause unregulated displacement of the potential tumor suppressor HP-1α. Further, Ikaros in its primary function as transcription factor (3) might have various direct transcriptional targets playing a role in growth control and/or maintenance of chromosomal stability

Monosomy 7 is a recurrent cytogenetic aberration in about 10% of adult and 5 % of childhood AML cases [175, 176]. Of the seven patients in our study exhibiting loss of *IKZF1*, two had monosomy 7. This result suggests that *IKZF1* may be the main tumor suppressor gene affected by monosomy 7. Monosomy 7 is a valuable prognostic marker in AML [97], and chromosome 7 defects are prominent cytogenetic lesions in PMF, present at increasing frequency after leukemic transformation [177]. Monosomy 7 and chromosome 7 deletions were

found to be associated with unfavorable prognosis in PMF [178]. Similarly, *IKZF1* deletions are associated with a very poor outcome and high relapse rate in B-cell ALL [179, 180]. The prognostic value of *IKZF1* loss in chronic phase MPN is limited since *IKZF1* deletions are rare in these patients. This is most likely due to rapid onset of leukemia after del7p acquisition. Although deletions targeting *IKZF1* were shown to be present at high frequencies in ALL, these defects have not yet been observed in de novo AML [150], or in other myeloid disorders. Our results show that deletions of *IKZF1* occur in 21% of post-MPN AML patients. Thus, Ikaros plays an important role not only in lymphoid malignancies but also in myeloid leukemogenesis especially if preceded by MPN.

5.2. Putative tumor suppressors in the del20q CDR

Besides Ikaros defects, we have studied one of the most frequent chromosomal aberrations in chronic phase MPN, which are deletions on chromosome 20q (del20q). We characterized three independent MPN patient cohorts (a total of 822 patients) for del20q, determined the role of del20q in the evolution of the malignant clone and described a multiple acquisition of the defect in the same patient. We further identified *MYBL2* and *TOP1* as two putative tumor suppressors on 20q by mimicking haploinsufficiency using different shRNA knock-down strategies in vitro. Assembling a del20q common deleted region (CDR) using microarray karyotyping of nine patients, we could see *TOP1* outside of the CDR, questioning the exclusive relevance of CDR mapping for the search for tumor suppressors in this genomic region.

The frequency of del20q in MPN is reported to be 5-10% [11, 20, 112-115], depending on the patient cohort analyzed. Our unbiased screen for del20q patients in three independent patient cohorts (Vienna, Austria; Pavia, Italy; Brno; Czech Republic) revealed much lower frequencies between 0% and 2%, with an average of 1.1%. This is likely to be due to the fact that we were using granulocyte DNA. Analyzing DNA representative for the whole granulocyte pool in the peripheral blood allowed us to detect the defect only if it is present in a substantial amount of cells. Thus, minor clones cannot be detected below a certain

threshold. Reports of higher frequencies are often based on single bone marrow cell analysis. The low frequencies in our granulocyte analysis are in accordance with previous reports, where the del20q clone was present in the bone morrow, but was absent in peripheral blood granulocytes. Clonal dominance has been observed to differ between the bone marrow stem cell pool and the peripheral blood [121]. However, information on bone marrow and peripheral blood both might provide important conclusions for MPN genetics.

MPN is characterized by genetic heterogeneity, showing a large variability of somatic mutations and chromosomal aberrations. Moreover, acquisition of several defects in the same patient results in a complex clonal diversity among patients. A multiple acquisition of the V617F mutation was observed to be present in the two different JAK2 alleles in the same clone [99]. There are reports about simultaneous presence of JAK2-V617F and MPL-W515L/K, and JAK2-V617F and JAK2 exon 12 mutations [37, 181] in the same patient, the latter pair proven to occur in two different clones [181]. Similarly, we could show that also del20q can be acquired multiple times in the same patient in different clones (Figures 4.2.2.1. and 4.2.2.2.). The facts that del20q is a non-phenotypic mutation [16] observed to occur before JAK2-V617F [125] might suggest a role for del20q in initiation of clonal hematopoiesis and chromosomal instability [2]. However, since del20q is acquired at increased frequency it is more likely that other factors, mutations or hereditary predispositions, are responsible for inducing the accumulation of genetic lesions such as del20q. JAK2-V617F was suggested to be such a factor responsible for chromosomal instability [100]. However, in patient 102, one of the del20q events occurred in a JAK2-V617F–negative cell (Figure 4.2.2.1), and patient 346 was negative for JAK2-V617F (Figure 4.2.2.1), suggesting that in these patients genomic instability is independent of JAK2-V617F.

Determining the order of acquisition of genetic lesions in the malignant clone is crucial for understanding the role of those defects. In a previous report of patients with del20q and JAK2-V617F it was shown that the size of the del20q clone by far exceeded the size of the clone carrying JAK2-V617F, suggesting that del20q preceded the acquisition of the JAK2-V617F mutation [125]. Our investigations on progenitor cell level now showed that the del20q

can occur also after JAK2-V617F (Figure 4.2.2.1.), arguing against the hypothesis that del20q represents a predisposing event for JAK2-V617F.

Mapping of common deleted regions recently led to the identification of TET2 and CBL defects in MPN, located on chromosomes 4q and 11q, respectively [38, 39]. Those two defects could be identified by detection of lesions targeting a single gene only. Huge efforts to achieve the same for del20q did not succeed yet. So far, high resolution microarray karyotyping failed to validate previously reported CDRs based on classical cytogenetic methods such as G-Banding and FISH. Assembling the mapping events recently reported by different groups [89, 108] and our own data combined from two patient cohorts (Vienna-Pavia) reveals most deletions to be rather large (Figure 5.2.). Thus, a CDR is unlikely to be defined by a single gene as it was the case for IKZF1 on chromosome 7p or for the defects which led to the identification of TET2 and CBL. Looking at the assembled data in Figure 5.2., the alternative possibility of reducing a CDR, finding a small overlap of two large deletions close to the two opposed breakpoints (centromeric-telomeric) seems unlikely too. However, there is and indication for clustering around the CDR based on Bench et al. [115], and the CDR based on reports by Buxhofer-Ausch et al. [17] and Gondek et al. [141]. Those are also the CDRs we used for our RNAi-based screens for del20q tumor suppressors. In case that multiple tumor suppressors are present on 20q, CDR mapping may become irrelevant and may even generate false conclusions. Our data indicates that a functional approach is a better choice in such tumor suppressor loci.

The two knock-down approaches mimicking haploinsufficiency for the del20q target genes led us to the identification of tumor suppressor features of *MYBL2* and *TOP1* in Baf3/EPO cells. Combining this functional data derived from in vitro studies with the genetic data from patient material, we could see *MYBL2* not only within the literature-derived CDRs, but also within the CDR base on our own Vienna-Pavia mapping data (Figure 5.2.). However, *TOP1* mapped outside of this CDR, thus, having today's knowledge, it would not have be included into a functional knock-down screen based on a CDR. It is therefore questionable whether tumor suppressors within a region relevant for the outgrowth of a malignant cell in any cancer should be assumed to be located exclusively within the CDR. Still, it is highly likely that there

is a tumor suppressor also within the CDR, especially if the deletion events are clustering around the CDR, as it is the case for MPN (Figure 5.2.).
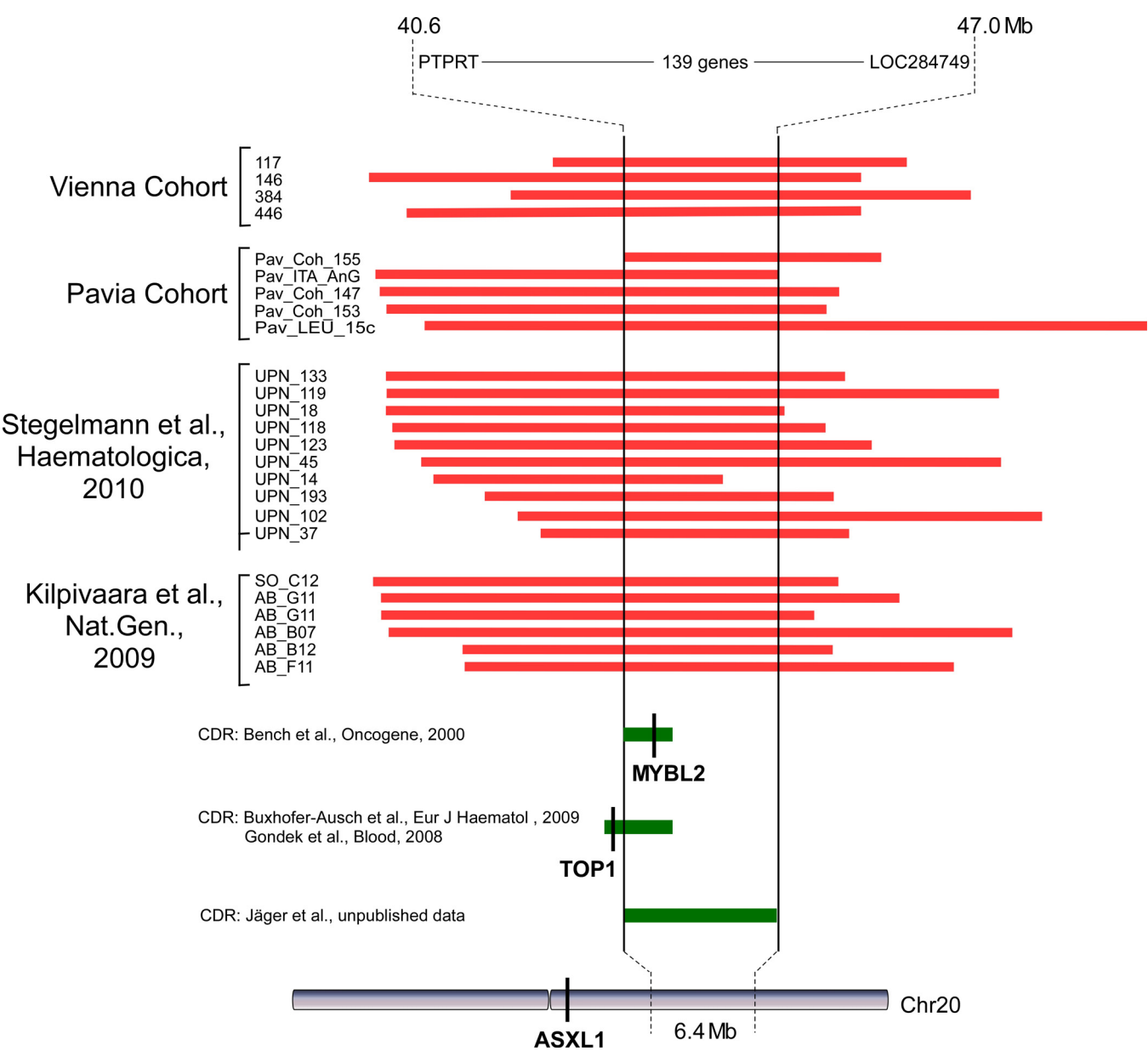
Figure 5.2. Assembled del20q CDRs and their relation to the putative tumor suppressors Our own mapping data (Vienna Cohort, Pavia Cohort) is shown together with the recently published del20q mapping in large cohorts by Stegelmann et al. and Kilpivaara et al. Red horizontal bars indicate size and physical positon of each deletion. The Vienna-Pavia common deleted region (physical position 40.6-47.0 Mb) contains 141 genes, from *PTPRT* to *LOC284749*. Green horizontal bars depict the CDRs derived from literature for the functional knock-down approached applied in chapters 4.2.4 and 4.2.5 and the CDR from our own Vienna-Pavia mapping (Jäger et al., unpublished data). The short black vertical lines depict the exact position of the MYBL2, TOP1 and ASXL1 genes in relation to the CDRs and chromosome 20q.

Nevertheless, there can be additional tumor suppressors outside the CDR, acting either alone or in combination with each other. A strong argument for several tumor suppressors on chromosome 20q is that in most cases del20q is a relatively large defect. Another finding in favor of additional 20q tumor suppressors is the identification of *ASXL1* mutations in patients suffering from myeloid malignancies [182]. *ASXL1* belongs to the enhancer of trithorax and polycomb gene family and is located on chromosome 20q close to the centromer, far outside of the Vienna-Pavia CDR (Figure 5.2.). Truncation exon 12 mutations have recently been described in 11% of patients with MDS, 43% of those with CMML, 7% with primary and 47% with secondary AML [182]. ASXL1 is thought to include a dual activator and suppressor activity toward transcription, including repression of retinoic and acid receptor-mediated transcription. It is still not clear whether *ASXL1* defects involve loss of tumor suppression or aberrant retinoic acid receptor signaling [183], thus, its relation to del20q and the newly identified putative tumor suppressors *MYBL2* and *TOP1* remains to be defined.

MYBL2, also known as *B-MYB*, is a member of the MYB transcription factor family. It has an essential function during embryonic development and is of general importance during the cell cycle [184]. In zebrafish, the "crash&burn " mutation in the Mybl2 homologue results in increased cancer susceptibility, defects in mitotic progression and spindle formation and genomic instability [185]. Investigations on the drosophila Mybl2 homologue revealed its presence in a transcriptional repressor complex with E2F2/RBF, pointing to a role in negative regulation of progression from G1 to S-phase in the cell cycle. Furthermore, drosophila Mybl2 was found to be involved in a more general regulation of S and M phase, being important for maintenance of chromosomal instability [186]. In accordance with that, the human Mybl2 protein was shown to be essential for S-phase progression and genomic stability in megakaryocytes [135].

TOP1 is encoding the topoisomerase I protein, a catalytic enzyme recognized for its key role in relaxing supercoiled DNA. Thus, the Top1 protein is involved in cellular processes, including DNA replication, transcription, recombination, and chromosome condensation [187]. Interestingly, the Top1 protein has also been reported to function as a splicing factor kinase

[188, 189], a transcriptional cofactor [190-192], and a p53 interacting protein [193, 194]. In contrast to *MYBL2, TOP1* defects were shown to be directly implicated in cancer. A NUP98-*TOP1* fusion is the result of the t(11;20)(p15;q11) chromosomal translocation associated with therapy-related myelodysplastic syndrome[195, 196]. A murine model of NUP98-*TOP1* shows a potent in vitro growth advantage and a block in differentiation in hematopoietic precursors, evidenced for a competitive growth advantage and a severe leukemia phenotype. However, there is strong evidence that these features are caused rather by complex effects of the fusion then by a translocation-caused TOP1 loss-of-function [197]. Furthermore, point mutations in TOP1 were found in patients with non-small cell lung cancer [198].

We could show clear tumor suppressor features for both *MYBL2* and *TOP1* in Baf3/Epo cells using different shRNA-based stable and transient knock-down strategies (Chapters 4.2.4 and 4.2.5.). Both candidate genes are prominently expressed three human hematopoietic compartments (CD34+, CD34- mononuclear cells and granulocytes) as well as in both murine progenitors (lin-) and differentiated (lin+) bone marrow (Figures 4.2.3.2, 4.2.5.1. and 4.2.5.2.). The proliferative advantage caused by the knock-downs is cytokine dependent, proving the relevance of the system for mimicking an MPN-associated defect, as cytokine hypersensitivity is the basis of MPN pathogenesis [20]. However, the direct link of *MYBL2* and *TOP1* defects to the disease is still missing, to date, no point mutations or other genetic defects restricted to those two putative tumor suppressors have been reported. It still remains to be elucidated whether those defects can be found in MPN patients and whether *MYBL2* and *TOP1* are acting as tumor suppressors not only in vitro but also in vivo.

5.3. Genetic complexity in MPN and implications for therapy

Our data of del20q occurring after JAK2-V617F in some patients weakens the putative role of del20q in initiation of clonal hematopoiesis and chromosomal instability. Furthermore, the clear presence of germ line predispositions in MPN pathogenesis decreases optimism for the identification of specific somatic lesions as the initial event responsible for this increased

mutability in MPN cells. However, regardless of its germ line or somatic origin, increased mutability in MPN leads to accumulation of chromosomal aberrations and oncogenic mutations. As also we could observe, multiple deletion events, independent progenitor clones and independently acquired combinations of mutations are often observed in the same patient [98, 99]. However, further investigations on the progenitor cell level will be required to examine all known defects in MPN for their role in the hierarchy of genetic lesions.

One key step in understanding the interaction of these genetic defects is to characterize their phenotypic role in MPN pathogenesis. Although contribution to clonal expansion is common to all defects present in the MPN clone, not all of them seem to be able to trigger a specific disease phenotype. At the time when patients present with hematological symptoms, the clone carrying oncogenic mutations such as JAK2-V617F has already reached a certain impact on blood production. Opposed to the phenotypic oncogenic mutations, a group of non-phenotypic mutations, beyond them del20q, do not trigger a specific hematological phenotype but rather contribute only to the increased growth potential of the progenitors [16].

When considering therapeutic approaches for MPN patients, it might be necessary to target the phenotype-inducing oncogenic mutations. JAK2-V617F is the most prominent oncogenic mutation in MPN and an obvious therapeutic target due to its uniformity and frequency in patients. Additionally, there is increasing evidence for a role of the JAK-STAT pathway as a common interface also for other defects in MPN as we could show for the Ikaros deletions. Moreover, there is evidence also that *CBL* defects result in activation of JAK-STAT signaling [81, 202]. Therefore, targeting the JAK-STAT pathway might provide a general benefit for reduction of myeloproliferation for a broader spectrum of genetic defects.

Specific inhibition of wild type *Jak2* or its V617F mutant protein turned out to be more complicated than expected when compared to the use of imatinib in CML [203]. However, Jak2 inhibitors are already undergoing clinical testing and the results seem to be promising [204]. "Addiction" of the MPN clone to survival mediated by the JAK-STAT signaling pathway can make the clone particularly sensitive to an anti-Jak2 therapy, and therefore makes Jak2 inhibition a promising therapeutic approach for patients carrying any of the defects related to

the JAK-STAT pathway. However, inhibition of mutant Jak2 may result in a competitive advantage of JAK2-V617F negative cells, which, based on the presence of a "mutator phenotype", might subsequently acquire other mutations, eventually resulting in resistance phenotypes or even acute malignancies such as AML. In addition, inhibitors targeting Jak2 often inhibit other kinases, which may facilitate the clonal outgrowth of cells acquiring additional leukemogenic mutations in different kinases such as Flt3, having a well described role in leukemia. As already mentioned in the context of Ikaros deletions, post-MPN leukemic transformation in patients positive for JAK2-V617F has been shown to frequently arise on a JAK2-V617F-negative background [128, 129].

Although targeting the phenotypic mutations should eliminate symptoms and complications, it remains to be seen whether molecular remission will result in a complete cure, including restoration of polyclonal hematopoiesis. For that happening, it will be necessary to target the primary clone in the patient's hematopoietic stem cell compartment. Targeting mutations acquired in a later differentiation stage or on already clonal background might significantly lower the success rate of therapy. The chances of complete cure might vary between patients, particularly as the amount and combination of genetic lesions and the putative presence of a mutator phenotype might define the power of the malignant clone. Besides targeting Jak2, it might be necessary to control clones harboring other lesions as they may further mutate and undergo selection in the presence of Jak2 inhibitors. Due to the genetic complexity in MPN this will require individualized therapeutic approaches based on a full characterization of the defects present in the patient's myeloid compartment. The question is whether this is feasible or whether general myelosuppression using currently applied classical cytoreductive drugs such as interferon alpha will turn out to be the most reasonable approach in future.

REFERENCES

1.   Jaffe ES, Harris NL, Stein H. World Health Organization Classification of Tumours. Pathology and Genetics of Tumours of Haematopoietic and Lymphoid Tissues. Lyon: IARC Press; 2001.

2.   Campbell PJ, Green AR. The myeloproliferative disorders. N Engl J Med 2006;355:2452-66.

3.   Tefferi A, Gilliland G. Classification of chronic myeloid disorders: from Dameshek towards a semi-molecular system. Best Pract Res Clin Haematol 2006;19:365-85.

4.   Passamonti F, Rumi E, Pungolino E, et al. Life expectancy and prognostic factors for survival in patients with polycythemia vera and essential thrombocythemia. Am J Med 2004;117:755-61.

5.   Cervantes F, Passamonti F, Barosi G. Life expectancy and prognostic factors in the classic BCR/ABL-negative myeloproliferative disorders. Leukemia 2008;22:905-14.

6.   Spivak JL. Polycythemia vera: myths, mechanisms, and management. Blood 2002;100:4272-90.

7.   Hibbin JA, Njoku OS, Matutes E, Lewis SM, Goldman JM. Myeloid progenitor cells in the circulation of patients with myelofibrosis and other myeloproliferative disorders. Br J Haematol 1984;57:495-503.

8.   Tefferi A. Myelofibrosis with myeloid metaplasia. N Engl J Med 2000;342:1255-65.

9.   Passamonti F, Rumi E, Arcaini L, et al. Prognostic factors for thrombosis, myelofibrosis, and leukemia in essential thrombocythemia: a study of 605 patients. Haematologica 2008;93:1645-51.

10.   Tefferi A. Essential thrombocythemia, polycythemia vera, and myelofibrosis: current management and the prospect of targeted therapy. Am J Hematol 2008;83:491-7.

11.   Reilly JT, Snowden JA, Spearing RL, et al. Cytogenetic abnormalities and their prognostic significance in idiopathic myelofibrosis: a study of 106 cases. Br J Haematol 1997;98:96-102.

12.   Cervantes F, Pereira A, Esteve J, et al. Identification of 'short-lived' and 'long-lived' patients at presentation of idiopathic myelofibrosis. Br J Haematol 1997;97:635-40.

13.   Rossi D, Deambrogi C, Capello D, et al. JAK2 V617F mutation in leukaemic transformation of philadelphia-negative chronic myeloproliferative disorders. Br J Haematol 2006;135:267-8.

14.   Murphy S, Peterson P, Iland H, Laszlo J. Experience of the Polycythemia Vera Study Group with essential thrombocythemia: a final report on diagnostic criteria, survival, and leukemic transition by treatment. Semin Hematol 1997;34:29-39.

15.   Sterkers Y, Preudhomme C, Lai JL, et al. Acute myeloid leukemia and myelodysplastic syndromes following essential thrombocythemia treated with hydroxyurea: high proportion of cases with 17p deletion Blood 1998;91:616-22.

16.   Kralovics R. Genetic complexity of myeloproliferative neoplasms. Leukemia 2008;22:1841-8.

17.   Buxhofer-Ausch V, Gisslinger H, Berg T, Gisslinger B, Kralovics R. Acquired resistance to interferon alpha therapy associated with homozygous MPL-W515L mutation and chromosome 20q deletion in primary myelofibrosis. Eur J Haematol 2009;82:161-3.

18.   Gangat N, Wolanskyj A, McClure R, et al. Risk stratification for survival and leukemic transformation in essential thrombocythemia: a single institutional study of 605 patients. Leukemia 2007;21:270-6.

19.   Finazzi G, Ruggeri M, Rodeghiero F, Barbui T. Second malignancies in patients with essential thrombocythaemia treated with busulphan and hydroxyurea: long-term follow-up of a randomized clinical trial. Br J Haematol 2000;110:577-83.

20.   Kralovics R, Skoda RC. Molecular pathogenesis of Philadelphia chromosome negative myeloproliferative disorders. Blood Rev 2005;19:1-13.

21.   Roder S, Steimle C, Meinhardt G, Pahl HL. STAT3 is constitutively active in some patients with Polycythemia rubra vera. Exp Hematol 2001;29:694-702.

22.   Pardanani A, Brockman SR, Paternoster SF, et al. FIP1L1-PDGFRA fusion: prevalence and clinicopathologic correlates in 89 consecutive patients with moderate to severe eosinophilia. Blood 2004;104:3038-45.

23.   Greipp PT, Dewald GW, Tefferi A. Prevalence, breakpoint distribution, and clinical correlates of t(5;12). Cancer Genet Cytogenet 2004;153:170-2.

24.   Golub TR, Barker GF, Lovett M, Gilliland DG. Fusion of PDGF receptor beta to a novel ets-like gene, tel, in chronic myelomonocytic leukemia with t(5;12) chromosomal translocation. Cell 1994;77:307-16.

25.   Garcia-Montero AC, Jara-Acevedo M, Teodosio C, et al. KIT mutation in mast cells and other bone marrow hematopoietic cell lineages in systemic mast cell disorders: a prospective study of the Spanish Network on Mastocytosis (REMA) in a series of 113 patients. Blood 2006;108:2366-72.

26.   Lauchle JO, Braun BS, Loh ML, Shannon K. Inherited predispositions and hyperactive Ras in myeloid leukemogenesis. Pediatr Blood Cancer 2006;46:579-85.

27.   Loh ML, Vattikuti S, Schubbert S, et al. Mutations in PTPN11 implicate the SHP-2 phosphatase in leukemogenesis. Blood 2004;103:2325-31.

28.   Shannon KM, O'Connell P, Martin GA, et al. Loss of the normal NF1 allele from the bone marrow of children with type 1 neurofibromatosis and malignant myeloid disorders. N Engl J Med 1994;330:597-601.

29.   Kralovics R, Passamonti F, Buser A, et al. A gain-of-function mutation of JAK2 in myeloproliferative disorders. N Engl J Med 2005;352:1779-90.

30.   Baxter EJ, Scott LM, Campbell PJ, et al. Acquired mutation of the tyrosine kinase JAK2 in human myeloproliferative disorders. Lancet 2005;365:1054-61.

31.   James C, Ugo V, Le Couedic JP, et al. A unique clonal JAK2 mutation leading to constitutive signalling causes polycythaemia vera. Nature 2005;434:1144-8.

32.   Levine RL, Wadleigh M, Cools J, et al. Activating mutation in the tyrosine kinase JAK2 in polycythemia vera, essential thrombocythemia, and myeloid metaplasia with myelofibrosis. Cancer Cell 2005;7:387-97.

33.   Scott LM, Tong W, Levine RL, et al. JAK2 exon 12 mutations in polycythemia vera and idiopathic erythrocytosis. N Engl J Med 2007;356:459-68.

34.   Pietra D, Li S, Brisci A, et al. Somatic mutations of JAK2 exon 12 in patients with JAK2 (V617F)-negative myeloproliferative disorders. Blood 2008;111:1686-9.

35.   Martinez-Aviles L, Besses C, Alvarez-Larran A, Cervantes F, Hernandez-Boluda JC, Bellosillo B. JAK2 exon 12 mutations in polycythemia vera or idiopathic erythrocytosis. Haematologica 2007;92:1717-8.

36.   Pikman Y, Lee BH, Mercher T, et al. MPLW515L is a novel somatic activating mutation in myelofibrosis with myeloid metaplasia. PLoS Med 2006;3:e270.

37.   Pardanani AD, Levine RL, Lasho T, et al. MPL515 mutations in myeloproliferative and other myeloid disorders: a study of 1182 patients. Blood 2006;108:3472-6.

38.   Grand FH, Hidalgo-Curtis CE, Ernst T, et al. Frequent CBL mutations associated with 11q acquired uniparental disomy in myeloproliferative neoplasms. Blood 2009;113:6182-92.

39.   Delhommeau F, Dupont S, Della Valle V, et al. Mutation in TET2 in myeloid cancers. N Engl J Med 2009;360:2289-301.

40.   Tefferi A, Lim KH, Abdel-Wahab O, et al. Detection of mutant TET2 in myeloid malignancies other than myeloproliferative neoplasms: CMML, MDS, MDS/MPN and AML. Leukemia 2009;23:1343-5.

41.   Druker BJ, Talpaz M, Resta DJ, et al. Efficacy and safety of a specific inhibitor of the BCR-ABL tyrosine kinase in chronic myeloid leukemia. N Engl J Med 2001;344:1031-7.

42.   Druker BJ, Sawyers CL, Kantarjian H, et al. Activity of a specific inhibitor of the BCR-ABL tyrosine kinase in the blast crisis of chronic myeloid leukemia and acute lymphoblastic leukemia with the Philadelphia chromosome. N Engl J Med 2001;344:1038-42.

43.   Shah NP, Tran C, Lee FY, Chen P, Norris D, Sawyers CL. Overriding imatinib resistance with a novel ABL kinase inhibitor. Science 2004;305:399-401.

44.   Kantarjian H, Sawyers C, Hochhaus A, et al. Hematologic and cytogenetic responses to imatinib mesylate in chronic myelogenous leukemia. N Engl J Med 2002;346:645-52.

45.   Kisseleva T, Bhattacharya S, Braunstein J, Schindler CW. Signaling through the JAK/STAT pathway, recent advances and future challenges. Gene 2002;285:1-24.

46.   Dameshek W. Some speculations on the myeloproliferative syndromes. Blood 1951;6:372.

47.   Levine RL, Belisle C, Wadleigh M, et al. X-inactivation-based clonality analysis and quantitative JAK2V617F assessment reveal a strong association between clonality and JAK2V617F in PV but not ET/MMM, and identifies a subset of JAK2V617F-negative ET and MMM patients with clonal hematopoiesis. Blood 2006;107:4139-41.

48.   Campbell PJ, Scott LM, Buck G, et al. Definition of subtypes of essential thrombocythaemia and relation to polycythaemia vera based on JAK2 V617F mutation status: a prospective study. Lancet 2005;366:1945-53.

49.   Antonioli E, Guglielmelli P, Pancrazzi A, et al. Clinical implications of the JAK2 V617F mutation in essential thrombocythemia. Leukemia 2005;19:1847-9.

50.   Jones AV, Kreil S, Zoi K, et al. Widespread occurrence of the JAK2 V617F mutation in chronic myeloproliferative disorders. Blood 2005;106:2162-8.

51.   Wolanskyj AP, Lasho TL, Schwager SM, et al. JAK2 mutation in essential thrombocythaemia: clinical associations and long-term prognostic relevance. Br J Haematol 2005;131:208-13.

52.   Campbell PJ, Griesshammer M, Dohner K, et al. V617F mutation in JAK2 is associated with poorer survival in idiopathic myelofibrosis. Blood 2006;107:2098-100.

53.   Tefferi A, Lasho TL, Schwager SM, et al. The JAK2(V617F) tyrosine kinase mutation in myelofibrosis with myeloid metaplasia: lineage specificity and clinical correlates. Br J Haematol 2005;131:320-8.

54.   Levine RL, Loriaux M, Huntly BJ, et al. The JAK2V617F activating mutation occurs in chronic myelomonocytic leukemia and acute myeloid leukemia, but not in acute lymphoblastic leukemia or chronic lymphocytic leukemia. Blood 2005;106:3377-9.

55.   Scott LM, Campbell PJ, Baxter EJ, et al. The V617F JAK2 mutation is uncommon in cancers and in myeloid malignancies other than the classic myeloproliferative disorders. Blood 2005;106:2920-1.

56.   Zhao R, Xing S, Li Z, et al. Identification of an acquired JAK2 mutation in polycythemia vera. J Biol Chem 2005;280:22788-92.

57.   Steensma DP, Dewald GW, Lasho TL, et al. The JAK2 V617F activating tyrosine kinase mutation is an infrequent event in both "atypical" myeloproliferative disorders and myelodysplastic syndromes. Blood 2005;106:1207-9.

58.   Jelinek J, Oki Y, Gharibyan V, et al. JAK2 mutation 1849G>T is rare in acute leukemias but can be found in CMML, Philadelphia chromosome-negative CML, and megakaryocytic leukemia. Blood 2005;106:3370-3.

59.   Tiedt R, Hao-Shen H, Sobas MA, et al. Ratio of mutant JAK2-V617F to wild-type Jak2 determines the MPD phenotypes in transgenic mice. Blood 2008;111:3931-40.

60.   Wernig G, Mercher T, Okabe R, Levine RL, Lee BH, Gilliland DG. Expression of Jak2V617F causes a polycythemia vera-like disease with associated myelofibrosis in a murine bone marrow transplant model. Blood 2006;107:4274-81.

61.   Rane SG, Reddy EP. JAK3: a novel JAK kinase associated with terminal differentiation of hematopoietic cells. Oncogene 1994;9:2415-23.

62.   Thomis DC, Gurniak CB, Tivol E, Sharpe AH, Berg LJ. Defects in B lymphocyte maturation and T lymphocyte activation in mice lacking Jak3. Science 1995;270:794-7.

63.   Walters DK, Mercher T, Gu TL, et al. Activating alleles of JAK3 in acute megakaryoblastic leukemia. Cancer Cell 2006;10:65-75.

64.   Saharinen P, Silvennoinen O. The pseudokinase domain is required for suppression of basal activity of Jak2 and Jak3 tyrosine kinases and for cytokine-inducible activation of signal transduction. J Biol Chem 2002;277:47954-63.

65.   Mullighan CG, Zhang J, Harvey RC, et al. JAK mutations in high-risk childhood acute lymphoblastic leukemia. Proc Natl Acad Sci U S A 2009;106:9414-8.

66.   Saharinen P, Vihinen M, Silvennoinen O. Autoinhibition of Jak2 tyrosine kinase is dependent on specific regions in its pseudokinase domain. Mol Biol Cell 2003;14:1448-59.

67.   Beer PA, Campbell PJ, Scott LM, et al. MPL mutations in myeloproliferative disorders: analysis of the PT-1 cohort. Blood 2008.

68.   Gurney AL, Wong SC, Henzel WJ, de Sauvage FJ. Distinct regions of c-Mpl cytoplasmic domain are coupled to the JAK-STAT signal transduction pathway and Shc phosphorylation. Proc Natl Acad Sci U S A 1995;92:5292-6.

69.   Pardanani A, Lasho TL, Finke C, et al. Extending Jak2V617F and MplW515 mutation analysis to single hematopoietic colonies and B and T lymphocytes. Stem Cells 2007;25:2358-62.

70.   Vannucchi AM, Antonioli E, Guglielmelli P, et al. Characteristics and clinical correlates of MPL 515W>L/K mutation in essential thrombocythemia. Blood 2008.

71.   Staerk J, Lacout C, Sato T, Smith SO, Vainchenker W, Constantinescu SN. An amphipathic motif at the transmembrane-cytoplasmic junction prevents autonomous activation of the thrombopoietin receptor. Blood 2006;107:1864-71.

72.   Kawamata N, Ogawa S, Yamamoto G, et al. Genetic profiling of myeloproliferative disorders by single-nucleotide polymorphism oligonucleotide microarray. Exp Hematol 2008;36:1471-9.

73.   Williams DM, Kim AH, Rogers O, Spivak JL, Moliterno AR. Phenotypic variations and new mutations in JAK2 V617F-negative polycythemia vera, erythrocytosis, and idiopathic myelofibrosis. Exp Hematol 2007;35:1641-6.

74.   Skoda RC. Thrombocytosis. Hematology Am Soc Hematol Educ Program 2009:159-67.

75.   Langemeijer SM, Kuiper RP, Berends M, et al. Acquired mutations in TET2 are common in myelodysplastic syndromes. Nat Genet 2009;41:838-42.

76.   Jankowska AM, Szpurka H, Tiu RV, et al. Loss of heterozygosity 4q24 and TET2 mutations associated with myelodysplastic/myeloproliferative neoplasms. Blood 2009;113:6403-10.

77.   Tefferi A, Levine RL, Lim KH, et al. Frequent TET2 mutations in systemic mastocytosis: clinical, KITD816V and FIP1L1-PDGFRA correlates. Leukemia 2009;23:900-4.

78.   Tefferi A, Pardanani A, Lim KH, et al. TET2 mutations and their clinical correlates in polycythemia vera, essential thrombocythemia and myelofibrosis. Leukemia 2009.

79.   Mullighan CG. TET2 mutations in myelodysplasia and myeloid malignancies. Nat Genet 2009;41:766-7.

80.   Tahiliani M, Koh KP, Shen Y, et al. Conversion of 5-methylcytosine to 5-hydroxymethylcytosine in mammalian DNA by MLL partner TET1. Science 2009;324:930-5.

81.   Sanada M, Suzuki T, Shih LY, et al. Gain-of-function of mutated C-CBL tumour suppressor in myeloid neoplasms. Nature 2009;460:904-8.

82.   Dunbar AJ, Gondek LP, O'Keefe CL, et al. 250K single nucleotide polymorphism array karyotyping identifies acquired uniparental disomy and homozygous mutations, including novel missense substitutions of c-Cbl, in myeloid malignancies. Cancer Res 2008;68:10349-57.

83.   Loh ML, Sakai DS, Flotho C, et al. Mutations in CBL occur frequently in juvenile myelomonocytic leukemia. Blood 2009;114:1859-63.

84.   Abbas S, Rotmans G, Lowenberg B, Valk PJ. Exon 8 splice site mutations in the gene encoding the E3-ligase CBL are associated with core binding factor acute myeloid leukemias. Haematologica 2008;93:1595-7.

85.   Caligiuri MA, Briesewitz R, Yu J, et al. Novel c-CBL and CBL-b ubiquitin ligase mutations in human acute myeloid leukemia. Blood 2007;110:1022-4.

86.   Mor A, Philips MR. Compartmentalized Ras/MAPK signaling. Annu Rev Immunol 2006;24:771-800.

87.   Birnbaum RA, O'Marcaigh A, Wardak Z, et al. Nf1 and Gmcsf interact in myeloid leukemogenesis. Mol Cell 2000;5:189-95.

88.   Tefferi A, Gilliland DG. Oncogenes in myeloproliferative disorders. Cell Cycle 2007;6:550-66.

89.   Stegelmann F, Bullinger L, Griesshammer M, et al. High-resolution single-nucleotide polymorphism array-profiling in myeloproliferative neoplasms identifies novel genomic aberrations. Haematologica 2009.

90.   Shannon K, Loh M. Cancer: More than kin and less than kind. Nature 2009;460:804-7.

91.   Kralovics R, Guan Y, Prchal J. Acquired uniparental disomy of chromosome 9p is a frequent stem cell defect in polycythemia vera. Exp Hematol 2002;30:229-36.

92.   Heinrichs S, Kulkarni RV, Bueso-Ramos CE, et al. Accurate detection of uniparental disomy and microdeletions by SNP array analysis in myelodysplastic syndromes with normal cytogenetics. Leukemia 2009;23:1605-13.

93.   Gondek LP, Tiu R, Haddad AS, et al. Single nucleotide polymorphism arrays complement metaphase cytogenetics in detection of new chromosomal lesions in MDS. Leukemia 2007;21:2058-61.

94.   Makishima H, Rataul M, Gondek LP, et al. FISH and SNP-A karyotyping in myelodysplastic syndromes: Improving cytogenetic detection of del(5q), monosomy 7, del(7q), trisomy 8 and del(20q). Leuk Res 2009.

95.   Szpurka H, Gondek LP, Mohan SR, Hsi ED, Theil KS, Maciejewski JP. UPD1p indicates the presence of MPL W515L mutation in RARS-T, a mechanism analogous to UPD9p and JAK2 V617F mutation. Leukemia 2008.

96.   Gondek LP, Dunbar AJ, Szpurka H, McDevitt MA, Maciejewski JP. SNP array karyotyping allows for the detection of uniparental disomy and cryptic chromosomal abnormalities in MDS/MPD-U and MPD. PLoS ONE 2007;2:e1225.

97.   Grimwade D, Walker H, Oliver F, et al. The importance of diagnostic cytogenetics on outcome in AML: analysis of 1,612 patients entered into the MRC AML 10 trial. The Medical Research Council Adult and Children's Leukaemia Working Parties. Blood 1998;92:2322-33.

98.   Schaub FX, Jager R, Looser R, et al. Clonal analysis of deletions on chromosome 20q and JAK2-V617F in MPD suggests that del20q acts independently and is not one of the predisposing mutations for JAK2-V617F. Blood 2009;113:2022-7.

99.   Olcaydu D, Harutyunyan A, Jager R, et al. A common JAK2 haplotype confers susceptibility to myeloproliferative neoplasms. Nat Genet 2009;41:450-4.

100.   Plo I, Nakatake M, Malivert L, et al. JAK2 stimulates homologous recombination and genetic instability: potential implication in the heterogeneity of myeloproliferative disorders. Blood 2008;112:1402-12.

101.   Beer PA, Jones AV, Bench AJ, et al. Clonal diversity in the myeloproliferative neoplasms: independent origins of genetically distinct clones. Br J Haematol 2009;144:904-8.

102.   Kralovics R, Stockton DW, Prchal JT. Clonal hematopoiesis in familial polycythemia vera suggests the involvement of multiple mutational events in the early pathogenesis of the disease. Blood 2003;102:3793-7.

103.   Bellanne-Chantelot C, Chaumarel I, Labopin M, et al. Genetic and clinical implications of the Val617Phe JAK2 mutation in 72 families with myeloproliferative disorders. Blood 2006;108:346-52.

104.   Rumi E, Passamonti F, Pietra D, et al. JAK2 (V617F) as an acquired somatic mutation and a secondary genetic event associated with disease progression in familial myeloproliferative disorders. Cancer 2006;107:2206-11.

105.   Saint-Martin C, Leroy G, Delhommeau F, et al. Analysis of the ten-eleven translocation 2 (TET2) gene in familial myeloproliferative neoplasms. Blood 2009;114:1628-32.

106.   Ding J, Komatsu H, Wakita A, et al. Familial essential thrombocythemia associated with a dominant-positive activating mutation of the c-MPL gene, which encodes for the receptor for thrombopoietin. Blood 2004.

107.   Jones AV, Chase A, Silver RT, et al. JAK2 haplotype is a major risk factor for the development of myeloproliferative neoplasms. Nat Genet 2009;41:446-9.

108.   Kilpivaara O, Mukherjee S, Schram AM, et al. A germline JAK2 SNP is associated with predisposition to the development of JAK2(V617F)-positive myeloproliferative neoplasms. Nat Genet 2009;41:455-9.
109.   Olcaydu D, Skoda RC, Looser R, et al. The 'GGCC' haplotype of JAK2 confers susceptibility to JAK2 exon 12 mutation-positive polycythemia vera. Leukemia 2009.
110.   Pardanani A, Lasho TL, Finke CM, et al. The JAK2 46/1 haplotype confers susceptibility to essential thrombocythemia regardless of JAK2V617F mutational status-clinical correlates in a study of 226 consecutive patients. Leukemia 2009.
111.   Tefferi A, Lasho TL, Patnaik MM, et al. JAK2 germline genetic variation affects disease susceptibility in primary myelofibrosis regardless of V617F mutational status: nullizygosity for the JAK2 46/1 haplotype is associated with inferior survival. Leukemia 2009.
112.   Rege-Cambrin G, Mecucci C, Tricot G, et al. A chromosomal profile of polycythemia vera. Cancer Genet Cytogenet 1987;25:233-45.
113.   Diez-Martin JL, Graham DL, Petitt RM, Dewald GW. Chromosome studies in 104 patients with polycythemia vera. Mayo Clin Proc 1991;66:287-99.
114.   Mertens F, Johansson B, Heim S, Kristoffersson U, Mitelman F. Karyotypic patterns in chronic myeloproliferative disorders: report on 74 cases and review of the literature. Leukemia 1991;5:214-20.
115.   Bench AJ, Nacheva EP, Hood TL, et al. Chromosome 20 deletions in myeloid malignancies: reduction of the common deleted region, generation of a PAC/BAC contig and identification of candidate genes. UK Cancer Cytogenetics Group (UKCCG). Oncogene 2000;19:3902-13.
116.   Westwood NB, Gruszka-Westwood AM, Pearson CE, et al. The incidences of trisomy 8, trisomy 9 and D20S108 deletion in polycythaemia vera: an analysis of blood granulocytes using interphase fluorescence in situ hybridization. Br J Haematol 2000;110:839-46.
117.   Najfeld V, Montella L, Scalise A, Fruchtman S. Exploring polycythaemia vera with fluorescence in situ hybridization: additional cryptic 9p is the most frequent abnormality detected. British Journal of Haematology 2002;119:558-66.
118.   Fenaux P, Morel P, Lai JL. Cytogenetics of myelodysplastic syndromes. Semin Hematol 1996;33:127-38.
119.   Heim S, Mitelman F. Cytogenetic analysis in the diagnosis of acute leukemia. Cancer 1992;70:1701-9.
120.   Asimakopoulos FA, White NJ, Nacheva E, Green AR. Molecular analysis of chromosome 20q deletions associated with myeloproliferative disorders and myelodysplastic syndromes. Blood 1994;84:3086-94.
121.   Asimakopoulos FA, Gilbert JG, Aldred MA, Pearson TC, Green AR. Interstitial deletion constitutes the major mechanism for loss of heterozygosity on chromosome 20q in polycythemia vera. Blood 1996;88:2690-8.
122.   Bench AJ, Aldred MA, Humphray SJ, et al. A detailed physical and transcriptional map of the region of chromosome 20 that is deleted in myeloproliferative disorders and refinement of the common deleted region. Genomics 1998;49:351-62.
123.   Bench AJ, Nacheva EP, Champion KM, Green AR. Molecular genetics and cytogenetics of myeloproliferative disorders. Baillieres Clin Haematol 1998;11:819-48.
124.   Douet-Guilbert N, Basinko A, Morel F, et al. Chromosome 20 deletions in myelodysplastic syndromes and Philadelphia-chromosome-negative myeloproliferative

disorders: characterization by molecular cytogenetics of commonly deleted and retained regions. Ann Hematol 2008;87:537-44.

125.   Kralovics R, Teo SS, Li S, et al. Acquisition of the V617F mutation of JAK2 is a late genetic event in a subset of patients with myeloproliferative disorders. Blood 2006;108:1377-80.

126.   Campbell P, Green A. The myeloproliferative disorders. N Engl J Med 2006;355:2452-66.

127.   Kralovics R, Passamonti F, Buser A, et al. A gain-of-function mutation of JAK2 in myeloproliferative disorders. N Engl J Med 2005;352:1779-90.

128.   Theocharides A, Boissinot M, Girodon F, et al. Leukemic blasts in transformed JAK2-V617F-positive myeloproliferative disorders are frequently negative for the JAK2-V617F mutation. Blood 2007;110:375-9.

129.   Campbell PJ, Baxter EJ, Beer PA, et al. Mutation of JAK2 in the myeloproliferative disorders: timing, clonality studies, cytogenetic associations, and role in leukemic transformation. Blood 2006;108:3548-55.

130.   Abdel-Wahab O, Manshouri T, Patel J, et al. Genetic analysis of transforming events that convert chronic myeloproliferative neoplasms to leukemias. Cancer Res 2010;70:447-52.

131.   Green A, Beer P. Somatic mutations of IDH1 and IDH2 in the leukemic transformation of myeloproliferative neoplasms. N Engl J Med 2010;362:369-70.

132.   Mardis ER, Ding L, Dooling DJ, et al. Recurring mutations found by sequencing an acute myeloid leukemia genome. N Engl J Med 2009;361:1058-66.

133.   Moffat J, Grueneberg DA, Yang X, et al. A lentiviral RNAi library for human and mouse genes applied to an arrayed viral high-content screen. Cell 2006;124:1283-98.

134.   Zufferey R, Nagy D, Mandel R, Naldini L, Trono D. Multiply attenuated lentiviral vector achieves efficient gene delivery in vivo. Nat Biotechnol 1997;15:871-5.

135.   Garcia P, Frampton J. The transcription factor B-Myb is essential for S-phase progression and genomic stability in diploid and polyploid megakaryocytes. J Cell Sci 2006;119:1483-93.

136.   Dunbar SA. Applications of Luminex xMAP technology for rapid, high-throughput multiplexed nucleic acid detection. Clin Chim Acta 2006;363:71-82.

137.   Georgopoulos K, Bigby M, Wang J, et al. The Ikaros gene is required for the development of all lymphoid lineages. Cell 1994;79:143-56.

138.   Winandy S, Wu P, Georgopoulos K. A dominant mutation in the Ikaros gene leads to rapid development of leukemia and lymphoma. Cell 1995;83:289-99.

139.   Wang J, Nichogiannopoulou A, Wu L, et al. Selective defects in the development of the fetal and adult lymphoid system in mice with an Ikaros null mutation. Immunity 1996;5:537-49.

140.   Kano G, Morimoto A, Takanashi M, et al. Ikaros dominant negative isoform (Ik6) induces IL-3-independent survival of murine pro-B lymphocytes by activating JAK-STAT and up-regulating Bcl-xl levels. Leuk Lymphoma 2008;49:965-73.

141.   Gondek LP, Tiu R, O'Keefe CL, Sekeres MA, Theil KS, Maciejewski JP. Chromosomal lesions and uniparental disomy detected by SNP arrays in MDS, MDS/MPD, and MDS-derived AML. Blood 2008;111:1534-42.

142.   Georgopoulos K, Moore D, Derfler B. Ikaros, an early lymphoid-specific transcription factor and a putative mediator for T cell commitment. Science 1992;258:808-12.

143.   Georgopoulos K. Haematopoietic cell-fate decisions, chromatin regulation and ikaros. Nat Rev Immunol 2002;2:162-74.

144.   Kirstetter P, Thomas M, Dierich A, Kastner P, Chan S. Ikaros is critical for B cell differentiation and function. Eur J Immunol 2002;32:720-30.

145.   Lopez RA, Schoetz S, DeAngelis K, O'Neill D, Bank A. Multiple hematopoietic defects and delayed globin switching in Ikaros null mice. Proc Natl Acad Sci U S A 2002;99:602-7.

146.   García P, Clarke M, Vegiopoulos A, et al. Reduced c-Myb activity compromises HSCs and leads to a myeloproliferation with a novel stem cell basis. EMBO J 2009;28:1492-504.

147.   Hahm K, Ernst P, Lo K, Kim GS, Turck C, Smale ST. The lymphoid transcription factor LyF-1 is encoded by specific, alternatively spliced mRNAs derived from the Ikaros gene. Mol Cell Biol 1994;14:7111-23.

148.   Klein F, Feldhahn N, Herzog S, et al. BCR-ABL1 induces aberrant splicing of IKAROS and lineage infidelity in pre-B lymphoblastic leukemia cells. Oncogene 2006;25:1118-24.

149.   Mullighan C, Miller C, Radtke I, et al. BCR-ABL1 lymphoblastic leukaemia is characterized by the deletion of Ikaros. Nature 2008;453:110-4.

150.   Iacobucci I, Storlazzi C, Cilloni D, et al. Identification and molecular characterization of recurrent genomic deletions on 7p12 in the IKZF1 gene in a large cohort of BCR-ABL1-positive acute lymphoblastic leukemia patients: on behalf of Gruppo Italiano Malattie Ematologiche dell'Adulto Acute Leukemia Working Party (GIMEMA AL WP). Blood 2009;114:2159-67.

151.   Luo H, Hanratty WP, Dearolf CR. An amino acid substitution in the Drosophila hopTum-l Jak kinase causes leukemia-like hematopoietic defects. EMBO J 1995;14:1412-20.

152.   Lacronique V, Boureux A, Valle V, et al. A TEL-JAK2 fusion protein with constitutive kinase activity in human leukemia. Science 1997;278:1309-12.

153.   Peeters P, Raynaud SD, Cools J, et al. Fusion of TEL, the ETS-variant gene 6 (ETV6), to the receptor-associated kinase JAK2 as a result of t(9;12) in a lymphoid and t(9;15;12) in a myeloid leukemia. Blood 1997;90:2535-40.

154.   Reiter A, Walz C, Watmore A, et al. The t(8;9)(p22;p24) is a recurrent abnormality in chronic and acute leukemia that fuses PCM1 to JAK2. Cancer Res 2005;65:2662-7.

155.   Murati A, Gelsi-Boyer V, Adélaïde J, et al. PCM1-JAK2 fusion in myeloproliferative disorders and acute erythroid leukemia with t(8;9) translocation. Leukemia 2005;19:1692-6.

156.   Griesinger F, Hennig H, Hillmer F, et al. A BCR-JAK2 fusion gene as the result of a t(9;22)(p24;q11.2) translocation in a patient with a clinically typical chronic myeloid leukemia. Genes Chromosomes Cancer 2005;44:329-33.

157.   Bousquet M, Quelen C, De Mas V, et al. The t(8;9)(p22;p24) translocation in atypical chronic myeloid leukaemia yields a new PCM1-JAK2 fusion gene. Oncogene 2005;24:7248-52.

158.   Mercher T, Wernig G, Moore S, et al. JAK2T875N is a novel activating mutation that results in myeloproliferative disease with features of megakaryoblastic leukemia in a murine bone marrow transplantation model. Blood 2006;108:2770-9.

159.   Kearney L, Gonzalez De Castro D, Yeung J, et al. Specific JAK2 mutation (JAK2R683) and multiple gene deletions in Down syndrome acute lymphoblastic leukemia. Blood 2009;113:646-8.

160.   Zhao R, Follows GA, Beer PA, et al. Inhibition of the Bcl-xL deamidation pathway in myeloproliferative disorders. N Engl J Med 2008;359:2778-89.

161.   Cramer K, Nieborowska-Skorska M, Koptyra M, et al. BCR/ABL and other kinases from chronic myeloproliferative disorders stimulate single-strand annealing, an unfaithful DNA double-strand break repair. Cancer Res 2008;68:6884-8.

162.   Slupianek A, Schmutte C, Tombline G, et al. BCR/ABL regulates mammalian RecA homologs, resulting in drug resistance. Mol Cell 2001;8:795-806.

163. Slupianek A, Hoser G, Majsterek I, et al. Fusion tyrosine kinases induce drug resistance by stimulation of homology-dependent recombination repair, prolongation of G(2)/M phase, and protection from apoptosis. Mol Cell Biol 2002;22:4189-201.

164. Chipoy C, Brounais B, Trichet V, et al. Sensitization of osteosarcoma cells to apoptosis by oncostatin M depends on STAT5 and p53. Oncogene 2007;26:6653-64.

165. Goetz CA, Harmon IR, O'Neil JJ, Burchill MA, Johanns TM, Farrar MA. Restricted STAT5 activation dictates appropriate thymic B versus T cell lineage commitment. J Immunol 2005;174:7753-63.

166. Hassel JC, Winnemoller D, Schartl M, Wellbrock C. STAT5 contributes to antiapoptosis in melanoma. Melanoma Res 2008;18:378-85.

167. Walz C, Lazarides K, Patel N, Hennighausen L, Zaleskas VM, Van Etten RA. Essential Role for Stat5a/b in Myeloproliferative Neoplasms Induced by BCR-ABL1 and Jak2 V617F. Blood (ASH Annual Meeting Abstracts) 2009;114:312-.

168. Hoelbl A, Schuster C, Kovacic B, et al. Stat5 is indispensable for the maintenance of bcr/abl-positive leukaemia. EMBO Mol Med;2:98-110.

169. Dawson MA, Bannister AJ, Gottgens B, et al. JAK2 phosphorylates histone H3Y41 and excludes HP1alpha from chromatin. Nature 2009;461:819-22.

170. Cummings WJ, Yabuki M, Ordinario EC, Bednarski DW, Quay S, Maizels N. Chromatin structure regulates gene conversion. PLoS Biol 2007;5:e246.

171. Yamagishi Y, Sakuno T, Shimura M, Watanabe Y. Heterochromatin links to centromeric protection by recruiting shugoshin. Nature 2008;455:251-5.

172. Panteleeva I, Boutillier S, See V, et al. HP1alpha guides neuronal fate by timing E2F-targeted genes silencing during terminal differentiation. EMBO J 2007;26:3616-28.

173. Luijsterburg MS, Dinant C, Lans H, et al. Heterochromatin protein 1 is recruited to various types of DNA damage. J Cell Biol 2009;185:577-86.

174. Brown KE, Guest SS, Smale ST, Hahm K, Merkenschlager M, Fisher AG. Association of transcriptionally silent genes with Ikaros complexes at centromeric heterochromatin. Cell 1997;91:845-54.

175. Luna-Fineman S, Shannon KM, Lange BJ. Childhood monosomy 7: epidemiology, biology, and mechanistic implications. Blood 1995;85:1985-99.

176. Wheatley K, Burnett A, Goldstone A, et al. A simple, robust, validated and highly predictive index for the determination of risk-directed therapy in acute myeloid leukaemia derived from the MRC AML 10 trial. United Kingdom Medical Research Council's Adult and Childhood Leukaemia Working Parties. Br J Haematol 1999;107:69-79.

177. Mesa R, Li C, Ketterling R, Schroeder G, Knudson R, Tefferi A. Leukemic transformation in myelofibrosis with myeloid metaplasia: a single-institution experience with 91 cases. Blood 2005;105:973-7.

178. Strasser-Weippl K, Steurer M, Kees M, et al. Chromosome 7 deletions are associated with unfavorable prognosis in myelofibrosis with myeloid metaplasia. Blood 2005;105:4146.

179. Mullighan C, Su X, Zhang J, et al. Deletion of IKZF1 and prognosis in acute lymphoblastic leukemia. N Engl J Med 2009;360:470-80.

180. Martinelli G, Iacobucci I, Storlazzi C, et al. IKZF1 (Ikaros) Deletions in BCR-ABL1-Positive Acute Lymphoblastic Leukemia Are Associated With Short Disease-Free Survival and High Rate of Cumulative Incidence of Relapse: A GIMEMA AL WP Report. J Clin Oncol 2009.

181.   Li S, Kralovics R, De Libero G, Theocharides A, Gisslinger H, Skoda RC. Clonal heterogeneity in polycythemia vera patients with JAK2 exon12 and JAK2-V617F mutations. Blood 2008;111:3863-6.

182.   Carbuccia N, Trouplin V, Gelsi-Boyer V, et al. Mutual exclusion of ASXL1 and NPM1 mutations in a series of acute myeloid leukemias. Leukemia 2010;24:469-73.

183.   Lee SW, Cho YS, Na JM, et al. ASXL1 represses retinoic acid receptor-mediated transcription through associating with HP1 and LSD1. J Biol Chem 2010;285:18-29.

184.   Sala A. B-MYB, a transcription factor implicated in regulating cell cycle, apoptosis and cancer. Eur J Cancer 2005;41:2479-84.

185.   Shepard JL, Stern HM, Pfaff KL, Amatruda JF. Analysis of the cell cycle in zebrafish embryos. Methods Cell Biol 2004;76:109-25.

186.   Lewis PW, Beall EL, Fleischer TC, Georlette D, Link AJ, Botchan MR. Identification of a Drosophila Myb-E2F2/RBF transcriptional repressor complex. Genes Dev 2004;18:2929-40.

187.   Pommier Y. Topoisomerase I inhibitors: camptothecins and beyond. Nat Rev Cancer 2006;6:789-802.

188.   Rossi F, Labourier E, Forne T, et al. Specific phosphorylation of SR proteins by mammalian DNA topoisomerase I. Nature 1996;381:80-2.

189.   Rossi F, Labourier E, Gallouzi IE, et al. The C-terminal domain but not the tyrosine 723 of human DNA topoisomerase I active site contributes to kinase activity. Nucleic Acids Res 1998;26:2963-70.

190.   Merino A, Madden KR, Lane WS, Champoux JJ, Reinberg D. DNA topoisomerase I is involved in both repression and activation of transcription. Nature 1993;365:227-32.

191.   Shykind BM, Kim J, Stewart L, Champoux JJ, Sharp PA. Topoisomerase I enhances TFIID-TFIIA complex assembly during activation of transcription. Genes Dev 1997;11:397-407.

192.   Kretzschmar M, Meisterernst M, Roeder RG. Identification of human DNA topoisomerase I as a cofactor for activator-dependent transcription by RNA polymerase II. Proc Natl Acad Sci U S A 1993;90:11508-12.

193.   Albor A, Kaku S, Kulesz-Martin M. Wild-type and mutant forms of p53 activate human topoisomerase I: a possible mechanism for gain of function in mutants. Cancer Res 1998;58:2091-4.

194.   Gobert C, Bracco L, Rossi F, et al. Modulation of DNA topoisomerase I activity by p53. Biochemistry 1996;35:5778-86.

195.   Ahuja HG, Felix CA, Aplan PD. The t(11;20)(p15;q11) chromosomal translocation associated with therapy-related myelodysplastic syndrome results in an NUP98-TOP1 fusion. Blood 1999;94:3258-61.

196.   Chen S, Xue Y, Chen Z, Guo Y, Wu Y, Pan J. Generation of the NUP98-TOP1 fusion transcript by the t(11;20) (p15;q11) in a case of acute monocytic leukemia. Cancer Genet Cytogenet 2003;140:153-6.

197.   Gurevich RM, Aplan PD, Humphries RK. NUP98-topoisomerase I acute myeloid leukemia-associated fusion gene has potent leukemogenic activities independent of an engineered catalytic site mutation. Blood 2004;104:1127-36.

198.   Tsurutani J, Nitta T, Hirashima T, et al. Point mutations in the topoisomerase I gene in patients with non-small cell lung cancer treated with irinotecan. Lung Cancer 2002;35:299-304.

199.   Beer PA, Delhommeau F, LeCouedic JP, et al. Two routes to leukemic transformation after a JAK2 mutation-positive myeloproliferative neoplasm. Blood 2009;115:2891-900.

200.   Ebert BL, Pretz J, Bosco J, et al. Identification of RPS14 as a 5q- syndrome gene by RNA interference screen. Nature 2008;451:335-9.

201.   Carette JE, Guimaraes CP, Varadarajan M, et al. Haploid genetic screens in human cells identify host factors used by pathogens. Science 2009;326:1231-5.

202.   Schmidt MH, Dikic I. The Cbl interactome and its functions. Nat Rev Mol Cell Biol 2005;6:907-18.

203.   Hantschel O, Rix U, Superti-Furga G. Target spectrum of the BCR-ABL inhibitors imatinib, nilotinib and dasatinib. Leuk Lymphoma 2008;49:615-9.

204.   Apostolidou E, Kantarjian HM, Verstovsek S. JAK2 inhibitors: A reality? A hope? Clin Lymphoma Myeloma 2009;9 Suppl 3:S340-5.

ACKNOWLEDGEMENTS

First of all I would like to thank Robert Kralovics for giving me the chance to be his first PhD student in his newly started up lab, thanks for trusting and believing in me. There was a lot to learn from Robert and I am grateful for the huge amount of support and time he spent on me.

I would like to thank Giulio Superti-Furga and Ulrich Jaeger for their time and input as my thesis committee members. Special thanks to Giulio for his enthusiasm in building up and leading CeMM, it was a big experience and privilege to be part of this great institute right from the beginning.

Special thanks to my colleagues in the Kralovics Lab, Tiina Berg, Ashot Harutyunyan, Thorsten Klampfl and Damla Olcaydu. Thank you so much for all the support, for all the discussions and especially for a good atmosphere and a lot of fun.

Thanks to our collaborators at the Medical Universtity Vienna, Heinz Gisslinger, Bettina Gisslinger and Nicole Bachofner. Special thanks to Matthias Mayerhofer for technical support and advice. Thanks also to our collaborators at the University Hospital Basel, Radek Skoda and Franz Schaub, and at the University of Pavia, especially to Elisa Rumi, Daniela Pietra, Francesco Passamonti and Mario Cazzola.

Special thanks to all people at CeMM, as already mentioned it was a privilege to be with you. The interaction with quite a lot of you was intense, productive and always relaxed and friendly. I would like to address special thanks to Omar Sharif, Oliver Hantschel and Florian Grebien, who provided me with a lot of theoretical and practical support. Special thanks also to the whole Nijman group, especially Sebastian Nijman, Nils Craig-Mueller and Markus Muellner. Markus had special impact on the Luminex-based screen, as he set up and optimized the system in the Nijman lab. Thank you for your kind supervision through the whole experiment. I further would like to thank Helen Pickersgill for critical reading of parts of my thesis.

CURRICULUM VITAE

Roland Jäger

A-4133 Niederkappel 6
AUSTRIA
Tel.: ++43 7286/8494
Mobile: ++43 650405172
e-mail: roland.jaeger@gmx.at

* 21. 09. 1981 in Linz
Nationality: Austrian

Education/Trainings/Occupations:

10/2006 –	PhD student at Ce-M-M- (Center for Molecular Medicine of the Austrian Academy of Sciences) and at the Medical University of Vienna under the supervision of Dr. Robert Kralovics; Project: Genetics of Myeloproliferative Neoplasms
10/2005 – 07/2006	Master thesis at the Semmelweis University, Budapest, Department of Genetics, Cell- and Immunobiology under the supervision of Dr. András Falus; Project: "The role of histamine in dendritic cell function: studies using "histamine-free" and "histamine-receptor-4 deficient" mouse models"
10/2004 -08/2006	Studies for the Master's degree in „Genetics and Biotechnology (Target: Immunology)" at the University of Salzburg
08/2004 - 09/2004	Work experience at the "National Research Institute for Radiobiology", Department for Cell Biology; Budapest, Hungary.
07/2003 - 08/2003	Work experience at the "Vienna General Hospital" (AKH Wien); Department of Clinical Pharmacology: Project: Determination of Fosfomycin in Plasma and Microdialysates by High Performance Capillary Electrophoresis
03/2002 – 03/2005	Studies for the Bachelor's degree in „Genetics and Molecular Biology" at the University of Salzburg
01/2001 - 03/2002	Military Service (compulsory) in the Austrian Military Band, Vienna

09/2000 - 12/2000	Temporary employment in the UK (Work Experience at City Center Restaurants, London)
09/1992 - 06/2000	Secondary school in Rohrbach
09/1988 - 07/1992	Elementary school in Niederkappel

Languages:

- German (native language)
- English (fluent)
- Hungarian (fluent)
- Italian (basics)

Publications:

Jäger R, Gisslinger H, Passamonti F, Rumi E, Berg T, Gisslinger B, Pietra D, Harutyunyan A, Klampfl T, Olcaydu D, Cazzola M, Kralovics R. Deletions of the transcription factor Ikaros in myeloproliferative neoplasms. Leukemia. 2010 May 27. [Epub ahead of print].

Jäger R, Kralovics R. Molecular basis and clonal evolution of myeloproliferative neoplasms. Haematologica. 2010 Apr;95(4):526-9.Review.

Olcaydu D, Harutyunyan A, **Jäger R**, Berg T, Gisslinger B, Pabinger I, Gisslinger H, Kralovics R. A common JAK2 haplotype confers susceptibility to myeloproliferative neoplasms. Nat Genet. 2009 Apr;41(4):450-4.

Schaub FX**, Jäger R**, Looser R, Hao-Shen H, Hermouet S, Girodon F, Tichelli A, Gisslinger H, Kralovics R, Skoda RC. Clonal analysis of deletions on chromosome 20q and JAK2-V617F in MPD suggests that del20q acts independently and is not one of the predisposing mutations for JAK2-V617F. Blood. 2009 Feb 26;113(9):2022-7.

Conferences:

12/2009	51th ASH annual meeting, San Francisco, Oral presentation: Deletions of the Transcription Factor Ikaros in Myeloproliferative Neoplasms at Transformation to Acute Myeloid Leukemia

12/2008   50th ASH annual meeting, San Francisco, CA
<u>Oral presentation:</u> Chromosomal Instability Causes Genetic and Clonal Heterogeneity in Myeloproliferative Neoplasms and Is Not Restricted to JAK2-V617F Positive Cells

02/2008   International Congress for Integrative Cancer Genomics, Munich, Germany

08/2007   1st CeMM conference, Drug Action and Chemical Biology in the Post-Genomic Era, Vienna, Austria

LIST OF PUBLICATIONS

Jäger R, Gisslinger H, Passamonti F, Rumi E, Berg T, Gisslinger B, Pietra D, Harutyunyan A, Klampfl T, Olcaydu D, Cazzola M, Kralovics R. Deletions of the transcription factor Ikaros in myeloproliferative neoplasms. Leukemia. 2010 May 27. [Epub ahead of print].

Jäger R, Kralovics R. Molecular basis and clonal evolution of myeloproliferative neoplasms. Haematologica. 2010 Apr;95(4):526-9.Review.

Olcaydu D, Harutyunyan A, **Jäger R**, Berg T, Gisslinger B, Pabinger I, Gisslinger H, Kralovics R. A common JAK2 haplotype confers susceptibility to myeloproliferative neoplasms. Nat Genet. 2009 Apr;41(4):450-4.

Schaub FX, **Jäger R**, Looser R, Hao-Shen H, Hermouet S, Girodon F, Tichelli A, Gisslinger H, Kralovics R, Skoda RC. Clonal analysis of deletions on chromosome 20q and JAK2-V617F in MPD suggests that del20q acts independently and is not one of the predisposing mutations for JAK2-V617F. Blood. 2009 Feb 26;113(9):2022-7.